European cooperation in the field of scientific and technical research

Meteorology

Mixing height and inversions in urban areas

Proceedings of the workshop

3 - 4 October 2001, Toulouse, France

COST Action 715

European Commission

COST Action 715

Meteorology Applied to Urban Air Pollution Problems

Mixing height and inversions in urban areas

Proceedings of the workshop

3 - 4 October 2001, Toulouse, France

Edited by:

Martin Piringer

Central Institute for Meteorology and Geodynamics,

Vienna, Austria

and

Jaakko Kukkonen

Finnish Meteorological Institute, Helsinki, Finland

Content

Introduction

Martin Piringer[1] and Jaakko Kukkonen[2]

[1]Central Institute for Meteorology and Geodynamics, Hohe Warte 38, A-1190 Vienna, Austria
e-mail: martin.piringer@zamg.ac.at

[2] Finnish Meteorological Institute, Air Quality Research, Sahaajankatu 20 E, FIN–00880 Helsinki, Finland
e-mail: jaakko.kukkonen@fmi.fi

Organisation of the expert meeting

COST-Action 715 held an expert meeting in Toulouse, France, on 3 - 4 October 2001, comprising of expert presentations on mixing heights and inversions in urban areas. COST is an acronym of "Co-operation in the fields of Science and Technology", financially supported by the European Commission to encourage and facilitate mutual scientific exchange among Member States. Each action is devoted to a specific topic whose main scientific goals are fixed in a so-called "Memorandum of Understanding", to be signed by COST Member States. An action lasts in general five years. COST Action 715, chaired by Bernard Fisher, University of Greenwich, U.K., and Michael Schatzmann, University of Hamburg, Germany, has been signed by 18 countries and will end in September 2003.

COST Action 715 is organised in four working groups, dealing with (1) urban wind fields, (2) surface energy budget and mixing height, (3) air pollution episodes in cities, and (4) meteorological input data for urban site studies. The Toulouse workshop was jointly organised by working groups 2 and 3 that are chaired by the editors of these proceedings.

Nine presentations were kept at the meeting in Toulouse, five on mixing heights, four on inversions. This volume contains the extended abstracts in the temporal order of the presentations kept at the meeting. The outcome of the general discussions is reflected in the conclusions that are presented at the end of these proceedings.

The session on mixing heights

Methods for the evaluation of mixing height were reviewed by A. Baklanov. In numerical weather prediction, the simple closure models do not work well. Nocturnal stable air in urban areas presents greatest difficulty for modellers. The performance of methods seems more acceptable in daytime than night. Inhomogeneity of surface types and thermal properties in a city should be modelled numerically.

R. Martens reviewed German regulatory models: a traditional Gaussian plume model and a new Lagrangian model. The latter uses turbulence components and Lagrangian time scales to evaluate the dispersion. In discussion, the problem of inhomogeneity over an urban surface reappeared.

The presentation of the ongoing experiment called BUBBLE (Basle Urban Boundary Layer Experiment) by M. Rotach showed the effort to set up a comprehensive network of tower and surface observations. Lidar, Sodar, wind profiler and tethered balloons were used to investigate the urban boundary layer in detail over a whole year, also for the purpose of subsequent numerical modelling.

The report of the recent UBL/ESCOMPTE experiment in the greater Marseilles area by F. Said described also the use of RASS, O_3 and particle Lidars. Real profiles showed often multiple layering, causing difficulty in detecting the mixing height from the Lidar measurements alone. A. Dandou tested the mixing height schemes within the meso-scale numerical model MM5 for the Lombardy area in Northern Italy, including Milan, and compared the results to the Milan radiosoundings.

The session on mixing heights concluded with considerable discussion of how are mixing heights best measured (e.g., via accumulated pollutants in the air, or by profiles, or by remote sensing) and what is really meant by them. In the context of numerical weather prediction (NWP), is the mixing height still a valid concept ? It seems that their practical usefulness in understanding episodes and in running the simpler types of pollution dispersion model renders the concept of mixing height useful, despite the agreed absence of precision in its definition.

The session on temperature inversions and air quality episodes

R. Sokhi presented the analysis and evaluation of air pollution episodes in several European cities. Examples of episodes of PM_{10}, NO_2 and O_3 were presented and the causes were examined in relation to local emissions and meteorological conditions. For both particulate matter and nitrogen oxides, low lying inversion and local low wind speeds are particularly important in that they tend to lead to high concentration of air pollutants. In case of PM_{10} episodes, resuspended particulate matter from street surfaces can also be important, especially in Northern and Central European cities.

E. Berge presented results from NWP modeling in Northern Europe during strong wintertime inversions, and discussed how realistic these simulations are. Air quality problems in Northern Europe are often linked to episodes of strong inversions, and high levels of air pollutants such as NO_2 and particulate matter ($PM_{2.5}$ or PM_{10}) often occur during such events. He utilised numerical results produced by two NWP models (HIRLAM and ECMWF), combined with the utilisation of the non-hydrostatic MM5 model. The numerical runs for Oslo using 10, 3 and 1 km nesting revealed the necessity of high resolution for resolving topographical features. He also simulated an episode in Helsinki that involved an extremely strong ground-based temperature inversion, and compared the predicted results with those measured at a radio tower of Kivenlahti.

A. Karppinen evaluated the meteorological data measured at a radio tower of 327 m height, called the Kivenlahti mast, situated in the Helsinki Metropolitan Area. The archived data contains wind speed and direction, ambient temperature and relative humidity values, since 1989. However, the data extracted from such measurements needs to be carefully evaluated in order to find out possible disturbances caused by the presence of the tower itself. The data has been utilised in evaluating the temporal evolution of temperature inversions in the course of episodes. As an example, the temperature profiles measured at the mast during 27-28 December 1995 showed a maximum vertical inversion of approximately 15˚C over the lowest 30 m of the atmosphere.

S. Finardi analysed three different episodes that occurred in cities of Northern Italy. These episodes were analysed based on synoptic meteorological information, local vertical profiles from soundings, and meteorological and chemical measurements performed at an air quality network. He showed that Milan is a city where topography plays an important role in winter inversions. Whilst high pressure may build the inversion, local processes determine the local wind field near the ground. The lower circulation may be decoupled from the synoptic scale, being driven by local and mesoscale effects.

Acknowlewgements

We wish to thank the former secretary of the COST 715 action, Mr. Zoltan Dunkel for taking care of supporting the expenses of the invited non-COST experts. Special thanks are due to the local organiser Meteo France, for providing good facilities in the city of Toulouse. We also wish to thank Douglas R. Middleton (UK Meteorological Office) for allowing us to utilise his previously written nice overview of this expert meeting. Finally, we express our thanks to all the speakers for their contributions and to the members of the working groups for helping us to organise this successful meeting.

The mixing height in urban areas - a review

Alexander Baklanov∗

∗ Danish Meteorological Institute (DMI), Lyngbyvej 100, DK-2100 Copenhagen, DENMARK,
e-mail: alb@dmi.dk

Abstract
The urban boundary layer (UBL), in comparison with 'rural' homogeneous PBLs, is characterised by greatly enhanced mixing, resulting from both the large surface roughness and increased surface heating, and by horizontal inhomogeneity of the mixing height (MH) and other meteorological fields due to variations in surface roughness and heating from rural to central city areas. So, it is reasonable to consider the UBL as a specific case of the atmospheric boundary layer over a non-homogeneous terrain. Most of the parameterisations of MH were developed for the conditions of a homogeneous terrain, so their applicability for urban conditions should be verified. Just a few authors suggested specific methods for MH determination in urban areas. Some authors tested the applicability of MH methods for specific urban sites, but a comprehensive analysis of the applicability does not exist yet. Proceeding from analysis of different methods of the MH estimation for urban areas, the following preliminary suggestions are discussed. For the estimation of the daytime MH, the applicability of common methods is more acceptable than for the nocturnal MH. For the convective UBL the simple slab models were found to perform quite well. The formation of the nocturnal UBL occurs in a counteraction with the negative 'non-urban' surface heat fluxes and positive anthropogenic/urban heat fluxes, so the applicability of the common methods for the SBL estimation is less promising. Applicability of some newly developed methods for the SBL height estimation, including diagnostic and prognostic equations and an improved Ri-method are also discussed.

Keywords:
Urban boundary layer, atmospheric stratification, urban canopy, internal boundary layer, dispersion models.

1. Introduction

Most of the urban atmospheric pollution models request the height of the mixing layer (MH) as input information. Despite the progress in numerical turbulent modelling during the last decades, this parameter is still one of the most important ones for correctly forecasting the air quality.

However, the mixing height (MH) is not observed by standard measurements, so in dispersion models it can be parameterised or obtained from profile measurements or simulations. The COST-Action 710 (Fisher *et al*., 1998) has reviewed different definitions and the practical determination of MH from measurements, by modelling and parameterisation and from output from NWP models. Moreover, it identified and tested pre-processors and computer routines to derive the mixing height and intercompared methods by using several non-urban data sets.

During the last decades many experimental studies of the mixing layer were realised for urban areas. This made it possible to analyse the peculiarities of the urban MH (UMH) and verify (or improve) different methods of the MH estimation versus measurement data sets from several types of urban areas.

So, the follow-up COST-Action 715 develops the scientific work achieved under COST-710 from rural to urban conditions. In particular, the Working Group 2 focuses on the specific problems in describing the surface energy balance and the mixing height in urban areas (Piringer, 2000; Piringer *et al.*, 2001). Within the WMO Global Atmosphere Watch programme the Urban Research Meteorology and Environment (GURME) project was also initiated in 1999 (Soudine, 2001).

2. Specificity and features of the urban boundary layer

The urban boundary layer (UBL), in comparison with 'rural' homogeneous PBLs, is characterised by greatly enhanced mixing, resulting from both the large surface roughness and increased surface heating, and by horizontal inhomogeneity of the MH and other meteorological fields due to variations in surface roughness and heating from rural to central city areas. So, it is reasonable to consider the UBL as a specific case of the PBL over a non-homogeneous terrain. This relates, first of all, to drastic changes of the surface roughness and urban surface heat fluxes. The scheme of vertical structure of the urban boundary layer can be simplified in the form presented in Figure 1.

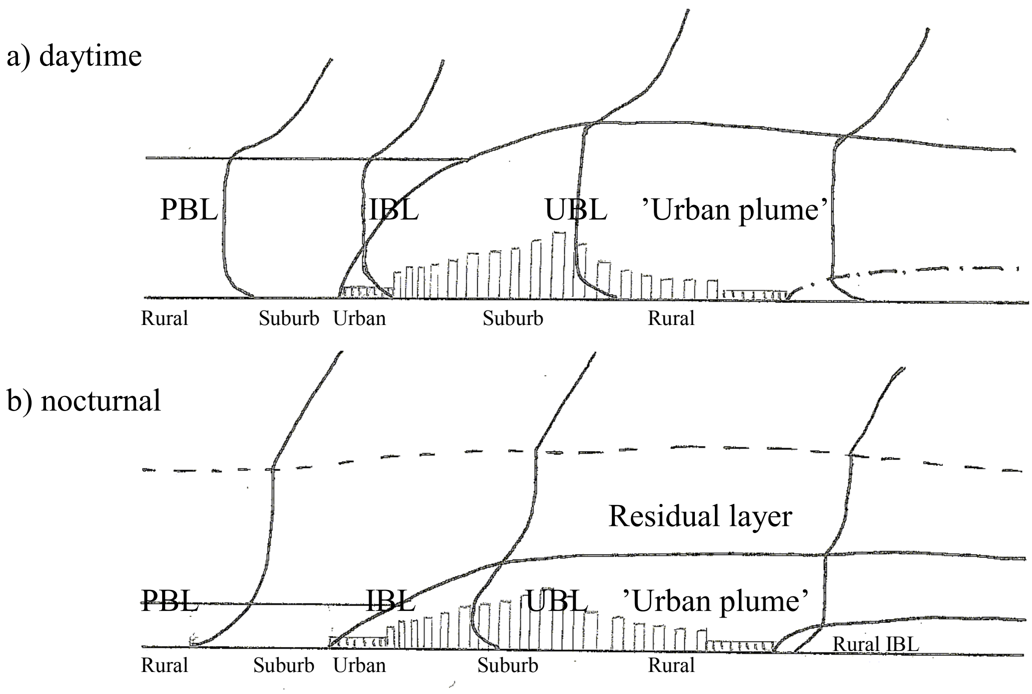

Figure 1: The simplified scheme of vertical structure of the urban boundary layer and typical potential temperature profiles: a) daytime UBL, b) nocturnal UBL.

As a result of the urban area features there are several aspects for analysing the urban MH, including:

(i) internal urban boundary layer (IBL),
(ii) elevated nocturnal inversion layer,
(iii) strong horizontal inhomogeneity and temporal non-stationarity,
(iv) so-called 'urban roughness island', zero-level of urban canopy, and $z_{0u} \neq z_{0T}$,
(v) anthropogenic heat fluxes from street to city scale,

(vi) downwind ‘urban plume’ and scale of urban effects in space and time,
(vii) calm weather situation simulation,
(viii) non-local character of urban MH formation,
(ix) effect of the water vapour fluxes.

3. Experimental studies of Urban Mixing Height

During the last decades many experimental studies of the mixing layer in urban areas were realised (see Table 1). In Northern America comprehensive studies of the urban boundary layer were done for the Lower Fraser Valley: Vancouver (Stein *et al*., 1997, Batcharova *et al*., 1999), Sacramento urban area, California (Cleugh and Grimmon, 2001), Mexico City (Cooper and Eichinger, 1994), St. Louis metropolitan area (Seaman, 1989; Westcott, 1989, Godovich *et al*, 1987). In Asia urban field experiments were carried out for Beijing and Shenyang cities in China (Zhang *et al*., 1991; Sang and Lui, 1990), for the city of Delhi (Kumari, 1985) and Japanese cities (e.g. Chen *et al*., 2001). For European cities experimental studies of the urban boundary layer and pollution episodes have already been performed for Basel (Rotach et al. 2001), Marseille (Said *et al*. 2001), Paris (Dupont *et al*., 1999), Vienna (Piringer *et al*., 1998) and Graz, Austria (Piringer and Baumann, 1999), Helsinki (Railo, 1997; Karppinen *et al*., 1998), the valley of Athens (Melas & Kambezidis, 1992; Frank 1997; Kambezidis *et al*., 1995), Copenhagen (Batcharova & Gryning 1989), Milan (Lena & Desiato, 1999), Sofia (Donev *et al*., 1995; Kolev *et al*., 2000), Moscow (Lokoshchenko *et al*., 1993).

This makes it possible to analyse the effects of the urban peculiarities and to verify different methods of the MH estimation versus measurement data sets from several types of urban areas.

Proceeding from the urban area features discussed above, there are the following important questions to answer for analysing the urban MH based on the experimental data:

1. How much does the MH in urban areas differ from the rural MH ?
2. How does the temporal dynamics of MH in urban areas differ from the rural MH ?
3. What is the scale of urban effects in space and time and for how long distance does the downwind ‘urban plume’ effect the MH ?
4. How important is the internal urban boundary layer in forming the MH?

Several experimental studies analysed the difference of MH in urban and rural sites for different geographical regions. There are several geographically different types of cities (e.g., on a flat terrain or in mountain valleys, coastal area cities, northern or southern cities), peculiarities of each type can affect the forming the urban boundary layer as well. For example, the stably stratified nocturnal boundary layer is not common for USA cities (Bornstein, 2001), it could be an elevated nocturnal inversion layer only. However, for European cities, especially in Northern Europe, the nocturnal SBL is very common (e.g., in Helsinki: see Railo, 1997). The mean profiles of the temperature at 00 and 12 UTC for the radiosonde station Jægersborg in Copenhagen (Rasmussen *et al*., 1999), presented in Figure 2, show clearly the stably stratified nocturnal BL.

Table 1: Experimental studies of the mixing layer in urban areas.

Experiment name and city	Publications
ESCOMPTE experiment in the Marseille area	*(Said et al, 2001)*
'Basel UrBan Boundary Layer Experiment' (*BUBBLE*)	*(Rotach et al., 2001)*
The *KONGEX* experiment in the Vienna area, Austria	*(Piringer et al., 1998)*
The Vienna Summer Aerosol Study (*VISAS*) during July and Aug. 1987	*(Piringer, 1988)*
The *ECLAP* experiment: the atmospheric boundary layer in Paris and its rural suburbs	*(Dupont, 1999)*
An environmental experiment over Athens urban area under sea breeze conditions	*(Kambezidis et al., 1995)*
The valley of Athens: the *MEDCAPHOT-TRACE* experiment, September 1994	*(Frank 1997; Batcharova & Gryning 1986)*
ATHens Internal Boundary Layer Experiment (*ATHIBLEX*) in summer 1989 and 1990	*(Melas & Kambezidis, 1992)*
Copenhagen: The internal boundary layer study	*(Batcharova & Gryning 1989; Rasmussen et al, 1997)*
The Milan urban area: Study of nocturnal mixing height during spring and summer 1996	*(Lena & Desiano 1999)*
Acoustic sounding of the urban boundary layer over Berlin-Adlershof in summer	*(Evers, 1987)*
The BL experiment, autumn 1991 over a flat, built-up urban area in Southeast Sofia	*(Donev et al., 1995, Donev et al., 1993)*
Lidar observation of the nocturnal boundary layer formation over Sofia, Bulgaria	*(Kolev et al., 2000)*
Studies of the atmospheric boundary layer over Moscow by remote sensing and in situ methods	*(Lokoshchenko et al., 1993)*
Sacramento urban area, California: boundary layer study	*(Cleugh and Grimmon, 2001)*
Lower Fraser Valley: Vancouver, in summer 1993: IBL over a coast region	*(Pottier et al, 1994, Stein et al., 1997, Batcharova et al., 1999)*
Study of the boundary layer over Mexico City	*(Cooper et al., 1994)*
METROMEX (Metropolitan Meteorological Experiment) and *RAPS* (Regional Air Pollution Study), St. Louis, MO, July 1975	*(Seaman, 1989; Westcott, 1989, Hildebrand & Ackerman, 1984)*
St. Louis metropolitan area: Observations of temperature profiles by a helicopter (35 morning experiments)	*(Godovich et al, 1987; Godovich 1986)*
Beijing, China: Study of wind and temperature profiles and sensible heat flux in July and December of 1986	*(Zhang & Sun, 1991)*
Shenyang City, Liaoning Province, China: the field experiments carried out in December 1984	*(Sang & Lui, 1990)*
One-year observation of urban mixed layer characteristics at Tsukuba, Tokio using a micro pulse lidar	*(Chen et al., 2001)*
The city of Delhi, 5 years of data: the mean diurnal variation of the mixing height in different months	*(Kumari, 1985)*

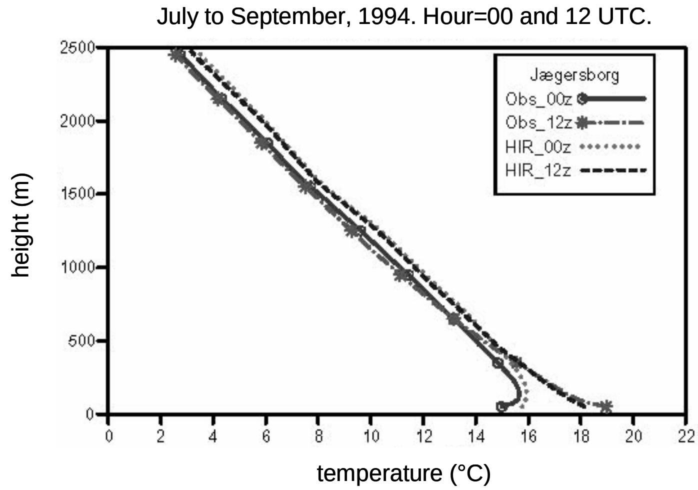

Figure 2: The mean measured and modelled profiles of the temperature at 00 and 12 UTC for the radiosonde station Jægersborg in the metropolitan Copenhagen area (Rasmussen et al.,

The ECLAP experiment (Dupont *et al*., 1999) has been performed during winter 1995 in order to study the influence of the urban area of Paris on the vertical structure and diurnal evolution of the atmospheric boundary layer. One urban site and one rural site have been instrumented with Sodars, Lidars and surface measurements. The sensible heat flux in Paris was generally found larger than in the rural suburbs (difference range from 25-65 W m^{-2}, corresponding to relative differences of 20-60%). The differences of unstable MH between both sites were less than 100 m most of the time. However, sodar and temperature data showed that the urban influence was enhanced during night-time and transitions between stable and unstable regimes.

Godowitch *et al*. (1987) analysed the spatial variation of the nocturnal urban boundary layer structure and the time variation of the MH (base of the inversion) in St. Louis. The nocturnal inversion top and strength after sunrise are presented for urban sites located upwind, downwind, and near the centre of the heat island, and at an upwind rural site. The nocturnal urban MH increased from the upwind edge of the urban area. Far downwind, in suburban and rural areas, a remnant of the urban boundary layer existed between a stable surface-based layer and an upper inversion that resembled the upwind rural inversion. The MH evolved in a parabolic manner after sunrise at the urban locations. Because of large horizontal temperature gradients associated with the urban heat island, cold air advection tended to counteract the urban-induced lifting effect by inhibiting mixing-height growth at urban locations upwind of the heat-island centre. Advection also caused the maximum height and fastest growth rate of the urban mixed layer to be shifted downwind of the urban area with time. However, mean MH growth rates at various urban locations did not differ significantly. The rural MH growth rate was about twice as large as urban values for as long as 3 hr after sunrise. Spatial differences in the MH became small near the time of inversion dissipation, which appeared to occur at about the same time at all locations.

In the previous St. Louis study (Godowitch *et al*., 1985), the evolutionary cycle of the nocturnal radiation inversion layer, from formation through the time of erosion under fair weather summer conditions, was investigated. This was done by time-series analyses of observations of inversion base and top heights and inversion strength at an urban and a nonurban site. A surface-based inversion, generally formed before sunset at the nonurban site, and the growth of the inversion top height have been described well by $(2K_T\ t)^{1/2}$, where K_T is the thermal eddy coefficient. The average time of formation of an elevated inversion layer at the urban site was 2.5 hr after sunset. The height of the nocturnal UBL decreased after formation under steady wind conditions. The urban MH was consistently higher during the morning than at the nonurban site, although the difference diminished with time since the nonurban MH growth rate was greater. The slower growth rate of the urban MH was attributed primarily to advection of relatively cold air and lower MHs from the upwind nonurban environment. An overall rise of the inversion top height after sunrise was believed to be due to urban-induced upward motions, caused by low-level convergence that produced increasing MH growth rates. The average time for the inversion layer to erode completely was 4 hr after sunrise at both sites.

Kambezidis *et al*. (1995) presented results from ATHens Internal Boundary Layer EXperiment (ATHIBLEX). This experiment was performed during June 1989 and June-July 1990. The aim of ATHIBLEX was to study the IBL formation over Athens urban area under sea breeze conditions and its association with the city environmental problems. The results showed a well established IBL over Athens basin. The orographic effect of Athens basin on the wind profiles was also demonstrated. u'-, v'- and w'-power spectral densities from a uvw propeller anemometer installed 4500 m downwind of the shoreline on the top of a hill 107 m a.m.s.l. exhibited the -5/3 law.

WG2 COST 715 (Piringer *et al*., 2001), on the basis of the above mentioned related experimental information, plans to review and assess pre-processors, schemes and models for determining the mixing height in urban areas. Unfortunately, many of the data sets mentioned above are not complete for a careful verification of the methods for the MH estimation. The group plans to use the following most suitable European urban data sets, as from the cities Paris, Basle, Milan, Marseille and Graz, to test and validate different parameterisations, pre-processors and models.

4. Methods for the urban MH estimation

Many parameterisations of the MH were developed for the conditions of a homogeneous terrain, so their applicability for urban conditions should be verified. Some authors suggested specific methods for MH determination in urban areas. They can be distinguished in two main categories: (i) with a local correction of the heat fluxes due to urban effects, and (ii) with estimations of the internal boundary layer (IBL) height growth. The first category usually uses the common methods for the homogeneous terrain with the urban heat fluxes and roughness. The second category based on the general methods for the IBL height estimation for areas with abrupt/drastic change of the surface roughness.

4.1. Estimation of the MH or eddy profile from meteorological models

One of the promising methods to estimate the MH or the eddy profile for dispersion models is using output from numerical meso-meteorological or weather prediction (NWP) models. Several possible ways are used in different publications.

First of all, it is possible to avoid the usage of the MH for dispersion models, which can directly use the eddy diffusivity profiles. Many advanced atmospheric dynamics and pollution models already follow this way (e.g., Baklanov, 2000a; Zhang *et al*., 2001; Kurbatskii, 2001). However, many models, especially regulatory models, are not coupled with meteorological models. They are based on *in situ* measurements of meteorological characteristics and need the MH as an input parameter.

Some meteorological models calculate the planetary boundary layer (PBL) height and then use it as the height of the simulation area. Such models were suggested by Penenko and Aloyan (1974, 1985). A simple version of this method was also realised by Arya & Byun (1987) and Byun & Arya (1990) for a 2-D numerical model of the urban BL. Such a method can be very useful for next-generation models, especially if meteorological models include the urban effects. However, such models are much more expensive in computation time.

During the last years, output data from 3-D NWP models were increasingly used for MH estimation based on different approaches, e.g.: turbulent kinetic energy models, k-ε models, subgrid scale turbulent closure models (incl. LES mode), second momentum turbulent closure models. The MH can be estimated from vertical profile of meteorological fields, e.g. based on:

- turbulent kinetic energy or eddy decay/depletion,
- Richardson-number method,
- different parameterisations and simple models.

Direct calculations of the MH from simulated turbulent kinetic energy or eddy profiles (so-called turbulent kinetic energy or eddy decay method) for the daytime urban boundary layers showed good and promising results (see e.g., Batchwarova *et al*., 1999). However, this way is very sensitive to the turbulent closure scheme, so it can be quite dangerous for practical use. E.g., Zhang *et al*. (2001) showed that local closure schemes gave considerable errors for the daytime MH as well. In spite of promising results for the CBL height, use of this method for the nocturnal MH (stably stratified BL) can give considerable problems and large uncertainties for the MH estimation, e.g. from TKE equations with a local closure. For example, a new version of the DMI-HIRLAM model (Saas *et al*., 2000; Nielsen and Saas, 2000) with the CBR turbulence scheme (Cuxard *et al*., 2000) tested a direct calculation of the PBL height from the turbulent energy profile by the TKE depletion approach. However, it was shown (Baklanov, 2000b) that this method gives a considerable underestimation of the height of the nocturnal PBL.

4.2. Applicability of common MH parameterisations and pre-processors for urban conditions

The most common way used in dispersion models to get the MH values is its calculation from different parameterisations and pre-processors. This way is suitable for using *in situ* measurements or NWP profiles. There are a number of different parameterisations and integral models for the MH estimation for homogeneous terrains (see an overview in Seibert *et al*., 1998). The following pre-processors and models for MH estimation are most common in practical applications and useful for 'non-urban' areas:

- OML (Berkowicz & Prahm, 1981; Olesen *et al*., 1992);
- HPDM (Hanna & Chang, 1992);
- RODOS (Mikkelsen *et al*., 1996);
- RAMMET-X (US EPA 1990; Berman *et al*, 1997);
- MIXEMUP (Benkley & Schulman, 1979);
- CALMET (Scire *et al*, 1995);
- SUBMESO (Anquetin *et al*., 1999).

Besides, there are several known routines for the MH calculation, e.g., UDM FMI routine (Karppinen *et al*., 1998), DMI routines (see Table 2), Sevizi Territorri Library (Seibert *et al*., 1998), etc.

Table 2: Routines for MH estimation realised and used at DMI.

Bulk Richardson number method	(Sørensen *et al*., 1997)
Corrected bulk Ri- method	(Vogelezang & Holtslag 1996)
Daytime MH growth model	(Bartchvarova & Gryning 1991)
Parcel method	(Seibert *et al*. 1998)
Turbulent kinetic energy decay method	(Nielsen and Saas, 2000)
Multi-limit SBL height formulation	(Zilitinkevich & Mironov 1996)
New diagnostic SBL height formulation	(Zilitinkevich *et al*. 2001)
Modified bulk Ri-method	(Zilitinkevich & Baklanov 2001)
Prognostic formulations for SBL height	(Zilitinkevich *et al*. 2001)
Library of ten common methods	(Baklanov 2001; Lena & Desiato 2000)

For MH estimation in urban areas most authors use common ‘rural’ methods (see, e.g., Schatzmann *et al*., 2001). Some authors tested the applicability of such methods for specific urban sites (e.g., Berman *et al*., 1997; Lena & Desiato, 1999), but a comprehensive analysis of the applicability does not exist yet.

In Berman et al. (1997) mixing heights derived from three algorithms, RAMMET-X, MIXEMUP, and CALMET, were compared with estimates derived from a 915-MHZ radar profiler and Radio Acoustic Sounding System (RASS) located at the urban site of Schenectady, NY. For the nine test days studied, mixing heights ranged from 1.6 km in midafternoon to 150-250 m at night, based on the refractive index structure parameter (Cn^2). The MHs obtained from CALMET and MIXEMUP were in good agreement with Cn^2 estimates throughout the day, especially in the afternoon when they agreed to within 100 m. In contrast, estimates from RAMMET-X displayed considerably less diurnal variation, with afternoon MHs 300-400 m lower than profiler estimates, and night-time values similarly too high. A separate "analytical method" based on an analysis of the profiler system's wind and temperature profiles, was offered as an alternate way for estimating the mixing height. MHs derived from the analytical method agreed well with Cn^2 estimates at the times of the maximum and minimum, but displayed a much faster growth rate during the morning and a slightly slower decay rate in the evening. The methods were not very suitable for estimating the nocturnal MH.

Lena and Desiato (1999) compared several algorithms for the MH estimation with measured urban data and showed that all the algorithms performed quite poorly. Ten indirect algorithms for the estimation of *h* in nocturnal, stable conditions, when the mixing was dominated by mechanical turbulence, were reviewed and compared with mixing heights derived from wind (SODAR) and temperature (RASS) profiles measured in the Milan urban area during spring and summer 1996. The test of the indirect algorithms indicated that a rash application of them to urban cases could lead to very inaccurate MH estimates and, as a consequence, to large errors in the vertical diffusivity. Among the others, the CALMET prescription showed a relatively good performance, but with underestimation or overestimation in low and high wind conditions, respectively.
However, this was done only for very simple algorithms for nocturnal conditions, so the bad correspondence with the measured MH was not very surprising and, probably, not due to the urban peculiarities. In Zilitinkevich and Baklanov (2001) and Baklanov (2001) most of the above mentioned methods together with several more advanced methods for SBL height estimation were analysed for the non-urban Cabauw data set (Vogelezang & Holtslag, 1996). Figure 3 demonstrates the scatter-plot diagrams for MH calculated by 8 methods (see Table 3) versus the measured SBL height.

Table 3. Empirical evaluation of different SBL height equations versus the Cabauw data (after Zilitinkevich and Baklanov, 2001).

#	Reference	SBL height equation	Bias	RMS error	Correlation coefficient
1	Aria, 1981 (*	$h = 0.42\,u_*^2 \mid fB_s \mid^{-1/2} + 29.3$	64.0	218	0.27
2	Niewstadt, 1984	$h = 0.4\,u_*^2 \mid fB_s \mid^{-1/2}$	24.4	173	0.27
3	Arya, 1981	$h = 0.089\,u_* / \mid f \mid + 85.1$	103	86.3	0.48
4	Mahrt, 1982	$h = 0.06\,u_* / \mid f \mid$	-24.4	18	0.48
5	Benkley & Schulman, 1979	$h = 125\,u_{10}$	208	264	0.48
6	Niewstadt, 1984	$h = 28\,u_{10}^{3/2}$	6.27	13.9	0.48
7	Zilitinkevich & Mironov, 1996	$\left\| \frac{fh}{0.5u_*} \right\|^2 + \frac{h}{10L} + \frac{Nh}{20u_*} + \frac{h\|f\|^{1/2}}{(u_* L)^{1/2}} + \frac{h\|Nf\|^{1/2}}{1.7u_*} = 1$	-33.8	33.8	0.38
8	Zilitinkevich et al., 2001a	$h = \frac{0.4u_*}{\|f\|}\left[\left(1+0.3\frac{w_h}{u_*}\right) \Big/ \left(1+\frac{0.16u_*(1+0.25NL/u_*)}{0.55L\|f\|}\right)\right]^{1/2}$	6.21	19.2	0.60

* Version modified after Zilitinkevich (1972) with re-estimated constants.

One can see the simple algorithms to perform quite poorly for the non-urban data as well. As it is seen, the new formulation of Zilitinkevich et al. (2001) is best supported by measurement data compared to the other seven formulations.

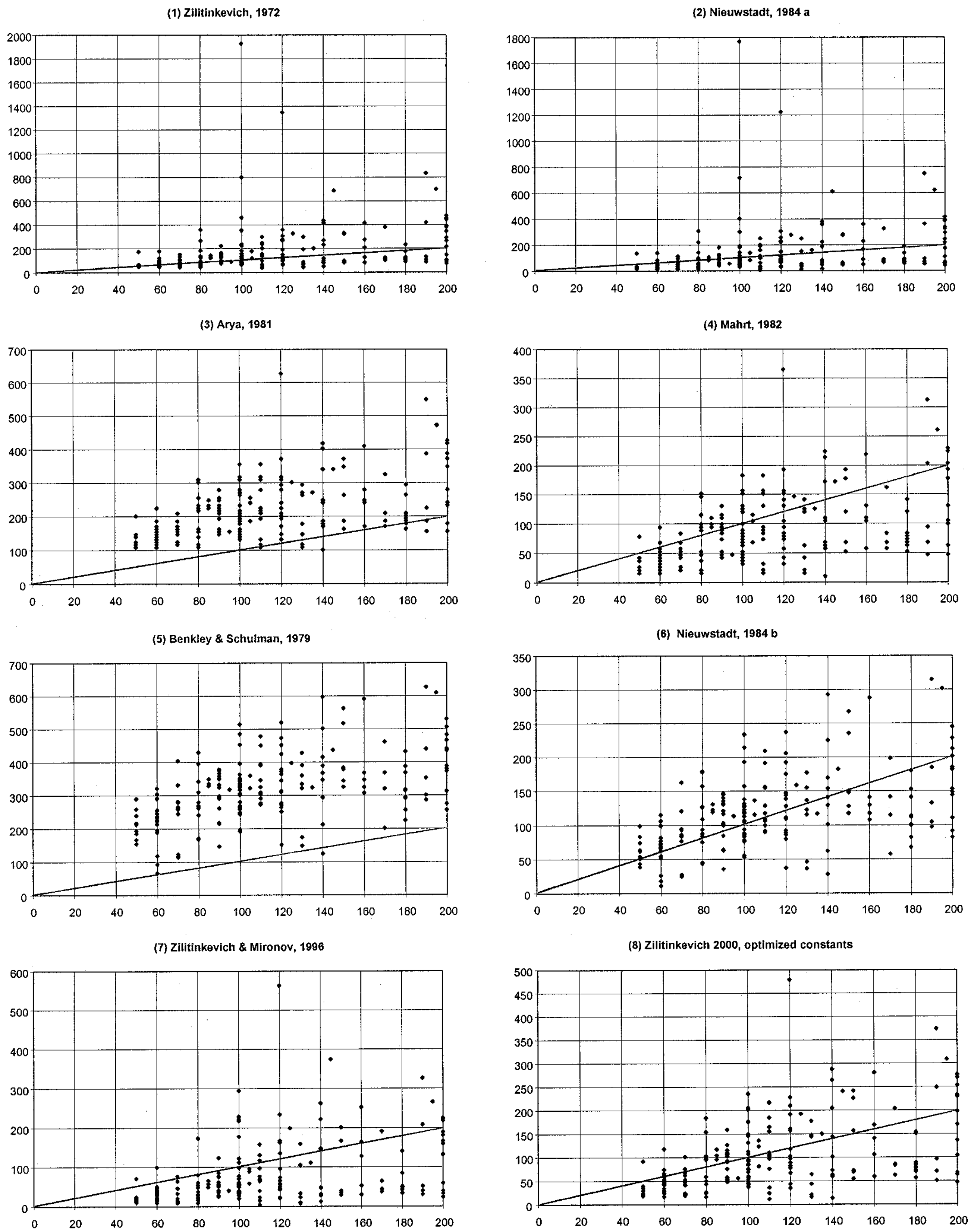

Figure 3. Simulation of SBL height by eight different parameterisations (see Table 3) for the Cabauw data: the vertical axis - the simulated SBL heights, h (in meters), the horizontal axis - the measured SBL height, h_{SBL} (in meters).

Another interesting method to be tested for urban conditions was suggested by Joffre *et al*. (2001). They investigated the variability of the stable and unstable boundary layer height applying different characteristic length scales and combinations of them (JKHK method). They found that, under stable conditions, a great deal of the variability of the mixing height is explained with the scales $L_N = u_*/N$ and L. For unstable conditions with buoyant and mechanical turbulence production, the MH is best determined with an expression based on a dimensionless form of the turbulence kinetic energy equation (Kitaigorodskii & Joffre, 1988) with the mixing height scaled by L and depending on the stability parameter $\mu_N = L_N/L$ and on N/f.

Another method, commonly proposed in scientific publications for the MH estimation, is based on the **Richardson number approach**. It differs in formulation, choice of the levels over which the gradients are determined and in value of the critical Richardson number, Ri_c, and it can underestimate the SBL height (Seibert et al., 1998; Baklanov, 2001). Following Zilitinkevich & Baklanov (2001), we can distinguish four different Ri methods.

1. Gradient Richardson number. Infinitesimal disturbances in a steady-state homogeneous stably stratified sheared flow decay if the gradient Richardson number Ri exceeds a critical value Ri_c,

$$\mathrm{Ri} \equiv \frac{\beta(\partial\theta_v / \partial z)}{(\partial u / \partial z)^2 + (\partial v / \partial z)^2} > \mathrm{Ri}_c = 0.25\,. \tag{1}$$

Accordingly, the turbulent boundary layer height, h_E, is deduced from inequalities $\mathrm{Ri} < \mathrm{Ri}_c$ at $z < h_E$ and $\mathrm{Ri} > \mathrm{Ri}_c$ at $z > h_E$.

2. Bulk Richardson number. An alternative, widely used method of estimating h employs, instead of the gradient Richardson number Ri, the boundary-layer bulk Richardson number, Ri_B, specified as

$$\mathrm{Ri}_B \equiv \frac{\beta\Delta\theta_v h}{U^2} \qquad => \qquad h_E = \frac{\mathrm{Ri}_{Bc} U^2}{\beta\Delta\theta_v} \tag{2}$$

through the wind velocity at the upper boundary of the layer, $U = \sqrt{u^2(h) + v^2(h)}$, and the virtual potential temperature increment across the layer, $\Delta\theta_v = \theta_v(h) - \theta_v(0)$.

3. Finite-difference Richardson number. The idea is to exclude the lower portion of the SBL and to determine a "finite-difference Richardson number", Ri_F, on the basis of increments $\delta\theta_v = \theta_v(h) - \theta_v(z_1)$ and $\delta U = \sqrt{u^2(z) + v^2(z)}\Big|_{z=z_2}^{z=h}$ over the height intervals $z_1 < z < h$ and $z_2 < z < h$. Assuming the existence of its standard critical value, Ri_{Fc}, the equilibrium SBL height formulation becomes

$$h_E \approx \frac{(h_E - z_2)^2}{h_E - z_1} = \frac{\mathrm{Ri}_{Fc}(\delta U)^2}{\beta \delta \theta_v}. \tag{3}$$

4. Modified Richardson number method. Analysis of different estimations of Ri_{bc} for calculation of h shows a broad variation of Ri_{bc} values from 0.11 to 3.0 (see Table 2 in Zilitinkevich & Baklanov, 2001). They showed that the SBL critical bulk Richardson number, Ri_{Bc}, is not a constant and evidently increases with increasing free flow stability and very probably depends on the surface roughness length, the Coriolis parameter and the geostrophic wind shear in baroclinic flows. The Richardson-number-based calculation techniques can be recommended only for rough estimates of the SBL height. For practical use Zilitinkevich and Baklanov (2001) recommended:

$$\mathrm{Ri}_{Bc} \approx 0.1371 + 0.0024 \frac{N}{|f|}. \tag{4}$$

For more accurate SBL height calculations within 1-D and 3-D models, respectively, the diagnostic and prognostic formulations (Zilitinkevich *et al.*, 2001) are recommended. It is necessary to mention that diagnostic methods for estimation of the urban MH are not good enough due to the strong horizontal inhomogeneity and temporal non-stationarity of the UBL and non-local character of urban MH formation. So, it is suggested within 3-D models to calculate the SBL height, h, more accurately on the basis of the prognostic formulation and accounting for the horizontal transport through the advection term and the sub-grid scale horizontal motions through the horizontal diffusivity K_h (Zilitinkevich & Baklanov, 2001):

$$\frac{\partial h}{\partial t} + \mathbf{V} \cdot \nabla h = -C_E \, |f| \, (h - h_{CQE}) + K_h \nabla^2 h, \tag{5}$$

where $\mathbf{V} = (u, v)$ is the horizontal velocity vector, C_E is a constant ($C_E \approx 1$), h_{CQE} is the equilibrium MH, calculated from a diagnostic formulation (e.g., Zilitinkevich *et al.*, 2001).

5. Specific methods for the urban or other IBL height estimation

Just a few authors suggested specific methods for MH determination in urban areas. As it was mentioned above they can be distinguished in two categories: (i) with correction of heat fluxes, and (ii) with estimation of IBL height growth. The first category is not very interesting for the analysis because it uses the above-discussed methods with corrected values of the urban heat flux and roughness. Let's consider the second category.

It should be considered in the bounds of general methods to estimate the growing height of the internal boundary layers with sudden changes of the surface roughness (smooth-to-rough or rough-to-smooth). Such approaches of the IBL or the blending height were actively developed for estimation of the IBL in coastal areas (see e.g., Panovsky & Dutton, 1984; Walmsley, 1989; Garratt, 1990; Wringht *et al.*, 1999). Such an approach can be used for the estimation of the height of the internal urban boundary layer, so-called downwind 'urban plume' and the rural IBL (see Figure 1).

E.g., Henderson-Sellers (1980) developed a simple model for the urban MH as a function of distance downwind into the city. Nkemdirim (1986) tested and further improved the Summers (1964) formulation for the UMH:

$$h_\alpha = \left[\frac{2Hx_k}{\rho c_p \alpha u_0} \right]^{1/2}, \tag{6}$$

where H is the cumulative heat flux between x_0 and x_k; x_k is the downwind distance. The formulation was verified for cities of New York and Calgary. It was shown that it could be used for a rough UMH estimation, but only for wind velocities $u < 4$ m/s.

Melas and Kambezidis (1992) studied the height of the thermal internal boundary layer over an urban area under sea-breeze conditions and compared it with the data of the ATHens Internal Boundary Layer Experiment (ATHIBLEX) in summer 1989 and 1990. For the IBL height estimation they analysed three slab methods: (i) - Gamo et al. (1983), (ii) – Venkatram (1986), (iii) - Gryning and Batchvarova (1990); one simple empirical diagnostic method as a function of the distance to city in wind direction, and one similarity model (Miyake, 1965). It was found that the similarity model of Miyake (1965) failed to give any reasonable prediction, indicating that models should not be extended beyond their stability and fetch range. Relations based on the slab models showed a high correlation with observations, but the observed thermal IBL heights were unpredicted unless both convective and mechanical turbulence were taken into account. The formulation proposed by Gryning and Batchvarova (1990) was found to be in good agreement with the measurements. In the bounds of the local equilibrium concept the thermal IBL height was suggested to grow as x^p where p depends upon several parameters of the IBL.

In Gryning and Batchvarova (1996) the above mentioned slab model on a zero-order scheme was extended for the internal boundary layer over terrain with abrupt changes of surface for near neutral and unstable atmospheric conditions. The equation for the height h of the internal boundary layer (Gryning and Batchvarova, 1996) is:

$$\left\{ \frac{h^2}{(1+2A)h - 2B\kappa L} + \frac{Cu_*^2 T}{\gamma g[(1+A)h - B\kappa L]} \right\} \left(\frac{\partial h}{\partial t} + u\frac{\partial h}{\partial x} + v\frac{\partial h}{\partial y} - w_s \right) = \frac{\left(\overline{w'\theta'}\right)_s}{\gamma}, \tag{7}$$

where u and v are the horizontal components of the mean wind speed in the internal boundary layer in the x and y directions, t is time, u_* is the friction velocity, $\left(\overline{w'\theta'}\right)_S$ - the kinematic heat flux, γ - the potential temperature gradient, w_s - the mean vertical air motion above the boundary layer, L the Monin-Obukhov scaling length, κ is the von Karman constant, and A, B and C empirical dimensionless constants. The model includes coastline curvature and spatially varying winds and was solved numerically for the height of the internal boundary layer. In the following

papers (Batchvarova & Gryning, 1998; Batchvarova *et al*., 1999; Gryning & Batchvarova, 2001) the authors applied this model for urban areas with a coastline and showed its good applicability.
E.g., Batchvarova *et al*. (1999) tested the ability of two quite different models to simulate the combined spatial and temporal variability of the internal boundary layer in an area of complex terrain and coastline during one day. The simple applied slab model of Gryning and Batchvarova (1996), and the Colorado State University Regional Atmospheric Modelling System (CSU-RAMS) were tested by comparison with data gathered during a field study (called Pacific '93) of photochemical pollution in the Lower Fraser Valley of British Columbia, Canada. The data utilised there were drawn from tethered balloon flights, free flying balloon ascents, and downlooking lidar operated from an aircraft flown at roughly 3500 m above sea level. Both models were found to represent the temporal and spatial development of the internal boundary-layer height over the Lower Fraser Valley very well, and reproduced many of the finer details revealed by the measurements.

Cleugh and Grimmond (2001) also assessed the validity of the simple slab model of the CBL - this was integrated forward in time using local-scale measured heat and water vapour fluxes, to predict the MH, temperature and humidity - for the Sacramento urban region, California. The prediction of the height of well-mixed CBLs using the slab model agreed fairly closely to the measured values. Of the four different CBL growth schemes used, the Tennekes and Driedonks (1981) model was found to give the best performance.

Proceeding from the above overview of different methods of the MH estimation for urban areas, we can conclude that for the convective and neutral daytime UBL the simple slab models (e.g. Gryning and Batchvarova, 2001) perform quite well. However, for the nocturnal UBL with stable and complex stratification most of the common methods perform not well enough. The urban SBL apparently needs a new theory for a better understanding of the SBL processes. One of such modern attempts is the parameterisation of Zilitinkevich *et al*. (2001), based on the newly developed non-local turbulence transport theory. Such methods need further adjustments for urban conditions and verifications versus urban data.

6. Concluding remarks

The urban boundary layer, in comparison with ‘rural’ homogeneous PBLs, is characterised by greatly enhanced mixing, resulting from both the large surface roughness and increased surface heating, and by horizontal inhomogeneity of the MH and other meteorological fields due to variations in surface roughness and heating from rural to central city areas. So, it is reasonable to consider the UBL as a specific case of the PBL over a non-homogeneous terrain. This related, first of all, to abrupt changes of the surface roughness and the urban surface heat fluxes. Specific methods for MH determination in urban areas can be distinguished in two categories: (i) with a local correction of the heat fluxes due to urban effects, and (ii) with estimations of the internal boundary layer (IBL) height growth.
General suggestions concerning the applicability of ‘rural’ methods of the MH estimation for urban areas:

- For estimation of the daytime MH, applicability of common methods is more acceptable than for the nocturnal MH.
- For the convective UBL the simple *slab models* (e.g. Gryning and Batchvarova, 2001) were found to perform quite well.
- The formation of the nocturnal UBL occurs in a counteraction with the negative 'non-urban' surface heat fluxes and positive anthropogenic/urban heat fluxes, so the applicability of the common methods for the SBL estimation is less promising.
- The determination of the SBL height needs further developments and verifications versus urban data. As a variant of the methodics for SBL MH estimation the new Zilitinkevich *et al*. (2001) parameterisation can be suggested in combination with a prognostic equation for the horizontal advection and diffusion terms (Zilitinkevich and Baklanov, 2001).
- Meso-meteorological and NWP models with modern high-order non-local turbulence closures give promising results (especially for the CBL), however currently the urban effects in such models are not included or included with great simplifications (Baklanov *et al.*, 2001).

Therefore, it is very important to test different MH schemes not specifically designed for the urban environment against urban MH or IBL schemes for different data sets (for nocturnal conditions first of all) from different urban sites to gain insight in the possible improvements. It would also be of use to know which of the parameterisations are most sensitive to changes of which environmental variables.

Reference

Anquetin, S., Chollet, J. P., Coppalle, A., Mestayer, P., and Sini, J. F. (1999). *The Urban Atmosphere Model SUBMESO*, Proc. EUROTRAC Symp. '98, P.M. Borrel & P. Borrel eds., WIT Press.

Arya, S. P. S., (1981). *Parameterizing the height of the stable atmospheric boundary layer*, J. Appl. Meteorol. **20**, 1192-1202.

Arya, S. P. S. and Byun, D. W., (1987) *Rate equations for the planetary boundary-layer depth (urban vs rural).* IN: Modeling the urban boundary-layer. American Meteorological Society, Boston, pp. 215-251.

Baklanov, A., (2000a) *Application of CFD methods for modelling in air pollution problems: possibilities and gaps*, Environmental Monitoring and Assessment, **65**: 181-190.

Baklanov, A. (2000b) *Possible improvements in the DMI-HIRLAM for parameterisations of long-lived stably stratified boundary layer*. DMI Internal Report, No. 00-15, 15 p.

Baklanov, A., (2001a). *NWP modelling for urban air pollution forecasting: possibilities and shortcomings*. DMI Technical Report, No. 01-12, 19 p

Baklanov, A. (2001b) *Parameterisation of SBL height in atmospheric pollution models*. NATO/CCMS International Technical Meeting on Air Pollution Modelling and its Application. ITM-2001, 15-19 October 2001, Louvain-la-Neuve, Belgium, pp. 303-310.

Baklanov, A., A. Rasmussen, B. Fay, E. Berge and S. Finardi, (2001). *Potential and Shortcomings of NWP Models in Providing Meteorological Data for UAP Forecasting*. Ext. abstract to the Third Urban Air Quality Conference, Loutraki, Greece. CD-ROM, paper PL.4.1.

Batchvarova, E. and Gryning, S.-E., (1991). *Applied model for the growth of the daytime mixed layer*. Boundary-Layer Meteorology, **56**(3): 261-274.

Batchvarova, E. and Gryning, S.-E., (1998). *Wind Climatology, Atmospheric Turbulence and Internal Boundary-Layer Development in Athens During the MEDCAPHOT-Trace Experiment*, Atmos. Environ. **32**, 2055-2069.

Batchvarova, E., Cai, X., Gryning, S.-E., Steyn, D., (1999). *Modelling internal boundary-layer development in a region with a complex coastline*. Boundary-Layer Meteorology, **90**: 1-20.

Benkley, C.W. and Schulman, L.L., (1979). *Estimating mixing depths from historical meteorological data*, Journal of Applied Meteorology, **18**, 772-780.

Berkowicz, R. and Prahm, L.P. (1982). *Sensible heat flux estimated from routine meteorological data by the resistance methode*. J. Appl. Meteorol., **21**, 1845-1864.

Berman, S., Ku, J.-Y., Zhang, J. & Rao, S. T. (1997). *Uncertainties in estimating the mixing depth: comparing three mixing-depth models with profiler measurements*. Atmospheric Environment, **31**(18): 3023-3039

Bornstein, R. D. (2001). *Currently used parameterisations in numerical models*. Workshop on Urban Boundary Layer Parameterisations. COST 715, Zürich, May 24-25 2001.

Byun, D. W. & Arya, S. P. S. (1990). *A two-dimensional mesoscale numerical model of an urban mixed layer. I: Model formulation, surface energy budget, and mixed layer dynamics*. Atmospheric Environment, **24**(4): 829-844.

Chen, W., H. Kuze, A. Uchiyama, Y. Suzuki and N. Takeuchi, (2001). *One-year observation of urban mixwed layer characteristics at Tsukuba, Tokio using a micro pulse lidar*. Atmospheric Environment, **35**: 4273-4280.

Cleugh, H. A. and Grimmond, C. S. B. (2001) *Modelling regional scale surface energy exchanges and CBL growth in heterogeneous, urban-rural landscape*. Boundary-Layer Meteorology, **98**: 1-31.

Cooper, D. I., Eichinger, W. E. (1994). *Structure of the atmosphere in an urban planetary boundary layer from lidar and radiosonde observations*. Journal of Geophysical Research, 99(D11): 22937-22948

Cuxart, J., Bougeault, P., and Redelsperger, J.-L. (2000). *A turbulence scheme allowing for mesoscale and large eddy simulations*, Q. J. R. Meteorol. Soc. **126**: 1-30.

Donev, E., Panchev, St., Kolev, I. & Zeller, K. (1993). *The morning boundary layer transition in response to the surface heat flux at an urban site in Sofia*. Bulgarian Journal of Meteorology and Hydrology, **4**(4): 186-195

Donev, E., Zeller, K., Panchev, St. & Kolev, I. (1995). *Boundary layer growth and lapse rate changes determined by lidar and surface heat flux in Sofia*. Acta Meteorologica Sinica, Beijing, China, **9**(1): 101-111

Dupont, E., Menut, L., Carissimo, B., Pelon, J., Flamant, P. (1999). *Comparison between the atmospheric boundary layer in Paris and its rural suburbs during the ECLAP experiment*. Atmospheric Environment, **33**(6): 979-994

Evers, K., Niesser, J. & Weiss, E. (1987). *Acoustic sounding of the urban boundary layer over Berlin-Adlershof in summer*. Zeitschrift für Meteorologie, **37**(5): 241-252 (German)

Fisher B., Erbrink J., Finardi S., Jeannet Ph., Joffre S., Morselli M., Pechinger U., Seibert P. & D. Thomson, (1998). *Harmonization of the Preprocessing of meteorological data for atmospheric dispersion models*. COST 710 Final Report, CEC Publication EUR 18195, Luxembourg, 431 pp.

Gamo, M., S. Yamamoto, O. Yokoyama and H. Yoshikado (1983). *Structure of the free convective internal boundary layer during the sea breeze*. J. Meteor. Soc. of Japan, **61**, 110-124.

Garratt, J. R., (1990). *The Internal Boundary Layer - A Review*, Boundary-Layer Meteorol. **50**, 171-203.

Godowitch, J. M. (1986). *Characteristics of vertical turbulent velocities in the urban convective boundary layer*. Boundary-Layer Meteorology, **35**(4): 387-407

Godowitch, J. M., Ching, J. K. S., Clark, J. F. (1985). *Evolution of the nocturnal inversion layer at an urban and nonurban location*. Journal of Climate and Applied Meteorology, **24**(8): 791-804.

Godowitch, J. M., Ching, J. K. S., Clarke, J. F. (1987). *Spatial variation of the evolution and structure of the urban boundary layer*. Boundary-Layer Meteorology, **38**(3): 249-272.

Gryning, S.-E. and E. Batchvarova (1990). *Analytical model for the growth of the coastal internal boundary layer during onshore flow*. Quarterly Journal of the Royal Meteorological Society, **116**(491): 187-203.

Gryning, S.-E. and E. Batchvarova (1996). *A model for the height of the internal boundary layer over an area with an irregular coastline*. Boundary-Layer Meteorology, **78**: 405-413.
Gryning, S.-E. and E. Batchvarova (2001). *Mixing height in urban areas: will 'rural' parameterisations work?* COST-Action 715 Workshop on Urban Boundary Layer Parameterisations. Zürich, May 24-25 2001, 10 p.
Hanna, S. R. & J. C. Chang, (1992). *Boundary-layer parameterizations for applied dispersion modeling over urban areas*. Boundary-Layer Meteorology, **58**(3): 229-259
Henderson-Sellers, A. (1980). *A simple numerical simulation of urban mixing depths*. Journal of Applied Meteorology, **19**: 215-218
Hildebrand, P.H. & Ackerman, B. (1984). *Urban effects on the convective boundary layer*. Journal of the Atmospheric Sciences, 41(1): 76-91
Joffre, S. M., M. Kangas, M. Heikinheimo, S. A. Kitaigorodskii, (2001). *Variability of the stable and unstable atmospheric boundary layer height and its scales over a boreal forest*. Boundary Layer Meteorol., **99**(3), 429-450.
Kambezidis, H. D., Peppes, A. A., Melas, D. (1995). *An environmental experiment over Athens urban area under sea breeze conditions*. Atmospheric Research, **36**(1-2): 139-156
Karppinen, A., J. Kukkonen, G. Nordlund, E. Rantakrans, and I. Valkama, (1998). *A dispersion modelling system for urban air pollution*. Finnish Meteorological Institute, Publications on Air Quality 28. Helsinki, 58 p.
Karppinen, A., S.M. Joffre and P. Vaajama (1997): *Boundary-layer parameterisation for Finnish regulatory despersion models*. Int. J. Environment and Pollution, **8**, 3-6, 557-564.
Kerschgens, M. J. & Suer, H. (1988). *Energetic feedback between urban climate and diffusion of atmospheric pollutants*. IN: International Symposium on Environmental Meteorology, 1st, Würzburg, W. Germany, Sept. 29-Oct. 1, 1987, Proceedings, Dordrecht, Holland, Kluwer Academic Publishers, 1988, p. 335-344.
Kitaigorodskii, S. A. and S. M. Joffre, (1988). *In search of a simple scaling for the height of the stratified atmospheric boundary layer*. Tellus **40A**(5), 419 - 433.
Kolev, I., P. Savov, B. Kaprielov, O. Parvanov and V. Simeonov, (2000). *Lidar observation of the nocturnal boundary layer formation over Sofia, Bulgaria*. Atmospheric Environment, **34**(19): 3223-3235.
Kumari, M. (1985). *Diurnal variation of mean mixing depths in different months at Delhi*. Mausam, New Delhi, **36**(1): 71-74
Kurbatskii, A.F. (2001) *Computational modelling of the turbulent penetrative convection above the urban heat island in a stably stratified environment*. J. Appl. Meteor., **40**: 1848-1761.
Lena, F. and Desiato, F. (1999) *Intercomparison of nocturnal mixing height estimate methods for urban air pollution modelling*. Atmospheric Environment, **33**(15): 2385-2393.
Liu, X. & Ohtaki, E. (1997) *An independent method to determine the height of the mixed layer*. Boundary-Layer Meteorology, **85**(3): 497-504.
Lokoshchenko, M. A., Isaev, A. A., Kallistratova, M. A. & Pekur, M. S. (1993). *Studies of the atmospheric boundary layer over Moscow by remote sensing and in situ methods*. Russian Meteorology and Hydrology, New York, NY, **9**: 13-24
Marsik, F. J., Fischer, K. W., McDonald, Tracey D., Samson, Perry J. (1995) *Comparison of methods for estimating mixing height used during the 1992 Atlanta Field Intensive*. Journal of Applied Meteorology, **34**(8): 1802-1814.
Melas, D., Kambezidis, H. D. (1992). *The depth of the internal boundary layer over an urban area under sea-breeze conditions*. Boundary-Layer Meteorology, **61**(3): 247-264
Miao, M. (1987). *Numerical modeling of the nocturnal PBL over the urban heat island in Changzhou city*. Boundary-Layer Meteorology, **41**(1/4): 41-56

Mikkelsen, T., S. Thykier-Nielsen, P. Astrup, J. M. Santabárbara, J.H. Sørensen, A. Rasmussen, L. Robertson, A. Ullerstig, S. Deme, R. Martens, J. G. Bartzis and J. Päsler-Sauer (1997). *MET-RODOS: A Comprehensive Atmospheric Dispersion Module*. Radiat. Prot. Dosim. **73**, 45–56.

Miyake, M., (1965). *Transformation of the ABL over inhomogeneous surfaces*. Sci. Report Contract (NR 307-252) 477(24).

Nielsen, N-W. and B.H. Saas, (2000). *A lower boundary condition for the mixing length in the CBR turbulence scheme*. HIRLAM Newsletter, **35**, 128-136.

Nieuwstadt , F.T.M., (1984). *Some aspects of the turbulent stable boundary layer*, Boundary-Layer Meteorology, **30**, 31-55.

Nieuwstadt, F.T.M., (1984). *The turbulent structure of the stable, nocturnal boundary layer*, J. Atmos. Sci. **41**, 2202-2216.

Nkemdirim, L.C. (1986). *Mixing depths and wind speed in an urban airshed: a note on the limits to a relationship*. Atmospheric Environment, **20**(9): 1829-1830

Olesen, H. R., Løfstrøm, P., Berkowicz, R. and Jensen, A. B., (1992). *An improved dispersion model for regulatory use: the OML model*. In: van Dop, Han and Kallos, George (eds.), Air pollution modeling and its application IX. New York, NY, Plenum Press, 1992. p. 29-38.

Panovsky, H.A. & J.A. Dutton, (1984). *Atmospheric turbulentce*. Wiley, NY, 397 pp.

Penenko, V.V. and A.E. Aloyan, (1974*). Numerical method for some meso-meteorological problems with free top of atmospheric mass*. Trudy ZapSibNII, Novosibirsk, 14, 52-66. (in Russian)

Penenko, V.V. and A.E. Aloyan, (1985). *Models and Methods for Environmental Problems*. Nauka:, Novosibirsk, 256 p. (pp. 49-55) (in Russian)

Piringer, M. (1988). *Determination of mixing heights by sodar in an urban environment*. IN: International Symposium on Environmental Meteorology, 1st, Würzburg, W. Germany, Sept. 29-Oct. 1, 1987, Proceedings, Dordrecht, Holland, Kluwer Academic Publishers, 1988, p. 425-444.

Piringer, M., A. Baklanov, K. De Ridder, J. Ferreira, S. Joffre, A. Karppinen, P. Mestayer, D. Middleton, M. Tombrou, R. Vogt, (2001). *The surface energy budget and the mixing height in urban areas: Status report of Working Group 2 of COST-Action 715*. Ext. abstract to the Third Urban Air Quality Conference, Loutraki, Greece. CD-ROM, paper Pl 1.3.

Piringer, M. and K. Baumann (1999): *Modification of a valley wind system by an urban area - experimental results.* Meteorol. Atmos. Phys. **71**, 117 - 125.

Piringer, M., Baumann, K. & Langer, M. (1998). *Summertime heights at Vienna, Austria, estimated from vertical soundings and by a numerical model*. Boundary-Layer Meteorology, **89**: 25-45.

Piringer, M., Editor (2000) *Surface energy balance in urban areas. Extended abstracts of an Expert Meeting*. WG-2 COST Action 715, Antwerp, Belgium, 12 April 2000 (submitted to EC-COST).

Railo, M., Editor (1997*). Urban Episodes. Problems and Action Plans*: Paris, Berlin, Helsinki, Turku. IImansuojelu. Special Issue. **6**, 29 pp.

Rasmussen, A., J.H. Sørensen and N.W. Nielsen. (1997). *Validation of Mixing Height Determined from Vertical Profiles of Wind and Temperature from the DMI-HIRLAM NWP Model in Comparison with Radiosoundings*. In: The Determination of the Mixing Height - Current Progress and Problems. EURASAP Workshop Proceedings, 1-3 October, 1997, Risø National Laboratory, Eds: S.-E. Gryning, F. Beyrich and E. Batchvarova, pp. 101-104

Rasmussen, A., J. H. Sørensen, N. W. Nielsen. and B. Amstrup (1999): *Uncertainty of Meteorological Parameters from DMI-HIRLAM*. Report RODOS (WG2)TN(99)12.

Rayner, K. N. & Watson, I. D. (1991). *Operational prediction of daytime mixed layer heights for dispersion modelling*. Atmospheric Environment, **25A**(8): 1427-1436.

Roth, M. (2000) *Review of atmospheric turbulence over cities*. Quart. J. Roy. Meteor. Soc, **126**(564): 941-990.

Rotach, M.W., V. Mitev and R. Vogt (2001) *BUBBLE - current status of the experiment and planned investigations/evaluations of the mixing height*. COST715 Workshop 'Mixing heights and inversions in urban areas', Meteo-France, Toulouse, 3-5.10.2001.

Sass, B. H., Nielsen, N. W., Jørgensen, J.U., Amstrup, B., and Kmit, M., (2000). *The operational HIRLAM system*, DMI Technical report 00-26. http://www.dmi.dk/f+u/publikation/tekrap/2000/Tr00-26.pdf.

Said, F., B. Campistron, A. Coppalle, A. Dabas, Ph. Drobinsky, E. Fréjafon, E. Gizard, A. Mériaux and P. Mestayer (2001) *Influence of sea breeze and relief on the mixing height during ESCOMPTE in the Marseille area*. COST715 Workshop 'Mixing heights and inversions in urban areas', Meteo-France, Toulouse, 3-5.10.2001.

Sang, J. & Liu, W. (1990). *An analysis on flow and temperature structure of wintertime urban boundary layer*. Acta Meteorologica Sinica, Beijing, China, **48**(4): 459-468

Schatzman, M., J. Brechler and B. Fisher, Editors, (2001). *Preparation of meteorological input data for urban site studies*. Proceedings of the workshop, 15 June 2000, Prague, Czech Republic. EC, Cost Action 715, EUR 19446, 101 pp.

Scire, J.S., E.M. Insley, R.J. Yamartino and M.E. Fernau, (1995). *A user's guide for the CALMET meteorological model*, EARTH TACH, 1995.

Seaman, N.L. (1989). *Numerical studies of urban planetary boundary-layer structure under realistic synoptic conditions*. Journal of Applied Meteorology, **28**(8): 760-781

Seibert, P., Beyrich, F., Gryning, S.-E., Joffre, S., Rassmussen, A. and Tercier, Ph., (1998). *Mixing Height Determination for Dispersion Modelling*. Report of Working group 2. COST Action 710. In: Fisher et al (Eds.), Preprocessing of Meteorological data for Dispersion Modelling. May 1997.

Soudine, A. (2001) *Personal communications*. October 2001. WMO.

Summers, P. W. (1965). *An urban heat island model: its role in air pollution problems with applications to Montreal.* First Canadian Conf. on Micrometeorology. Toronto, CMOS, 22 pp.

Summers, P. W. (1977). *Application of the urban mixing-depth concept to air pollution problems*. IN: United States Forest Service, Northeastern Experiment Station, Upper Darby, PA., General Technical Report NE-25, 1977, p. 273-277.

Sørensen, J.H., A. Rasmussen and H. Svensmark, (1996). *Forecast of Atmospheric Boundary-Layer Height for ETEX Real-time Dispersion Modelling*, Phys. Chem. Earth, Vol **21**, No. 5-6, pp. 435-439.

Tennekes, H. and A. G. M. Driedonks, (1981). *Basic entrainment equations for the atmospheric boundary layer*. Boundary-Layer Meteorology, **20**(4): 515-531

US EPA, (1990). U*ser's guide for the Urban Airshed Model.* Vol.2: User's manual for the UAM modeling system, EPA-450/4-90-007B.

Venkatram, A. (1986). *An examination of methods to estimate the height of the coastal internal boundary layer*. Boundary-Layer Meteorology, **36**: 149-156.

Vogelezang, D.H.P. and Holtslag, A.A.M., (1996). *Evolution and model impacts of the alternative boundary layer formulations*. Boundary-Layer Meteor., **81**, 245-269.

Walmsley, J.L. (1989). *Internal boundary-layer height formulae – a comparison with atmospheric data*. Boundary-Layer Meteor., **47**, 251-262.

Westcott, N. (1989). *Influence of mesoscale winds on the turbulent structure of the urban boundary layer over St. Louis*. Boundary-Layer Meteorology, **48**(3): 283-292

Wringht, S.D., Elliot, L., Ingham, D.B. & Hewson, M.J.C. (1999). *The adaptation of the atmospheric boundary layer to a change in surface roughness*. Boundary-Layer Meteorology,

Zhang, A., Sun, C. & Yi, T. (1991). *Observing results of the atmospheric mixed layer in Beijing area and the evaluation of theoretical models*. Acta Meteorologica Sinica, Beijing, China, **5**(5): 541-550

Zhang, K., Mao, H., Civerolo, K., Berman, S., Ku, Y.-Y., Rao, S. T., Doddridge, B., Philbrick, C. R., Clark, R. (2001). *Numerical investigation of boundary layer evolution and nocturnal low-level jets: local versus non-local PBL schemes*. Envir. Fluid Mechanics, **1**: 171-208.

Zilitinkevich, S. & Baklanov, A. (2001). *Calculation of the height of stable boundary layers in operational models*. Boundary Layer Meteorology (accepted), (available also as DMI Scientific Report, No. 01-07 http://www.dmi.dk/f+u/publikation/vidrap/2001/Sr01-07.pdf)

Zilitinkevich, S. & Mironov, D. (1996). *A multi-limit formulation for the equilibrium depth of a stably stratified boundary layer*. Boundary-Layer Meteorology, **81**(3-4): 325-351.

Zilitinkevich, S., A. Baklanov, J. Rost, A.-S. Smedman, V. Lykosov, P. Calanca, (2001). *Diagnostic and prognostic equations for the depth of the stably stratified Ekman boundary layer*. Quart. J. Roy. Meteor. Soc., **128** (579).

A recommendation for turbulence parameterisation in German guidelines for the calculation of dispersion in the atmospheric boundary layer – improvements and remaining problems –

K. Maßmeyer* and R. Martens**[1]

* Fachhochschule Lippe und Höxter - University of Applied Sciences -, Abteilung Höxter, Fachbereich Technischer Umweltschutz, An der Wilhelmshöhe 44, D 37671 Höxter

** Gesellschaft für Anlagen- und Reaktorsicherheit mbH, Schwertnergasse 1, D 50667 Köln

Keywords:
Dispersion modelling, turbulence parameters, standard deviations of wind speed components, Lagrangian time scales

Abstract

Common approaches for the turbulence parameterisation (standard deviations of wind speed components σ_{ui} *and Lagrangian time scales* T_{Li}*) for practical purposes within dispersion models are based on similarity theory with empirical formulas derived from meteorological field experiments. The principal shape of these formulas is derived via the theory of homogeneous and stationary turbulence accounting for the inhomogeneity of the boundary layer by empirical corrections. A great variety of such formulas exists in which the state of the atmosphere is characterised by the following input parameters: roughness length, Monin-Obukhov length, friction velocity and mixing layer height which have to be derived via a meteorological pre-processor. These formulas give different results for the same atmospheric stability, discontinuities and jumps at the transition between different stability regimes of the atmosphere.*

Based on a review of parameterisations a working group of the German Association of Engineers (VDI) recommended formulas which might be used for practical purposes. The criterion of choice are consistency with similarity theory, a consistent formulation for all types of dispersion models and a smooth transition between different turbulence regimes.

The formulas will be incorporated in the appendix of the amended version of the German Technische Anleitung zur Reinhaltung der Luft (TA-Luft, Technical Instruction on Air Quality Control) which deals with atmospheric dispersion calculations (AUSTAL2000). Results of different dispersion experiments have been used as a validation data base.

---

[1] *Further members of the working group:*

D. Etling, Institut für Meteorologie und Klimatologie, Universität Hannover
M.J. Kerschgens, Institut für Geophysik und Meteorologie, Universität zu Köln
W. Mix, Institut für Physik, Humboldt-Universität zu Berlin
K. Nester, Institut für Meteorologie und Klimaforschung, Forschungszentrum Karlsruhe
H. Nitsche, Deutscher Wetterdienst, Offenbach
U. Pechinger, Zentralanstalt für Meteorologie und Geodynamik, Wien
M. Wichmann-Fiebig, Air Quality Unit-Environment DG, European Commission

1 Introduction

In the Commission on Air Pollution Prevention of VDI and DIN – Standards Committee (KRdL) experts from science, industry and administration, acting on their own responsibility, establish VDI guidelines and DIN standards in the field of environmental protection. They describe the state of the art in science and technology in the Federal Republic of Germany and serve as a decision–making aid in the preparatory stages of legislation and application of legal regulations and ordinances.

For a long time the Gaussian plume model served as a working horse for a lot of different type of applications connected to environmental protection purposes. Dispersion parameters applied in German guidelines were derived from dispersion experiments carried out at the research centres of Juelich and Karlsruhe for specified emission heights (50, 100 and 160 m) and 6 stability categories (GMBl, 1986; Bundesanzeiger, 1990). The orography at both sites is nearly flat and the roughness length lies in the order of 1 m. Stability categories for routine applications at other sites usually are defined on the basis of synoptic oberservations – i.e. cloud cover, wind speed and time of the day – and carried out by the national weather service (DWD). Such datasets are available for more than 100 sites all over Germany.

Based on the results of recent boundary layer modelling theory – which follows the ideas of the so-called similarity theory – these meteorological datasets can also be applied to calculate (similarity) parameters characterising the turbulent state of the atmospheric boundary layer via a meteorological pre-processor (e.g. Holtslag, 1986; Holtslag, 1987; van Ulden, 1985). Using these similarity parameters a "universal" turbulence parameterisation (i.e. standard deviations of wind speed components σ_{ui}, Lagrangian time scales T_{Li}) depending upon surface roughness and height can be established and applied to all types of atmospheric dispersion models. The parameterisation is based on the theory of homogeneous and stationary turbulence accounting for the inhomogeneity by empirical corrections. The state of the atmosphere within the parameterisation is characterised by boundary layer parameters:

- roughness length z_0,
- Monin-Obukhov length L,
- friction velocity u_* and
- height of the mixing layer z_i.

During the last years several new technical guidelines have been developed in Germany and put into operation. They describe the characteristics and the application of different types of atmospheric flow and dispersion models (i.e. Gaussian plume and puff models, Lagrangian models, Eulerian models) (VDI3783/6, 1992; VDI3945/1, 1995; VDI3945/3, 2000). Common approaches for the parameterisation of turbulence for practical purposes within these dispersion models are based on similarity theory with empirical formulas based on experiments. However, turbulence parameterisations available from literature often give different results for the same atmospheric stability; they exhibit discontinuities and jumps at the transition between different stability regimes of the atmosphere (Kerschgens et al., 2000).

Based on a review of parameterisations of σ_{ui} and T_{Li} a working group of the VDI recommended formulas to be used for practical purposes. The criterion of choice are consistency with similarity theory (we recommend a von Karman constant of $k = 0.4$ and a "universal" Kolmogorov constant of $C_0 = 5.7$), a consistent formulation for all types of dispersion models and a smooth transition between different turbulence regimes. The formulas are briefly summarised in the following Chapter 2.

2. Vertical profiles of mean wind speed and turbulence parameters

The parameterisations presented below were derived from a literature survey of meteorological field experiments (Kerschgens et al., 2000) and are strictly valid only in the surface boundary layer – which roughly extends between surface and a normalised height of $z/z_i = 0.1$. Contrary to the former parameterisation via dispersion parameters the recommended parameterisation is explicitly not a result of tracer experiments but based on meteorological field data in connection with contemporary boundary layer modelling.

2.1 Vertical wind profile

Once the boundary layer parameters are known the vertical variation of wind speed can be derived via equation (1) as a function of stability (see e.g. Businger, 1971; Buyn, 1990; Paulson, 1970):

$$u(z) = \begin{cases} \frac{u_*}{\kappa} \cdot \left[\ln\frac{z}{z_0} - 2 \cdot \ln\frac{1+X}{1+X_0} - \ln\frac{1+X^2}{1+X_0^{\,2}} + 2 \cdot \arctan X - 2 \cdot \arctan X_0 \right] & \text{for } \frac{z}{L} \le 0 \\ \frac{u_*}{\kappa} \cdot \left[\ln\frac{z}{z_0} + 5 \cdot \left(\frac{z - z_0}{L} \right) \right] & \text{for } 0 \le \frac{z}{L} < 0{,}5 \\ \frac{u_*}{\kappa} \cdot \left[8 \ln\left(2\frac{z}{L} \right) + 4{,}25 \left(\frac{z}{L} \right)^{-1} - 0{,}5 \left(\frac{z}{L} \right)^{-2} \right. & \text{for } 0{,}5 \le \frac{z}{L} < 10 \\ \quad \left. - \ln\left(2\frac{z_0}{L} \right) - 5\frac{z_0}{L} - 4 \right] & \\ \frac{u_*}{\kappa} \cdot \left[0{,}7585 \frac{z}{L} + 8 \ln 20 - 11{,}165 - \ln\left(2\frac{z_0}{L} \right) - 5\frac{z_0}{L} \right] & \text{for } 10 \le \frac{z}{L} \end{cases} \tag{1}$$

with: $X = \left(1 - 15 \cdot \frac{z}{L} \right)^{\frac{1}{4}}$; $X_0 = \left(1 - 15 \cdot \frac{z_0}{L} \right)^{\frac{1}{4}}$; for: $z \ge z_0$.

2.2 Vertical profiles of turbulence parameters

Within the framework of the VDI-guidelines different types of dispersion models are incorporated. The parameterisation of atmospheric turbulence is handled via model specific turbulence parameters as shown in Table 1:

Table 1: Type of dispersion model and associated turbulence parameters within VDI-guideline framework

Model type	Model specific turbulence parameters
Gaussian plume model	Horizontal (σ_y) and vertical (σ_z) dispersion parameters, dependent upon source distance
Gaussian puff model	Horizontal (σ_x, σ_y) and vertical (σ_z) dispersion parameters, dependent upon travelling time of pollutant
Lagrangian particle model	Standard deviations of the wind velocity components (σ_u, σ_v, σ_w), Lagrangian time scales (T_{Lx}, T_{Ly}, T_{Lz}), dependent on local roughness
Eulerian model	Diffusion coefficients (K_x, K_y, K_z), depending on local roughness

In the following subsections formulas are summarised which enable the model specific turbulence parameterisation based on identical input information, i.e. the standard deviations of the wind speed components and the Lagrangian time scales.

2.2.1 Standard deviations of wind speed components

Most of the parameterisation schemes for the standard deviations of the wind speed components available from literature can be rewritten in the form:

$$\sigma_{u_i} = \left((a_{u_i} \cdot u_*)^n + (b_{u_i} \cdot w_*)^n \right)^{\frac{1}{n}} \qquad (2).$$

The coefficients a_{ui} and b_{ui} vary approximately by 10 %, the exponent n is usually set to values of 2 or 3 (Kerschgens et al. 2000).

For a neutral to unstable stratification the following parameterisations are recommended by the working group:

$$\sigma_u = \left[(2.4 u_*)^3 + (0.59 w_*)^3 \right]^{\frac{1}{3}} \exp\left(-\frac{z}{z_i} \right) \qquad (3)$$

$$\sigma_v = \left[(1.8 u_*)^3 + (0.59 w_*)^3 \right]^{\frac{1}{3}} \exp\left(-\frac{z}{z_i} \right) \qquad (4)$$

$$\sigma_w = \left(\left(1.3 u_* \exp(-\frac{z}{z_i}) \right)^3 + \left(1.3 (\frac{z}{z_i})^{\frac{1}{3}} (1 - 0.8 \frac{z}{z_i}) w_* \right)^3 \right)^{\frac{1}{3}} \qquad (5).$$

In equations (3) and (4) the exponential function is acting on both terms on the right hand side of the equations yielding higher near surface values of the standard deviations of the horizontal wind speed components than in upper regions of the boundary layer. The height dependence via exp(-z/z_i) avoids undefined Lagrangian time scales for heights $z = z_i$. The height dependence in the convective part of equation (5) – which is scaled with w_* – was introduced by (Lenschow, 1980) and was validated by different authors (see Caughey, 1982; Carruthers, 1992). For convective situations the standard deviations of the vertical wind speed component are rather small near the surface and near the top of the atmospheric boundary layer while the expected maximum of σ_w occurs approximately in the region of $z/z_i = 0.3$. This behaviour is reproduced by equation (5).

For stable stratification we propose the following formulas:

$$\sigma_u = 2.4 u_* \exp\left(-\frac{z}{z_i} \right) \qquad (6)$$

$$\sigma_v = 1.8 u_* \exp\left(-\frac{z}{z_i} \right) \qquad (7)$$

$$\sigma_w = 1.3 u_* \exp\left(-\frac{z}{z_i} \right) \qquad (8).$$

The parameterisations (6) – (8) do not show discontinuities in the transition between unstable and stable stratification of the atmosphere.

2.2.2 Lagrangian time scales

Contrary to the commonly applied parameterisation schemes for the standard deviation of the wind speed components (which show rather small differences) pronounced variations must be stated for the available formulas for the parameterisation of the Lagrangian time scale. Based on the theory of Kolmogorov in (Luhar, 1989; Rodean, 1996; Du, 1997) a parameterisation applying the turbulent velocity variance σ_{ui}^2, the dissipation rate ε of turbulent kinetic energy and the Kolmogorov-constant C_0 is proposed. The underlying equation (9) is strictly valid only in homogeneous turbulence. In situations with inhomogeneous turbulence – occurring in a convective boundary layer – such kind of parameterisation must not be applied because no unique time scale exists (Luhar, 1989). The probability density function of tracer particles then has to be derived from the dissipation of turbulent kinetic energy as well as from the skewness of the probability distribution of the turbulent wind speed components (Shao, 1992). However, because the skewness of the probability density function of the turbulent wind speed fluctuations is small in the lower part of the boundary layer the following equation for the turbulent time scale is recommended nevertheless:

$$T_{L_i} = \frac{2\sigma_{u_i}^{\;2}}{C_o \varepsilon} \qquad (9).$$

The values of the Kolmogorov-constant C_0 reported in the literature vary between 2 and 10, depending on atmospheric stability and coordinate direction (Kerschgens et al., 2000; Du, 1997; Rotach, 1996; Anfossi, 1998). Due to reasons of consistency with similarity theory we propose a value of C_0=5.7 which should be used for all three coordinate directions.

For neutral to unstable stratification the rate of dissipation of turbulent kinetic energy as a function of height above ground and stability can be calculated according to (Kerschgens et al., 2000):

$$\varepsilon = \max\left[\frac{u_*^{\;3}}{k \cdot z} \cdot \left[\left(1 - \frac{z}{z_i}\right)^2 + 2.5 \cdot k \cdot \frac{z}{z_i}\right] + \frac{w_*^{\;3}}{z_i} \cdot \left[1.5 - 1.3\left(\frac{z}{z_i}\right)^{\frac{1}{3}}\right], \frac{u_*^3}{kz}\right] \qquad (10).$$

For stable stratification the dissipation rate reads as

$$\varepsilon = \frac{u_*^{\;3}}{k \cdot z} \cdot \phi_\varepsilon \qquad \text{with } \phi_\varepsilon = \phi_m - \frac{z}{L} \text{ and } \Phi_m = 1 + 5\frac{z}{L} \qquad (11).$$

2.2.3 Turbulence parameters for Gaussian puff and plume models

Supposing stationary and homogeneous turbulence the growth of a puff released to the atmosphere can be calculated as a function of time t as follows (Hanna, 1990):

$$\sigma_x(t) = \sigma_u t \frac{1}{\sqrt{1 + 0.5\frac{t}{T_{Lx}}}}, \sigma_y(t) = \sigma_v t \frac{1}{\sqrt{1 + 0.5\frac{t}{T_{Ly}}}}, \sigma_z(t) = \sigma_w t \frac{1}{\sqrt{1 + 0.5\frac{t}{T_{Lz}}}}, \qquad (12).$$

For stationary meteorological conditions – especially for constant wind speed – the time dependent dispersion parameters $\sigma_X(t)$, $\sigma_Y(t)$ and $\sigma_Z(t)$ can be recalculated as a function of distance, i.e. $\sigma_X(x)$, $\sigma_Y(x)$ and $\sigma_Z(x)$, using equation (13):

$$t = \frac{x}{u} \qquad (13).$$

2.2.4 Diffusion coefficients for Eulerian models

On the basis of the parameterisations given in chapters 2.2.1 and 2.2.2 the turbulent diffusion coefficients for use in Eulerian diffusion models can be calculated as follows:

$$K_x = \sigma_u^2 \cdot T_{L_u} \quad (14)$$

$$K_y = \sigma_v^2 \cdot T_{L_v} \quad (15)$$

$$K_z = \sigma_w^2 \cdot T_{L_w} \quad (16).$$

3. Typical vertical profiles of the turbulence parameters

For specified boundary layer parameters (friction velocity, Monin-Obukhov-length and mixing layer height) all turbulence parameters described in Chapter 2 can be calculated as a function of height above ground and atmospheric stability. In Table 2 typical combinations of boundary layer parameters for unstable, neutral and stable stratification of the atmosphere are presented for a site with a roughness length of 1.5 m which is representative for the Research Centre at Karlsruhe. In Figures 1 to 3, the associated vertical profiles of the standard deviations of the wind speed components, the Lagrangian time scales and the diffusion coefficients are shown, respectively.

Table 2: Boundary layer parameters for different regimes of atmospheric stability

Boundary layer parameters / stratification	Wind speed at a height of 10 m (m/s)	Friction velocity (m/s)	Monin-Obukhov-length (m)	mixing layer height (m)
Stable	2	0.396	350	780
Neutral	3	0.632	99999	800
Unstable	2	0.453	-190	1100

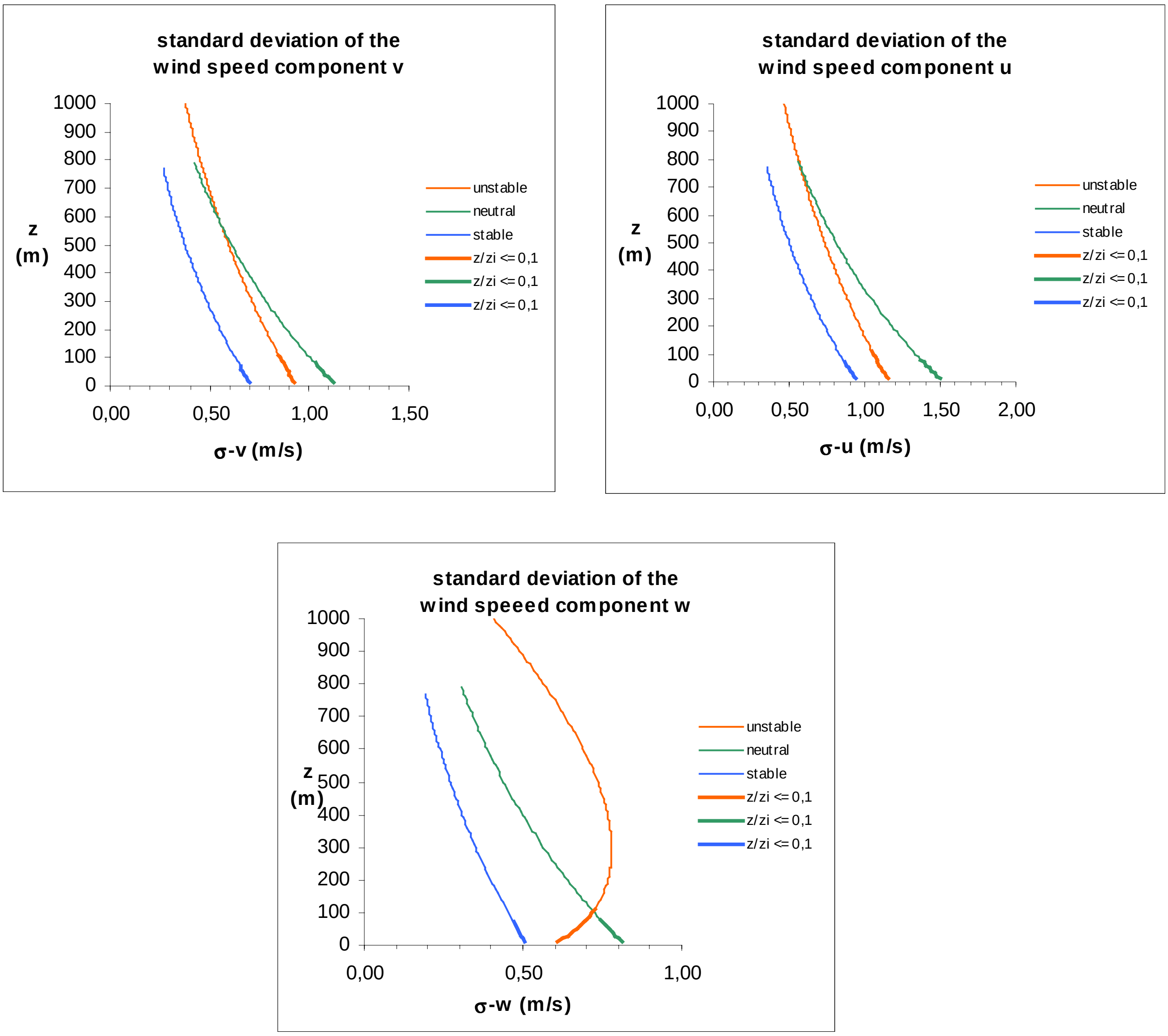

Figure 1: Vertical profiles of the standard deviations of the wind speed components for a site with a surface roughness of 1.5 m and varying atmospheric stratification. The profiles are shown within the stability dependent range of the mixing layer height given in Table 2. Bold lines characterise the regions where the underlying theory is strictly applicable (i.e. $z/z_i<0.1$).

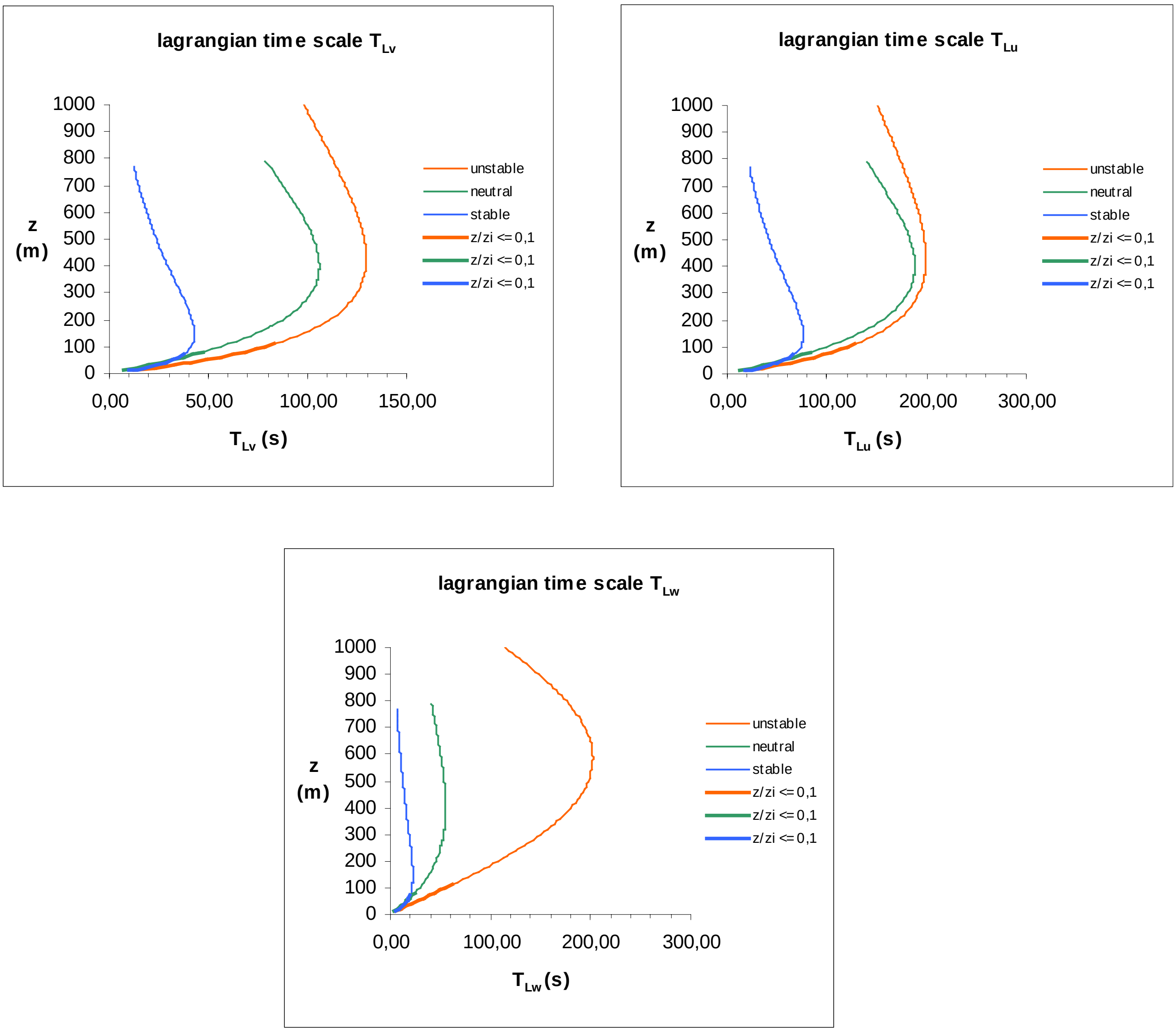

Figure 2: Vertical profiles of the lagrangian time scales for a site with a surface roughness of 1.5 m and varying atmospheric stratification. The profiles are shown within the stability dependent range of the mixing layer height given in Table 2. Bold lines characterise the regions where the underlying theory is strictly applicable (i.e. $z/z_i<0.1$).

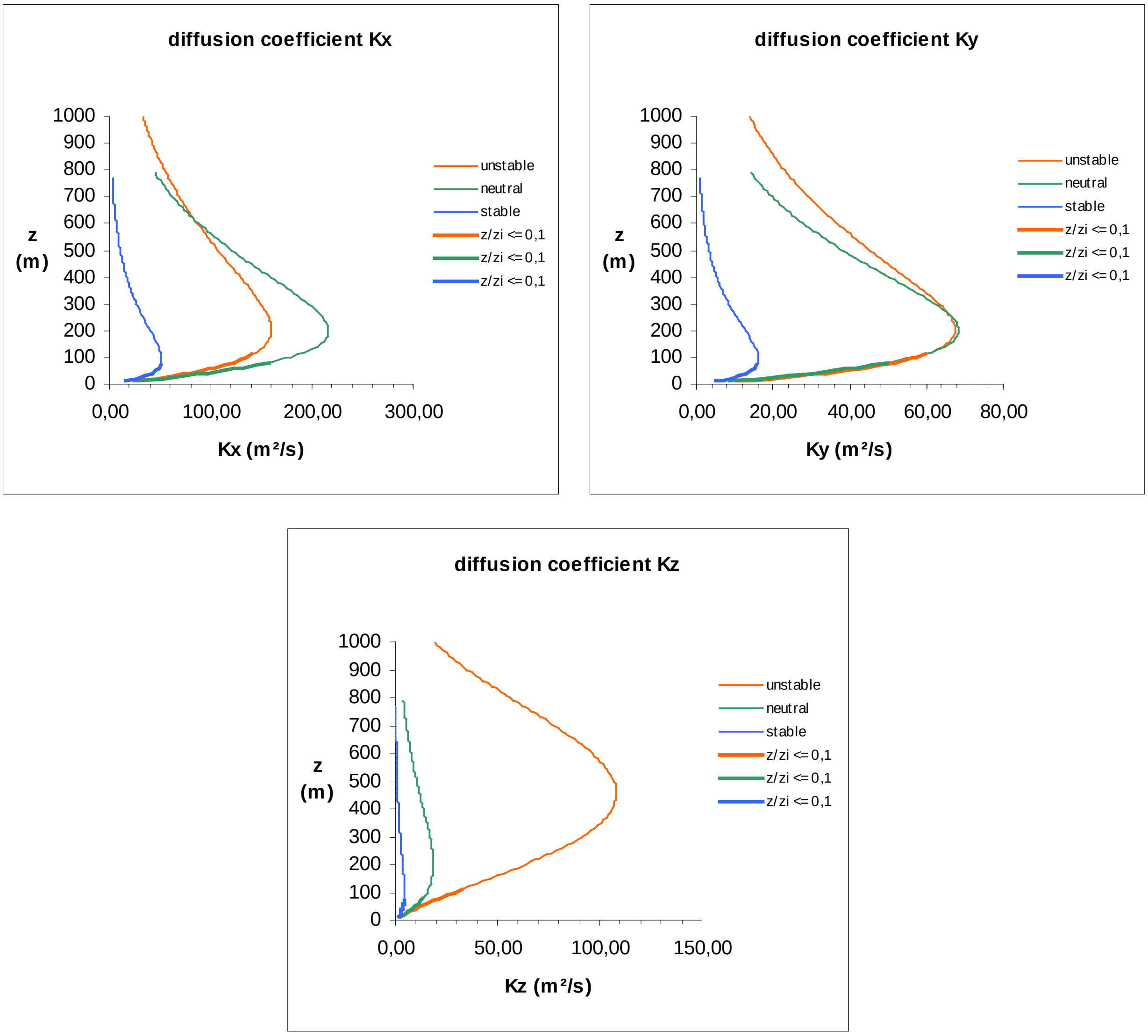

Figure 3: Vertical profiles of the diffusion coefficients for a site with a surface roughness of 1.5 m and varying atmospheric stratification. The profiles are shown within the stability dependent range of the mixing layer height given in Table 2. Bold lines characterise the regions where the underlying theory is strictly applicable (i.e. $z/z_i<0.1$).

4. Validation

The recommended formulas for the turbulence parameterisation were applied together with a Lagrangian particle model (VDI3945/3, 2000) in order to compare calculated tracer concentrations with observed concentrations from appropriate tracer experiments (KSP-Bericht, 2000, Barad, 1958).

4.1 Experiments in a wind tunnel

For neutral stratification, a roughness length of z_0=0,7 m and source heights of 60 m and 100 m near surface measurements of tracer concentration distributions c(x,y,0) are available (KSP-Bericht, 2000). Cross wind integrated concentrations at fixed source distances $c_y(x)$ = $c(x, y, 0)dy$ are not influenced by lateral plume meandering. This parameter was determined with a Lagrangian particle model for a Monin Obuchov length of 9999 m and a fixed value for the mixing layer height of 800 m. In Figure 4 the normalised concentration data $C_y = c_y \cdot H \cdot u_q / Q$ (source strength Q, source height H, wind speed at source height u_q) are presented as a function of source distance x.

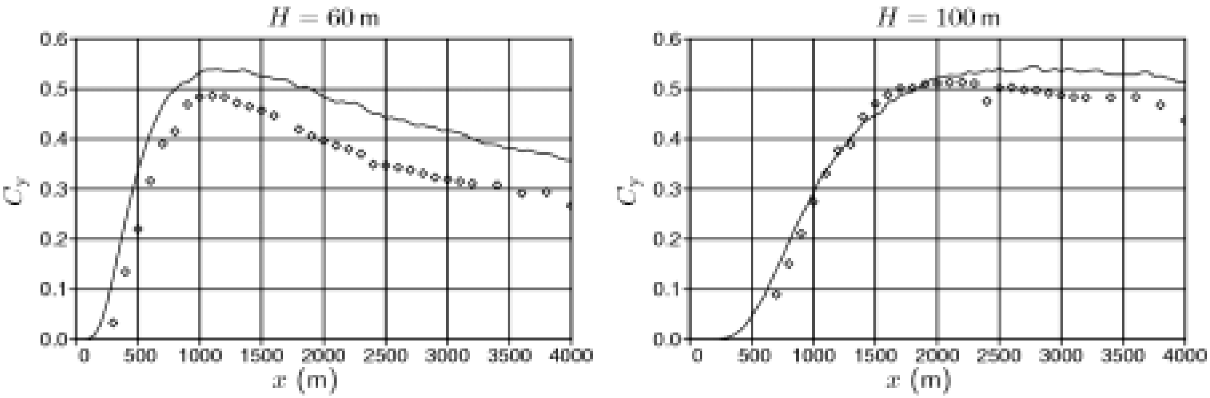

Figure 4: Comparison of the cross wind integrated tracer concentration normalised with the factor $Q/(H\ u_q)$ as a function of source distance x (open symbols: measured data, solid line: model results).

For a source height of 100 m and distances between source and the concentration maximum the calculated concentrations fit quite well to the measured ones. The calculated maximum concentration is slightly larger than the measured maximum. The source distance of the calculated maximum concentration is found to be a little bit larger than the measured maximum value.

For a source height of 60 m the calculated concentrations give conservative results: for all evaluated distances the calculated concentration data are slightly higher than the measured ones. The position of the measured/calculated maximum concentration values show only minor differences.

4.2 Prairie Grass Experiment

The Prairie Grass experiments were carried out in O'Neill, Nebraska/USA (Barad, 1958). The orography near O'Neill is flat with a roughness length of approximately 0.008 m. For a time period of 10 minutes SO_2-gas was emitted continuously at an emission height of 0.46 m above ground. Within source distances between 50 m and 800 m downwind tracer sampling stations were installed with an angular distance of 1 – 3 degrees. All datasets listed in (Barad, 1958) were recalculated with a Lagrangian particle model together with the recommended turbulence parameterisation.

For three source distances (50 m, 200 m and 800 m) observed and calculated values of:

- the cross wind integrated tracer concentration ($C_y \cdot u_2/Q$; u_2 is the wind speed measured in a height of 2 m above ground) and
- the plume width (σ_y)

were compared. The results are shown in figures 5 and 6 as a function of thermal stability.

The plume widths show a good agreement between measurement and calculation for all source distances. For unstable to neutral stratification the calculated and observed normalised concentration data agree very well. In cases of unstable stratification and for larger source distances the differences between calculation and measurement are more pronounced. A larger scatter in the measured data is obvious. In situations with extreme unstable stratification the tracer gas will be transported rather quickly in upper regions of the atmosphere. These convective situations can not be handled appropriately by the underlying theory and the recommended parameterisation respectively. In the results from dispersion modelling a larger part of the tracer remains near the ground resulting in higher concentration values.

5. Conclusions

Based on a literature study a set of formulas comprising the common understanding of atmospheric boundary layer modelling was proposed allowing the description of atmospheric turbulence applicable for different atmospheric dispersion models based on the same synoptic dataset. The recommended formulas show neither discontinuities nor jumps between different states of atmospheric stability as other commonly used formulas do. Comparative calculations of tracer experiments applying a Langrangian particle model together with the recommended turbulence parameterisation show a satisfactory level of agreement.

The formulas will be incorporated in the appendix of the amended version of the German Technische Anleitung zur Reinhaltung der Luft (TA-Luft, Technical Instruction on Air Quality Control) which deals with atmospheric dispersion calculations (AUSTAL2000).

However, some (practical) problems are not yet solved. They concern the modelling of time series with sequences of descending mixing heights, the description of the wind profile above z_i, the modelling of dispersion inside canopy/urban canopy layer, the application to non-level terrain, and the necessity of fixing a minimum time scale for Lagrangian particle models. Finally the universality of C_0 is still an open question.

Acknowledgements

The authors wish to thank Dr. Ulf Janicke, Ingenieurbüro Janicke, for carrying out the calculations with the Lagrangian particle model and the comparisons with measured data presented in Chapter 4.

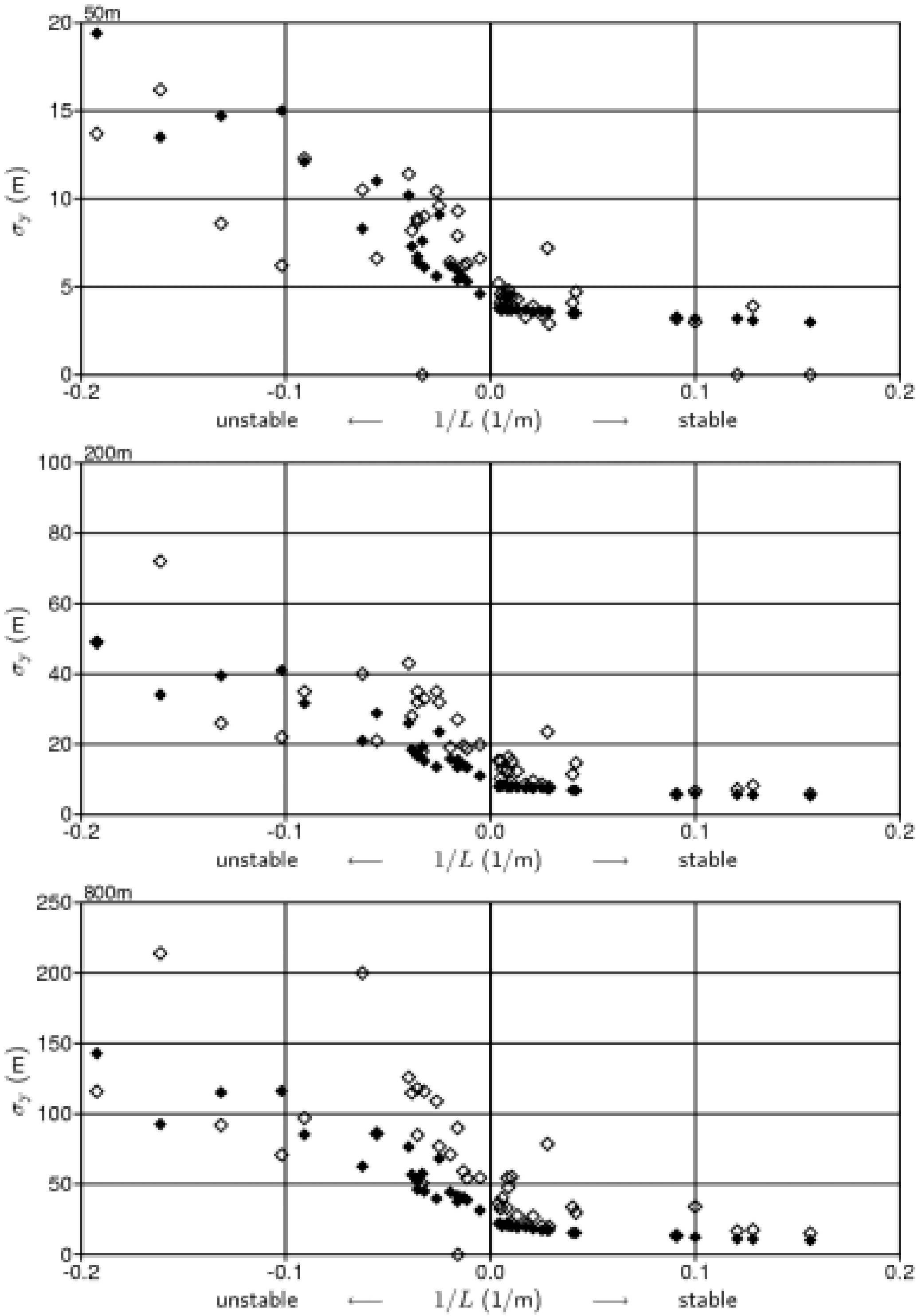

Figure 5: Comparison of plume widths measured during the Prairie grass experiments and calculated with the recommended turbulence parameterisation implemented in a Lagrangian particle model for 3 source distances as a function of atmospheric stability (open symbols: measured values, solid symbols: model results).

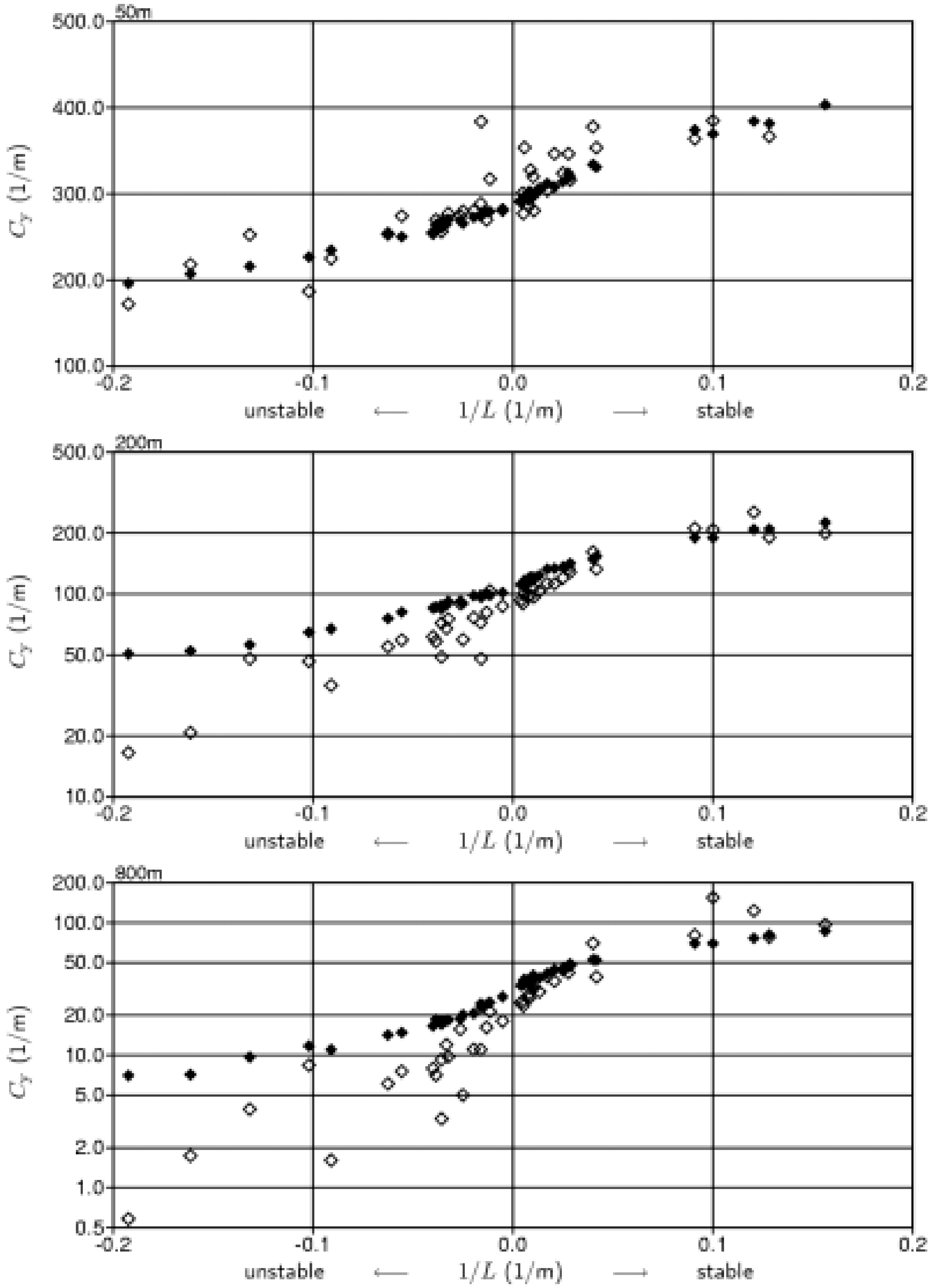

Figure 6: Comparison of cross wind integrated tracer concentration data as measured during the Prairie grass experiments and calculated using the recommended turbulence parameterisation together with a Lagrangian particle model for three source distances as a function of atmospheric stability (open symbols: measured data, closed symbols: model results).

References

Anfossi, D., G. Degrazia, E. Ferrero, S.E. Gryning, M.G. Morselli & S. Trini Castelli (1998). *Estimation of Kolmogorov constant C_0 from sonic anemometer measurements in the atmospheric surface layer.* 23rd NATO/CCMS International technical meeting on air pollution modelling and its application, preprints, Volume II, 443 – 449.

Barad, M.L. (1958). *Project Prairie Grass; a field program in diffusion; Vol. 1.* Geophysics Research Paper No. 59, Geophysics research directorate, Air Force Cambridge Research Center, Bedford, Massachusetts.

Bundesanzeiger (1990). *Allgemeine Verwaltungsvorschrift zu § 45 Strahlenschutz-verordnung: Ermittlung der Strahlenexposition durch die Ableitung radioaktiver Stoffe aus kerntechnischen Anlagen oder Einrichtungen.* Bundesanzeiger vom 31.03.1990.

Businger, J.A. et al. (1971). *Flux profile relationships in the atmospheric surface layer.* Journal of the atmospheric sciences, **28**, 181 - 189.

Buyn, D.W. (1990). *On the analytical solution of flux profile relationships for the atmospheric surface layer.* Journal of applied meteorology, **29**, 652 - 657.

Carruthers, D.J., R.J. Holroyd, J.C.R. Hunt, W.S.Weng, A.G. Robins, D.D. Apsley, F.B. Smith, D.J. Thomson & B. Hudson (1992). *UK Atmospheric dispersion modelling system.* Air pollution modelling and its application IX (eds. H. van Dop and G. Kallos), Plenum Press, New York.

Caughey, S.J. (1982). *Observed characteristics of the atmospheric boundary layer.* Atmospheric turbulence and air pollution modelling (eds. Nieuwstadt, F.T.M. and H. van Dop), D. Reidel Publ..

Du, S. (1997). *Universality of the Lagrangian velocity structure function constant (C_O) across different kinds of turbulence.* Boundary layer meteorology, **83**, 207 - 219.

GMBl (1986), *Erste allgemeine Verwaltungsvorschrift zum Bundes-Immissionsschutzgesetz (Technische Anleitung zur Reinhaltung der Luft – TA Luft) vom 27.02.1986.* GMBl., Ausg. A, **Bonn 28.02.1986**, 93 – 144.

Hanna, S.R. & D. G. Strimaitis (1990). *Rugged Terrain Effects on Diffusion(Chapter 6 in: Atmospheric Processes over Complex Terrain).* Meteorological Monographs, **23** (45), American Meteorological Society.

Holtslag, A.A.M. & F.T.M Nieuwstadt (1986). *Scaling the atmospheric boundary layer.* Boundary layer meteorology. **36**, 201 - 209.

Holtslag, A.A.M. & F.T.M Nieuwstadt (1987). *Reply to comments on 'Scaling the atmospheric boundary layer'.* Boundary layer meteorology, **38**, 415 - 416.

Kerschgens, M.J., C. Noelle & R. Martens (2000). *Comments on turbulence parameters for the calculation of dispersion in the atmospheric boundary layer.* Meteorologische Zeitschrift, **9**, 155 – 163.

KSP-Bericht (2000). *Validierung des "Kinematic Simulation Particle Model" (KSP-Modell) für Anwendungen im Vollzug des BImSchG*. Meteorologisches Institut der Universität Hamburg, Auftrag des Bundesumweltamtes, Forschungsbericht 98-295 43 354.

Lenschow, D.H. & J.C. Wyngaard (1980). *Mean field and second moment budgets in a baroclinic, convective boundary layer.* Journal of the atmospheric sciences, **37**, 1313-1326.

Luhar, A.K. & R.E. Britter (1989). *A random walk model for dispersion in inhomogeneous turbulence in a convective boundary layer.* Atmospheric environment, **23**, 1911-1989.

Paulson, C.A. (1970). *The mathematical representation of wind speed and temperature profiles in the unstable atmospheric surface layer.* Journal of applied meteorology, **9**, 857 - 861.

Rodean, H.C. (1996). *Stochastic Lagrangian models of turbulent diffusion.* Meteorological monographs, American meteorological society, **26** (48).

Rotach, M.W., S.E. Gryning & C. Tassone (1996). *A two dimensional Lagrangian stochastic dispersion model for daytime conditions.* Quarterly journal of the royal meteorological society, **122**, 367 - 389.

Shao, Y. (1992). *Turbulent dispersion in coastal atmospheric boundary layers: An application of a Lagrangian model*. Boundary layer meteorology, **59**, 363-385.

van Ulden, A.P. & A.A.M. Holtslag (1985). *Estimation of atmospheric boundary layer parameters for diffusion applications.* Journal of Climate and Applied Meteorology, **24**, 1196 - 1207.

VDI3783/6 (1992). *Regionale Ausbreitung von Luftverunreinigungen über komplexem Gelände, Modellierung des Windfeldes 1*, VDI-Handbuch Reinhaltung der Luft, Band 1, Beuth Verlag GmbH, Berlin.

VDI3945/1 (1995). *Gaußsches Wolken-Modell (Puffmodell)*, VDI-Handbuch Reinhaltung der Luft, Band 1, Beuth Verlag GmbH, Berlin.

VDI3945/3 (2000). *Atmosphärische Ausbreitungsmodelle – Partikelmodell.* VDI-Handbuch Reinhaltung der Luft, Band 1, Beuth Verlag GmbH, Berlin.

BUBBLE – current status of the experiment and planned investigation of the urban mixing height

Mathias W. Rotach[1], Valentin Mitev[2], Roland Vogt[3], Alain Clappier[4], Hans Richner[1] and Dominique Ruffieux[5]

[1]Swiss Federal Institute of Technology, Institute for Atmospheric and Climate Science, Zürich, Switzerland

[2]Observatory of Neuchâtel, Switzerland

[3]University of Basel, MCR-Lab, Switzerland

[4]Swiss Federal Institute of Technology, Laboratory of Soil and Air Pollution, Lausanne, Switzerland

[5]MeteoSwiss, Payerne, Switzerland

Introduction

BUBBLE stands for '**B**asel **U**r**B**an **B**oundary **L**ayer **E**xperiment' and is a research project directly associated to COST 715. Due to funding restrictions it has been a number of only Swiss research groups interested in urban meteorology (see list of authors) who have initiated this project. However, important commitments for contributing to the instrumentation and specific research objectives have been made by a large number of foreign institutions (Table I). While the Swiss 'core project' mainly covers the continuous long-term observations (Section 2.3), many of the supplementary projects during periods of intensive observation (IOPs), will be covered by research groups from all over the world.

The philosophy of BUBBLE is based on the recognition that over complicated and essentially inhomogeneous urban surfaces both the near-surface turbulence exchange processes and the entire boundary layer structure have to be observed at the same time. Often in the past only detailed near-surface observations were performed over urban surfaces, without taking into consideration the larger scales (e.g., Rotach 1993, Feigenwinter et al. 1999). On the other hand, in studies dealing with the entire urban boundary layer (e.g., Argentini et al. 1999; Menut et al. 1999) the near-surface observations are often missing or very sparse. Only in very recent urban studies such as ESCOMPTE (see F. Said, this volume), similar attempts as in BUBBLE were undertaken in order to combine remote sensing and near-surface in situ observations.

The present contribution summarises the observational and modelling strategies within BUBBLE and gives an overview over the mixing height determination means that will be available from the data set.

2 Observations

2.1 Near-surface sites

Two urban ('U'), one suburban ('S') and a rural reference ('R') surface sites are presently being set up. Such a site usually consists of the following components:

- Profiles up to a height larger than twice the obstacle height.
- U-sites: 6 levels of sonic anemometers (some of the levels: fast response hygrometers); S- and R-sites: 2 to 3 levels.
- Full radiation balance

- Additional observations such as mean meteorological observations; also at the urban sites, detailed measurements concerning the canyon thermal and radiative properties and turbulent fluxes of CO_2 are planned for short periods (IOP).

An overview of the city of Basel is shown in Fig. 1, where the sites are indicated. Additional 'industrial sites' are included for planning purposes, but the current budget and manpower doesn't allow for a realisation of those sites.

At the time of writing this report the four surface sites are being instrumented (Fig. 2 as an example) and it is expected that all of them are operational in late fall 2001.

Institution	**Country**	**Area of interest**	**Responsible scientist**
UBC	Canada	Radiative and thermal properties of street canyon	T.R. Oke
University of Western Ontario	Canada	Thermal properties of street canyon	J. Voogt
Indiana University	USA	Urban energy balance	C.S.B. Grimmond
Ohio State University	USA	Street canyon energy budget and climate models	A.J. Arnfield
National University of Singapore	Singapore	Turbulent exchange in the urban roughness sublayer	M. Roth
University of Tasmania	Australia	Radiative and thermal properties of street canyon	M. Nunez
Forschungs-zentrum Karlsruhe	Germany	Near-surface processes; thermal structure of urban boundary layer	N. Kalthoff
University of Freiburg	Germany	Urban boundary layer structure	H. Mayer
TU Dresden	Germany	Near-surface processes	Ch. Bernhofer
University of Padova	Italy	Near-surface processes	A. Pitacco

Table I Contributions to BUBBLE from institutions outside the 'core project'.

An instrument inter-comparison has been performed for some of the sonic anemometers prior to the mounting of the instruments. The analysis of this data set will be performed in a similar manner as in earlier projects (Christen et al. 2000) and will allow for a distinction between measurement uncertainties and true physical differences in the turbulence statistics of interest.

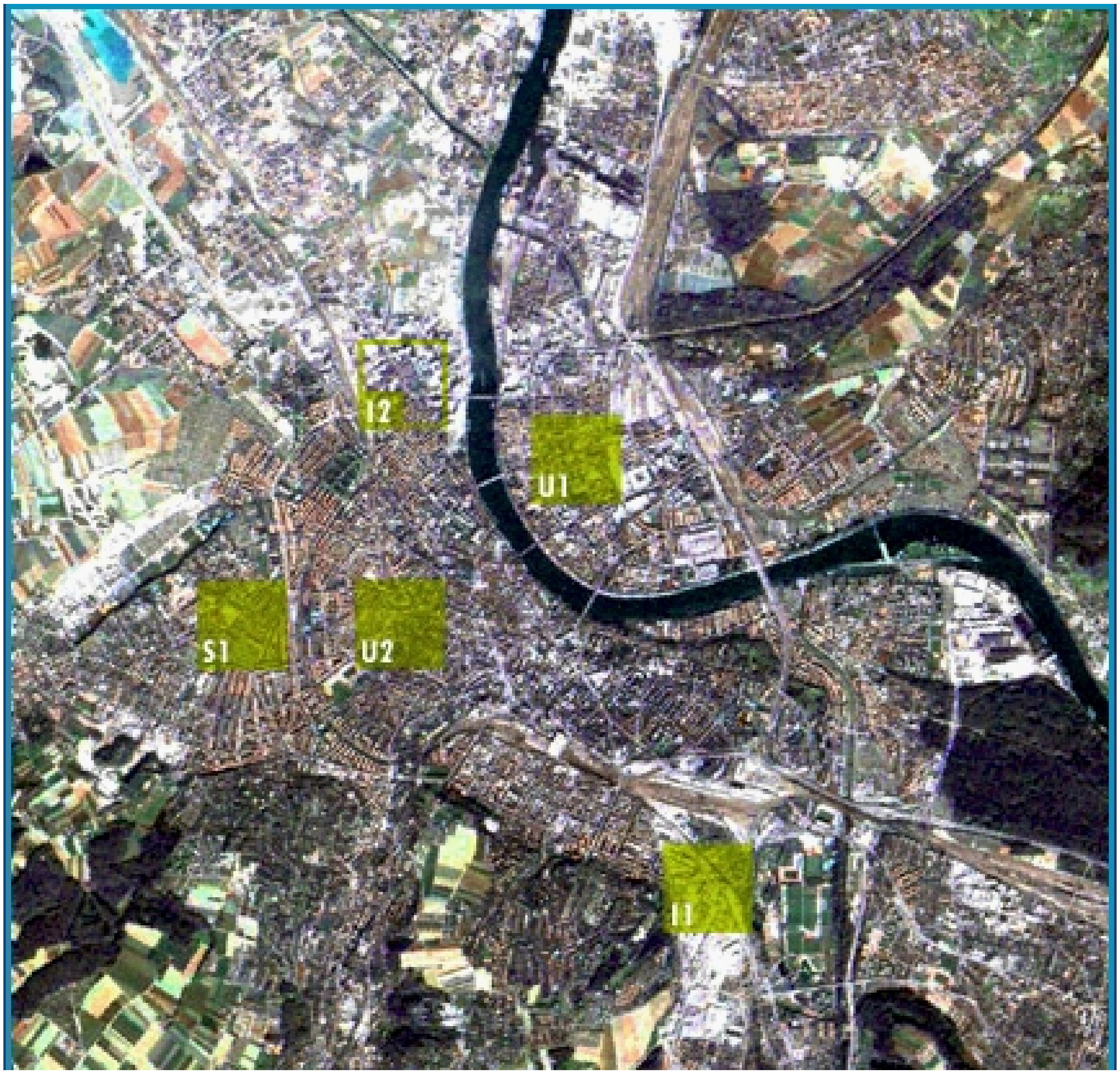

Fig. 1 Experimental programme of BUBBLE. Sites I1 and I2 (industrial surfaces) are not realised during the continuous observations, but possibly for an IOP. The rural site is situated in the northwest of the shown extract (Scale: approx. 1:5000).

2.2 Remote sensing

A Wind Profiler (pulsed Doppler Radar operating at 1290 MHz) has been installed in June 2001 at site U2 and is continuously measuring the profile of the three-dimensional mean wind speed since then. The instrument can be operated in a high-resolution mode (first gate at 83m, vertical resolution 45m) or at a lower resolution (first gate at 165m, vertical resolution 400m) and reaches a height of 4300m under ideal atmospheric conditions. It is expected to also retrieve profiles of some turbulence statistics from the profiler observations.

An aerosol backscatter Lidar has been installed during the month of October, also at site U2 and is continuously recording the aerosol distribution within the urban boundary layer and aloft. Its vertical resolution varies between 12 and 33m and it ranges up to a height of 3500m.

Fig. 2 Installation of tower at site U1 (Sperrstrasse). Some of the measurement levels within the street canyon are yet missing or not visible.

2.3 Observational period

All the mentioned observational systems will *continuously* be operated until August 2002, i.e., for almost one year. Additional instrumentation to probe the urban boundary layer structure (several Sodars, RASS, tethered balloon) is foreseen for selected periods of operation, i.e. Intensive Operation Periods (IOP's). Similarly, during the summer IOP (July 2002), additional efforts will be undertaken to probe in detail the thermal and radiative properties of the street canyon at site U1. These measurements will be performed by some of the foreign project partners.

3 Mixing height detection

A continuous detection of the urban boundary layer height will be available from the backscatter LIDAR signal at site U2. As a standard algorithm to retrieve the BL height from the LIDAR signal, the derivative of the backscatter signal profile will be used. Fig. 3 shows an example of this procedure, which does not stem from Basel but from the nearby small Swiss City of Neuchâtel. Between 600 and 900m a quite complex layering structure can be observed. Still, a clear shift in the range-corrected signal is observed around 800m. The derivative of this signal (Fig. 4) then indicates that the largest gradient occurs at 780m. Fig. 4 furthermore gives some evidence that higher levels are at least influenced by entrainment processes. Only for heights larger than 1000m this influence seems to be negligible.

Note that the example of Figs. 3 and 4 is a selected nice case. Much more complicated spatial and temporal structures in the urban boundary layer are expected to frequently occur in the city of Basel.

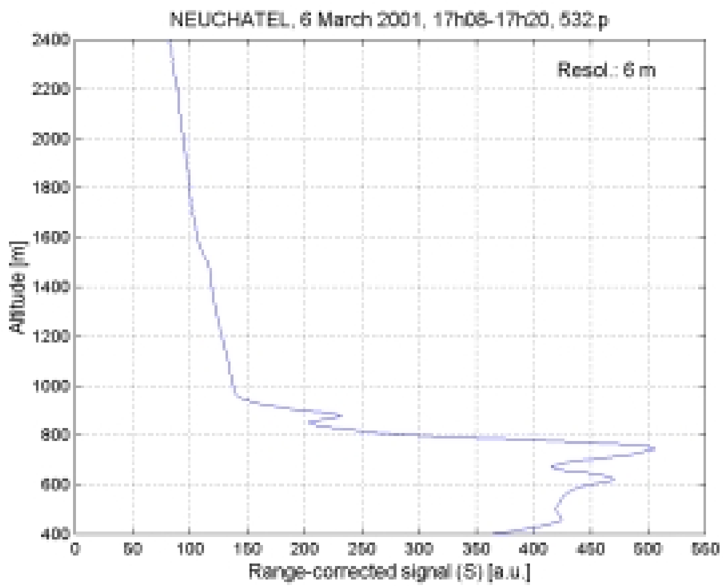

Fig. 3 *Backscatter Lidar range-corrected signal profile detected above Neuchâtel on March 6 2001. Time integration: 12 minutes; Altitude resolution: 6m; Altitude is above ground level.*

Other detection algorithms such as the one by Steyn et al. (1999) which is based on a prescribed profile of the backscatter signal will also be tested. During special periods the spatial and temporal evolution of the mixing height will be assessed from additional Sodar profiles (4 Sodars spread over the city), tethered balloon soundings outside the city centre and RASS.

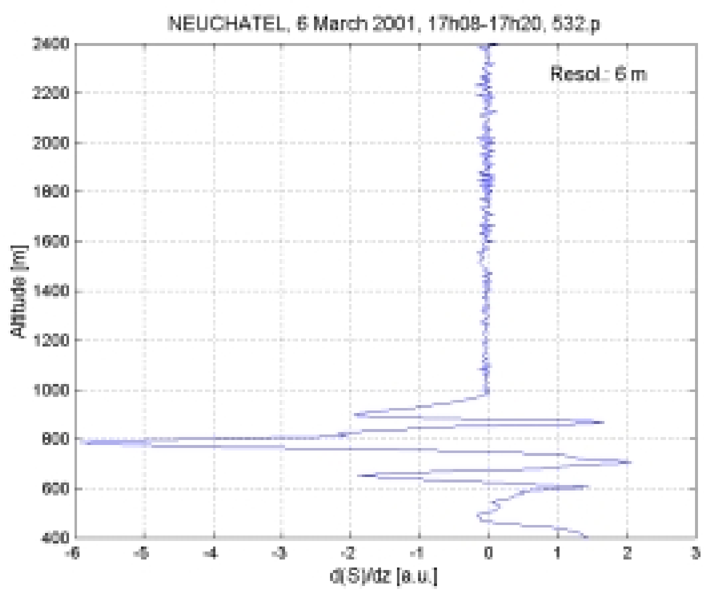

Fig. 4 *Gradient of the signal presented in Fig. 3. Time integration: 12 minutes; Altitude resolution: 6m; Altitude is above ground level.*

In addition, the abundance of available surface data will allow the evaluation of existing bulk- or slab-models (e.g., Batchvarova and Gryning 1991, Gryning and Batchvarova 1996). Even if these originally were not developed for urban surfaces, Gryning and Batchvarova (2001) argue that *in principle*, there is no reason why these approaches shouldn't apply – provided that representative 'surface' fluxes are available. With all the observed near-surface turbulence data it will be possible to assess to what extent these models can be used over urban surfaces. In summary we may recognise that large parts of instruments and methods as listed by Seibert et al. (2000) for the determination of the mixing height will be available during certain periods of BUBBLE.

4 Modelling

The observational activities within BUBBLE will yield a detailed data set covering the entire urban boundary layer over several months duration. This probably unprecedented data set will be exploited in order to investigate, validate and possibly improve the surface exchange parameterisation of Martilli (2001) which takes into account not only the rough character but also the modified thermodynamic and radiative properties of an urban surface. While the 'urban modification' in mesoscale numerical models is often restricted to modifying the roughness length (Craig and Bornstein, 2001) or only takes into account the thermodynamic aspect (e.g., Masson 2000), this approach allows for assessing the *relative* importance of roughness and thermodynamic properties, respectively over urban surfaces (Martilli 2002). Martilli et al. (2002a) show that this surface exchange parameterisation is able to reproduce many observed near-surface turbulence characteristics and Martilli et al. (2002b) successfully apply the numerical model in a case study in the region of Athens.

Dispersion modelling in the city of Basel will be performed using the approach of Rotach (2001) in which a Lagrangian particle dispersion model has been modified in such a way that observed near-surface turbulence characteristics are reproduced. Tracer experiments over urban surfaces are successfully reproduced with this model – but so far only cases with high sources are available. On the one hand, BUBBLE will provide more turbulence data from different types of urban surfaces in order to improve the employed empirical turbulence parameterisations. On the other hand, it is hoped to realise a tracer experiment with a low source height in the vicinity of roof level taking advantage of the detailed meteorological measurements during the experiment. De Haan et al. (2001) have modified a Gaussian plume dispersion model in a similar manner and have obtained large improvements with respect to 'traditional' approaches when simulating year-long NO_x surface concentrations in the city of Zürich. Similar simulations will be performed for the city of Basel using the network pollutant observations available there as a reference.

Acknowledgements

The BUBBLE project is supported by the Swiss Federal Ministry of Education and Science through contract # C00.0068. Substantial financial support is furthermore available through project or personal grants of the individuals listed in Table I.

References

Argentini, S; Mastrantonio, G. and Lena, F.: 1999, 'Case studies of the wintertime convective boundary-layer structure in the urban area of Milan, Italy', *Boundary-Layer Meteorol.*, **93**, 253-267.

Batchvarova, E. and Gryning S.E.: 1991, 'Applied model for the growth of the daytime mixed layer', *Boundary-Layer Meteorol*., **56** (3), 261-274.
Christen A.; van Gorsel, E; Andretta, M.; Calanca, P.; Rotach, M.W. and Vogt, R.: 2000, 'Field intercomparison of ultrasonic anemometers during the MAP-Riviera project', *Preprints Ninth Conference on Mountain Meteorology*, August 7–11 2000, Aspen, CO, 130-131.
Craig, K.J. and Bornstein, R.D.: 2001, ' Urbanisation of Numerical Mesoscale Models', in: Rotach, M.W.; Fisher, B. and Piringer, M. (Eds.): Workshop on 'Urban Boundary Layer Parameterisations', COST publication, subm. to the European Commission, 17-30.
Feigenwinter, C.; Vogt, R. and Parlow, E.: 1999, 'Vertical structure of selected turbulence characteristics above an urban canopy', *Theor. Appl. Clim*., **62** (1-2), 51-63.
De Haan, P.; Rotach, M.W. and Werfeli, M: 2001, 'Modification of an Operational Dispersion Model for Urban Applications', *J. Appl. Meteorol.*, **40**, No 5, 864-879.
Gryning, S.-E., and Batchvarova, E.: 'Mixing heights in urban areas: will 'rural' parameterisations work?', in: Rotach, M.W.; Fisher, B. and Piringer, M. (Eds.): Workshop on 'Urban Boundary Layer Parameterisations', COST publication, subm. to the European Commission, 99-109.
Gryning, S.-E., and Batchvarova, E.: 1996, 'A model for the height of the internal boundary layer over an area with an irregular coastline', *Boundary-Layer Meteorol.* **78**, 405-413.
Martilli, A.: 2001: 'Development of an Urban Turbulence Parameterisation for Mesoscale Atmospheric Models', Swiss Federal Institute of Technology Lausanne (EPFL), Dissertation # 2445, 176pp.
Martilli, A.: 2002: 'A Numerical study of the impact of an urban area on the airflow: sensitivity to synoptic wind speed and urban morphology', subm. to *J. Appl. Meteorol.*
Martilli, A.; Clappier, A. and Rotach, M.W.: 2002a, 'A Parameterisation of the Interactions between Urban Surfaces and the Atmosphere for Mesoscale Models', accepted *Boundary-Layer Meteorology*
Martilli, A.; Roulet, Y.A.; Jeunier, M.; Kirchner, F.; Rotach, M.W. and Clappier, A.: 2002b, 'Effect of an Urban Area on Air Pollution: the Athens Case', subm. to *Atmospheric Environ.*
Masson, V.: 2000, 'A physically-based scheme for the urban energy budget in atmospheric models', *Boundary-Layer Meteorol*., **94** (3): 357-397
Menut, L.; Flamant, C. and Pelon, J.: 1999, 'evidence of interaction between synoptic and local scales in the surface layer over the Paris area', *Boundary-Layer Meteorol*., **93**, 269-286.
Rotach, M.W.: 2001, 'Simulation of urban-scale dispersion using a Lagrangian stochastic dispersion model', *Boundary-Layer Meteorol.,* **99**, 379-410.
Rotach, M.W.: 1993, 'Turbulence Close to a Rough Urban Surface Part I: Reynolds Stress', *Boundary-Layer Meteorol.*, **65**, 1-28.
Seibert, P., Beyrich, F., Gryning, S-E., Joffre, S., Rasmussen, A. and Tercier, P.: 2000, 'Review and intercomparison of operational methods for the determination of the mixing height'. Atmospheric Environment **34**, 1001-1027.
Steyn, D.G.; Baldi, M. and Hoff, R.M.: 1999, 'The detection of mixed layer depth and entrainment zone thickness from Lidar backscatter profiles', *J Atmos. Oceanic Technol.*, **16** (7), 953-959

Influence of sea breeze and relief on the mixing height during ESCOMPTE in the Marseille area

Frédérique Said*, Bernard Campistron, Alexis Coppalle, Alain Dabas, Philippe Drobinsky, Emeric Fréjafon, Emmanuel Gizard, Alain Mériaux and Patrice Mestayer

*Laboratoire d'Aérologie UMR 5560, OMP, 14av. E. Belin, Toulouse, France

Introduction

ESCOMPTE 2001 is a field experiment that took place in the Marseille-Fos-Berre area, a polluted region of roughly 100x100 km in the South of France, from June 11 to July 13, 2001, with the aim of understanding transformation and transport of chemical constituents and to improve numerical models devoted to pollution study and forecasting. The Urban Boundary Layer program UBL/CLU was part of this overall experiment and the objective was to collect data to be able to study the specificity of the Marseille urban boundary layer and to improve local and mesoscale parameterisations of the agglomeration.

Experimental means to measure the Urban Boundary Layer Height during ESCOMPTE

The level of the mixing height was pointed out as a major information to be able to get, so several means were deployed to reach this information (see table).

Instrumentation	Location	Operation
Radiosoundings (CNRM)	Observatoire	June 26, 12 – 14 – 16 h, June 29, 10 – 14 h
Sodar (ECN-CNRS)	St. Jérome	June 12 – July 13, 7:00 – 16:00
Mini-Sodar (CORIA)	Near Ste. Marguerite	June 6-8; 11-15; 19-22; 25-29 July 2-6; 9-10, 6:30 – 20:00
UHF Profiler (CNRM)	Observatoire	Continuous operation
Sodar MERASS (Alliance Technologies)	Vallon Dole	June 12 ; 14-15 ; 20-23 July 2-5 ; 9-13, 7:00 – 17:30
Ozone Lidar (INERIS)	Observatoire Vallon Dole	July 10 – 13 July 14 - 15
Doppler Lidar LVT (LMD)	Vallon Dole	June 22-26 July 02-04, 7:00-19:00
Merlin flights	Marseille	6 flights
Falcon crossings	Marseille	7 flights
Fokker 27 crossings	Marseille	several

The knowledge of the mixing height is of major interest since it defines the layer where the effect of the town may be sensed and the possibility for an internal boundary layer to develop and to interfere with the surroundings. As far as this aspect is concerned, the problem is complicated in this peculiar area by the effect of sea-breeze and relief since Marseille is close to the sea and bordered by ridges to the South and to the East. For instance, the town temperature may differ from the surroundings which may shift the time, direction and strength of the sea-breeze. So the peculiar effect of this position is studied by comparison with the sea-breeze and valley flows in the non-urban areas, with the help of UHF radars and aircraft.

Preliminary results

Sodars and mini sodars can be used to detect the mixing height Z_i through the echo strength measurement. This method has not be validated yet. The Minisodar was situated on a building roof 15 m above ground near Ste. Marguerite hospital, SW of the town centre. The Minisodar's altitude range is limited to 15 – 200 m, with 5 m increments. Thus, it allows for the detection of Z_i within that range only, primarily at night-time. The RASS system associated to an UHF radar in Vallon Dole provides information on Z_i from a larger vertical range, but this has also not been validated yet.

An angular ozone lidar was operated at Vallon Dole. The extinction coefficient retrieved through an angular exploration towards the town shows several layers with varying aerosol concentration, inside the mixed layer and above. The ozone profiler operated at Cadarache, to the north of the ESCOMPTE area, outside of Marseille, confirms the temporal variation of the stratification through the ozone concentration.

The positioning of the UHF radars inside the town as well as at St. Chamas outside Marseille allows for a comparison of urban and rural conditions. IOP (Intensive Operation Period) 2 was divided into a Mistral episode between 21 and 23 June and a sea breeze episode between 24 and 26 June. The Mistral episode was characterized by strong North West synoptic wind both at St Chamas as well as inside the town, the latter station showing higher windspeeds between 1 and 3 km above ground. The sea breeze in the low layers was captured similarly by both instruments. The radar also provides an information about the turbulence through the dissipation rate of the turbulent kinetic energy which shows stronger rates of turbulence inside the town by a factor of about 10. The evolution of Cn^2 with maximum values during the day time, which enables to provide the upper boundary of the mixed layer, shows the same evolution at the two sites. A comparison between the urban UHF and radiosounding estimates of Z_i for 26 June indicates the influence of the sea breeze for the mixed layer, reducing, on that particular day, the mixing height in the afternoon from about 1030 to 830 m within two hours.

The mobile wind lidar LVT was implemented at Vallon Dole and operated according to 2 different operation schemes: In the scheme "Escompte", six vertical planes on a circle with 30° increments were used for turbulence measurements; in the scheme UBL/CLU, 18 vertical planes on half a circle with 10° increments directed towards Marseille were used. A scan along two planes (one towards the town and the other towards the sea), taken on 26 June during IOP 2b, clearly allows to distinguish the aerosol layer corresponding to the mixed layer in both cases, and the radial velocity field will enable to compare the vertical development of the sea breeze.

The Merlin aircraft from Meteo France performed several flights especially devoted to the UBL project. On 26 June, it took two tracks crossing the town, with three levels in the mixed layer and and one above (maximum height about 3000 m). The condensation level can be assumed to be the mixed layer upper boundary in case of low level clouds. In this case, there were no low level clouds and the condensation level was rejected upwards. It may be noted that the crossing of Marseille only takes 3 minutes with the Merlin, and half this time with the Falcon.

On 25 June, 16:00 to 16:30, the Falcon performed another town crossing with the WIND lidar on board which provided the vertical distribution of the horizontal wind vector along the flight track. Crossing the Marseille area on that particular day, the area of the sea breeze could well be discerned from that of the synoptic wind.

The stratification of the lower troposphere that has been highlighted with the other means is also seen in the aircraft data. On a vertical sounding performed by the ARAT (outside Marseille) on 25 June, 11:00, distinct superposed layers can be observed through various parameters such as water vapor content, ozone, aerosols. These stable layers are also visible on the radar reflectivity profiles in Marseille or at St Chamas and raise 2 problems: a metrological problem which is the difficulty to detect the top of the mixed layer; a scientific question which is to understand the interaction of these stratified layers and the underlying mixed layer.

Conclusion

Summing up, the status of the different means to detect Z_i is as follows:

The most promising means are the lidars and radars that provide the time variation of Z_i. These data have to be validated due to non-academic aerosol, ozone and water vapour layers. The Lidar-equipped airplane is potentially useful, however, it had a very short crossing time of Marseille. Aircraft with in-situ measurements will only provide few information since low level clouds necessary to deduce the mixing height from the condensation level, were seldom present. Therefore, the complexity of the vertical stratification of the low boundary layer implies to validate also the usual methodologies used to retrieve Z_i, as the echo profiles from Minisodars or the virtual temperature profile from the Sodar/RASS.

Mixing Heights calculations by MM5 and simple pre-processors for atmospheric dispersion modelling

A. Dandou, M. Tombrou, E. Akylas and D. Boucouvala

Department of Physics, University of Athens, Greece

Correspondence address:
Ass. Professor Maria Tombrou
National and Kapodistrian University of Athens
Department of Physics, Division of Applied Physics
Laboratory of Meteorology
Panepistimioupolis, Bd. Physics V,
GR - 157 84 Athens, Greece
Tel: + 3010-72.76.935 / 837
Fax: + 301-72.95.281
E-mail: mtombrou@cc.uoa.gr

Keywords: Mixing Height, Planetary Boundary Layer, Nocturnal Boundary Layer

Abstract
In the present study, the mixing height was calculated by the meso-scale MM5 model, by using different parameterization closure schemes. The domain of study was the extended area of Lombardy in Italy and the simulations were performed for one winter and one autumn day. The model's results were compared with radiosondes, available at Milan's station.

1. Introduction

The mixing height is an important meteorological parameter to the prediction of pollutant concentrations, so large effort is being made in order to improve its estimation. Convection or mechanical turbulence disperses the pollutants released at the surface vertically, within an hour or less, up to the upper level, which is defined by the mixing height (Beyrich at. al., 1996). Nonetheless, there is still no unique definition and no overall accepted method of calculating the mixing height. As a result, the determination of the mixed layer depth is often ambiguous under realistic atmospheric conditions, even over relatively homogeneous terrain. Apart from the radiosonde ascents that still provide the most common database for mixing height estimation, also sodars, wind profiler/RASS systems and lidars are increasingly used to determine reliable values for the mixing height (Piringer et al., 1998). However, mixing height values derived from measurements are available, if at all, at specific sites and partly also for limited time periods only, so that parameterizations are widely used. The so-called meteorological pre-processors that have been developed to compute the mixing height are based on the 'horizontal homogeneity' approximation. In complex terrain however, the effects of horizontal advection need also to be included in the calculations. In these cases meteorological dynamical models are used to supply the atmospheric dispersion models with the necessary input parameters.

Due to the ambiguity on the definition of the mixing height, various parameterization schemes have been implemented in the meteorological dynamical models, in order to attend different meteorological conditions. This results to the user's confusion in selecting the most appropriate scheme for his application. In this work, the meteorological dynamic model Penn

State/NCAR Mesoscale Model MM5 (Anthes and Warner, 1978) was used to calculate the mixing height (MH) in an area with strong horizontal in-homogeneity. In particular, the various parameterization closure schemes, provided by the model, were tested in the greater Lombardy area in Northern Italy for both day and night on 6-2-1998 and on 12-9-1999. The model's results were compared with the available radiosoundings for each day, performed in Milan's station.

2. Models / Parameterization Schemes

The Penn State/NCAR Mesoscale Model MM5 is a numerical weather prediction model, which can be used for a broad spectrum of theoretical and real time studies, including applications of both predictive simulation and four-dimensional data assimilation to monsoons, hurricanes and cyclones. On the smaller meso-beta and meso-gamma scales (2-200 km), the model can be used for studies involving mesoscale convective systems, fronts, land-sea breezes, mountain-valley circulation and urban heat islands. The model can be either hydrostatic or non-hydrostatic.

The model includes 7 different schemes in order to parameterize the planetary boundary layer processes:

- *Bulk PBL*, based on bulk-aerodynamic parameterization, suitable for coarse vertical resolution in the boundary layer, e.g.>250m vertical grid sizes. It considers two stability regimes.
- *High-resolution Blackadar PBL*, (Zhang and Anthes, 1982), suitable for high resolution PBL, e.g. 5 layers in the lowest km, surface layer<100m thick. Four stability regimes, including free convective mixed layer.
- *Burk-Thomson PBL*, based on Mellor-Yamada formulas (Burk and Thompson, 1989). Suitable for high resolution PBL. Predicts TKE (Turbulent Kinetic Energy) for use in vertical mixing. It has its own force-restore ground temperature prediction.
- *Eta PBL*, Mellor-Yamada scheme (Janjic, 1990, 1994). It predicts TKE and has local vertical mixing.
- *Gayno-Seaman PBL*, based on Mellor-Yamada TKE prediction (Ballard et al., 1991). It uses liquid-water potential temperature as a conserved variable, allowing the PBL to operate more accurately in saturated conditions.
- *MRF PBL,* based on Troen-Mahrt representation for countergradient term and K profile in the well mixed PBL (Hong and Pan, 1996)
- *Pleim-Chang PBL*, the Asymmetric Convective Model, using a variation on Blackadar's non-local vertical mixing (Pleim and Chang, 1992)

The first 5 schemes are based on local parameters while the last 2 involve non-local parameters and are considered more suitable for strongly unstable conditions.

3. PBL calculations with different parameterization schemes

The area, where we applied the model, is the greater Lombardy area in Northern Italy (Fig.1). The area of interest is the 2nd nested domain in the model. At the borders the boundary conditions provided by the 1st domain prevail. Thus, the values at the edges are expected to have lower reliability. The model runs continuously for one winter day, the 6th of February 1998 and one autumn day, the 12th of September 1999, for each one of the selected parameterization schemes. In this particular study the MRF, the High-resolution Blackadar and the Gayno-Seaman parameterization schemes were applied with the version V3-4 of the MM5 model.

The model's simulations show a homogeneous mixing height in the basin, which is well explained by the hour of the calculation. In the mountainous area, both North and South of the domain, the mixing height strongly varies following the local topography. The maximum values of mixing heights were calculated above the mountain crests. In particular, for the winter day the values of mixing heights at the basin, provided by the local parameterization schemes, were the lowest. For the Blackadar scheme (Fig. 2) the heights reach altitudes of 250-300m, while for the Gayno-Seaman (Fig. 3) they are up to 200-250m. The corresponding values, provided by the MRF non-local scheme, were much higher, up to 400-500m (Fig. 4). During the autumn day the mixing heights were estimated substantially larger in accordance with the atmospheric conditions that were prevailing in the basin. The local scheme of Blackadar indicated values around 1100-1300m (Fig.5) while the MRF showed values up to 1800-2000m (Fig.6). During the night the two non-local schemes give almost zero values of the mixing height for both days, while the MRF scheme gives values around 50m on the winter day and around 100-150m on the autumn day. In Figs. 1 to 6, the numbers on both axes refer to grid cell numbers. The (x 2km) refers to the resolution of the grid cell.

Thereafter, the calculated diurnal variation of the mixing height by using different PBL parameterization schemes (Fig 7 and 9) is compared with the available radiosoundings, taken from Milan, for both days. The potential temperature profiles taken from Milan's station are given in Figures 8 and 10. It should be mentioned that the height presented in the radiosoundings is Above Sea Level (ASL), so the station's elevation (103m) should be abstracted in order to compare the model's results with the inversion height.

The estimation of mixing heights from the radiosoundings was performed using a technique suggested by Heffter (1980). In this method, potential temperature profiles are computed for each sounding. The profiles are analyzed for the existence of a 'critical inversion', which is assumed to mark the top of the mixed layer. In this scheme, a critical inversion is defined as the lowest inversion that meets the following two criteria:

$$\Delta\theta / \Delta Z \geq 0.005 K m^{-1} \qquad (1)$$

$$\theta_{top} - \theta_{base} \geq 2K \qquad (2)$$

where $\Delta\theta / \Delta Z$ is the potential temperature lapse rate in the inversion layer and θ_{top} and θ_{base} refer to the potential temperatures at the top and bottom of the critical inversion layer. The height of the mixing layer is that point in the inversion layer at which the temperature is 2^{o}K above the temperature at the inversion base. This method was selected for use because it recognizes the likelihood of mixing (caused by buoyant thermals) to overshoot the base of the critical inversion. This physical process is overlooked in many similar schemes. This scheme has also been considered in the studies of Marsik et al., 1995 and Piringer et al., 1998.

On 6-2-1998 a mixing height of 379m ASL at 12:00 UT is deduced from the potential temperature profile (Fig. 8), based on the method described above. This value is in relative good accordance with the Blackadar scheme (Fig. 7). During the night a temperature inversion is apparent; thus, the development of mixing height can only be attributed to the wind shear. The value of 50m provided by the MRF scheme is considered more reliable than the zero value, calculated by the other two local schemes. On the autumn day, the mixing height derived from the potential temperature's profile (Fig. 10), using the same method, is up to 1980m ASL at 12:00 UT. This is in good agreement with the values calculated by the MRF scheme, as presented in Figure 9. During the night, the non-local MRF scheme gives a mixing height up to 100m (Fig. 9), which is also in good relation with the radiosounding's inversion height.

4. Conclusions-Future work

From the limited results presented above, it is apparent that during strong convection the MRF seems to be the most appropriate closure scheme. However, during the winter day it seems to overestimate the mixing height. The nocturnal mixing height, which depicts the layer where the pollutants are blended, is poorly predicted by the examined schemes.

Further to the above work, an effort is made to implement current advanced parameterization schemes (Zilitinkevich et al., 1998, Akylas et al., 2001) into the model. In particular we focus on the strongly unstable regimes over rough areas.

Especially for the Nocturnal Boundary Layer (NBL), the work will be continued with the collaboration with San Jose University. The area under investigation is the basin of Los Angeles, where datasets of surface measurements from 110 surface sites, performed during the Southern California Ozone Study (SCOS97) as well as data from profilers and rawinsondes are available. Moreover, the simple meteorological pre-processors addressed for the Nocturnal Boundary Layer, (Tombrou et al., 1998) will be applied in the Los Angeles basin for the 4-7 August 1997. In this case, the calculations of mixing heights will be performed by considering two sets of data, separately: a) surface measurements and b) the atmospheric parameters calculated by the MM5 model, with the Mellor-Yamada parameterization scheme (Ballard et al., 1991). Thereafter, the resulting NBL values will be compared to vertical measured data (profilers and rawinsondes) through the maximum winds and inversion heights as well as to the theoretical calculations from the MM5 model.

Figures

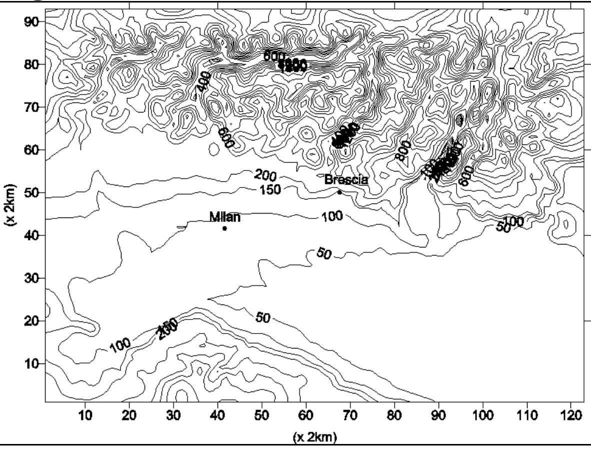

Figure 1: The greater Lombardy area (Northern Italy)

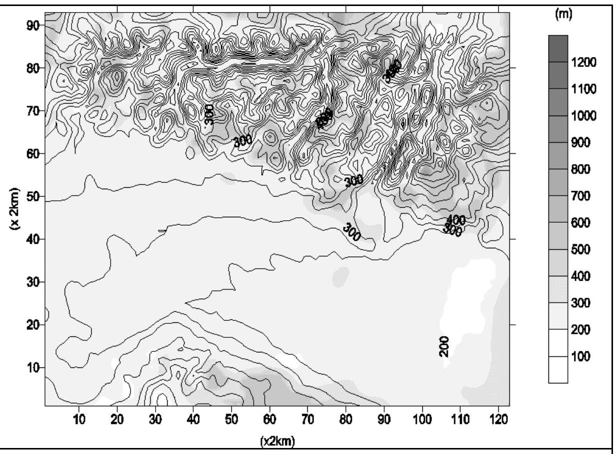

Figure 2: High-resolution Blackadar PBL mixing heights on 6-2-1998 at 12:00 UT

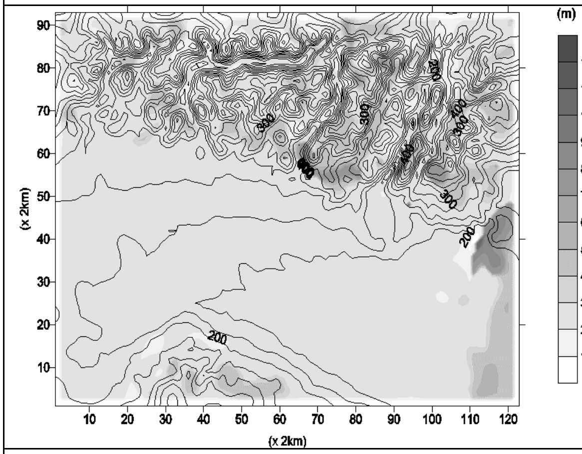

Figure 3: Gayno-Seamen PBL mixing heights on 6-2-1998 at 12:00 UT

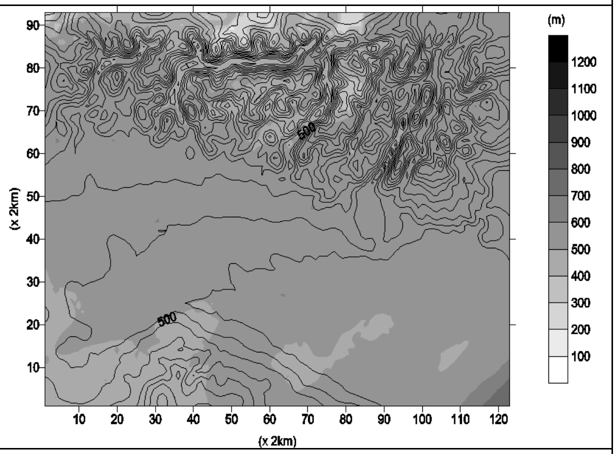

Figure 4: MRF PBL mixing heights on 6-2-1998 at 12:00 UT

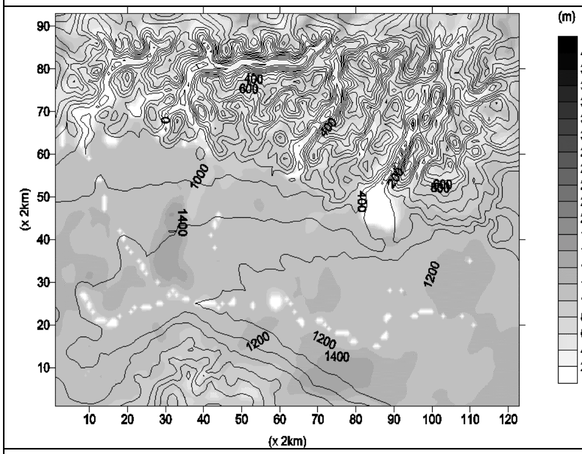

Figure 5: High-resolution Blackadar PBL mixing heights on 12-9-2-1999 at 12:00 UT

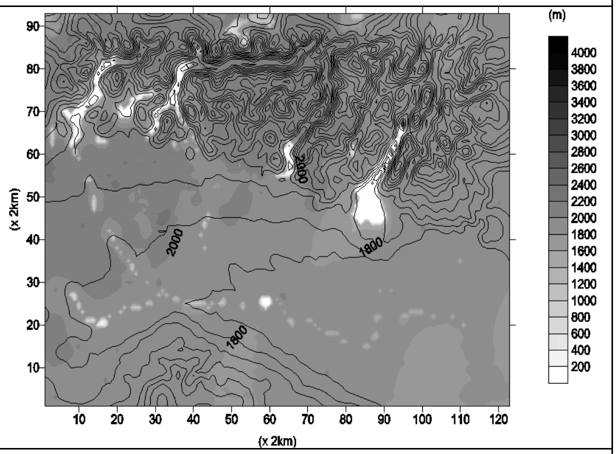

Figure 6: MRF PBL mixing heights on 12-9-1999 at 12:00 UT

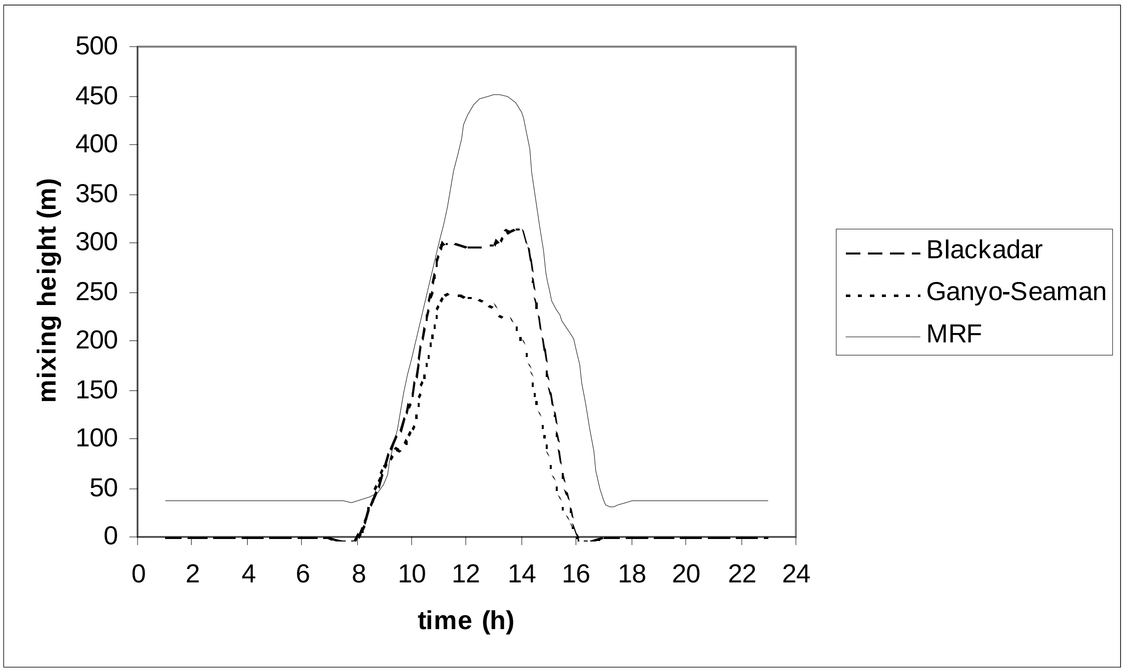

Figure 7: Diurnal variation of mixing height with differnet PBL schemes in Milan on 6-2-1998

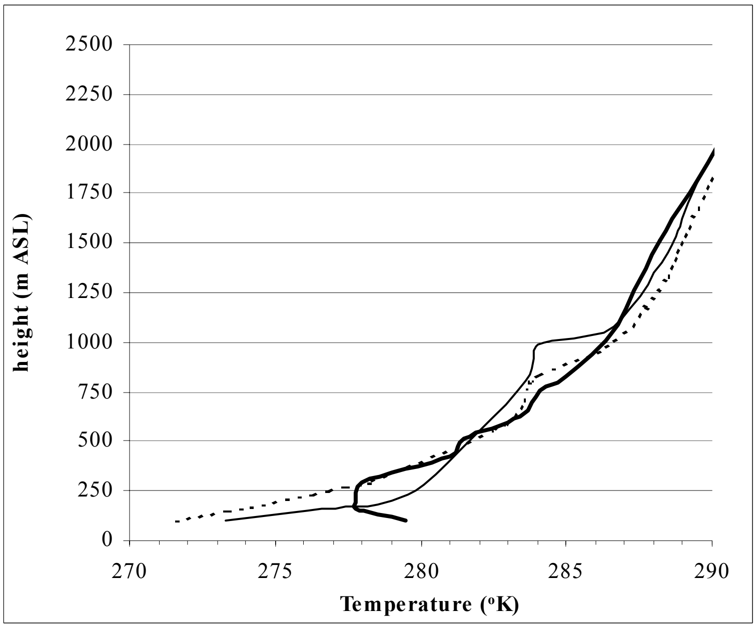

Figure 8: Potential temperature profiles taken from Milan's station on 6-2-1998 at a) 0:00 UT (——) b) 6:00 UT (..........) and c) 12:00 UT (▬▬)

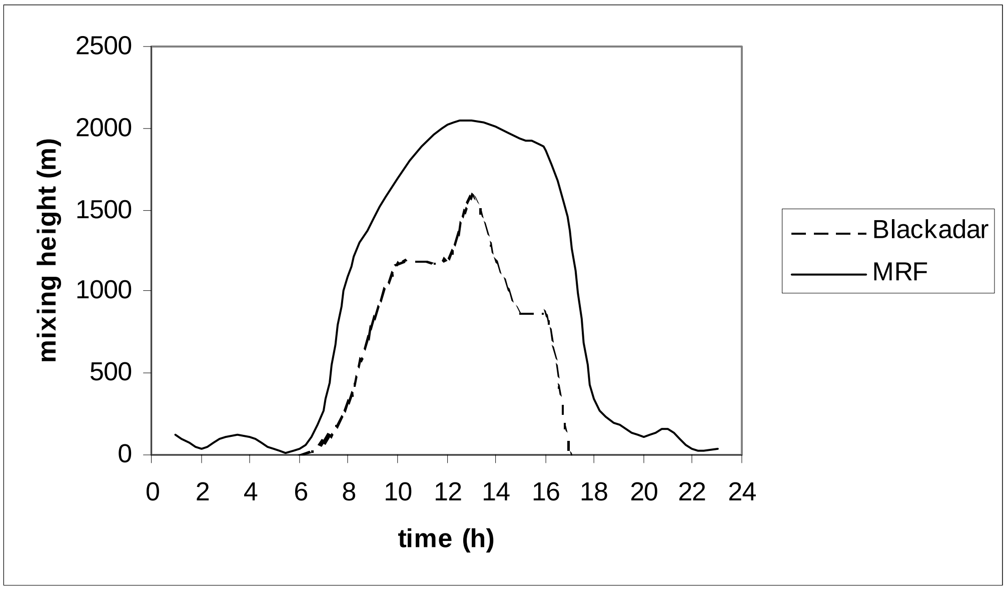

Figure 9: Diurnal variation of mixing height with differnet PBL schemes in Milan on 12-9-1999

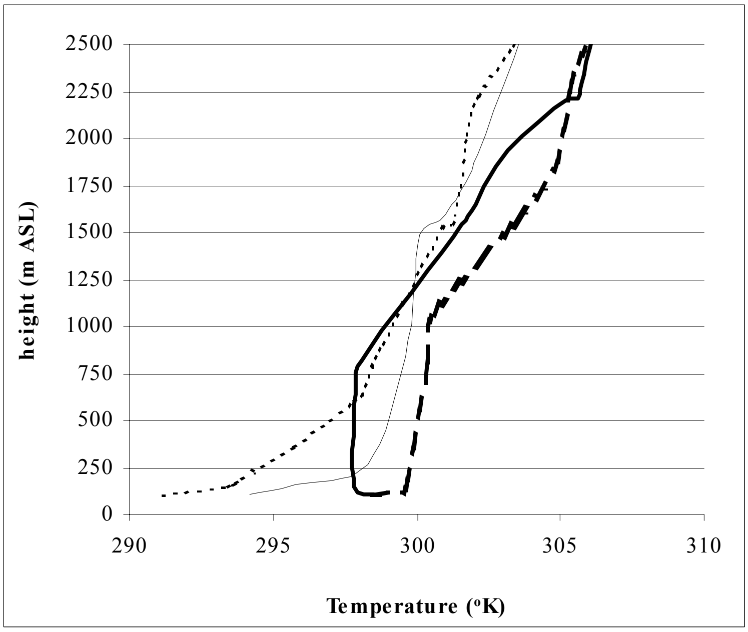

Figure 10: Potential temperature profiles taken from Milan's station on 12-9-1999 at a) 0:00 UT ( ) b) 6:00 UT ( ) c) 12:00 UT ( ) and d) 18:00 UT ( )

References

Akylas, E., M. Tombrou, D. Lalas, and S. Zilitinkevich, (2001a). '*Surface fluxes under shear-free convection'*. Quart. J. Roy. Meteorol. Soc., **127**, pp.1-15.

Anthes, R.A. and Warner, T.T., (1978). *'Development of hydrodynamic models suitable for air pollution and other meso-meteorological studies'*, Mon. Wea. Rev., **106**, pp. 1045-1078.

Ballard, S.P., Golding B.W. and Smith R.N., (1991). *'Mesoscale model experimental Forecasts of the Haar of Northeast Scotland'*, Mon. Wea. Rev., **119**, pp. 2107-2123.

Beyrich, F., Gryning, S.E., Joffre, S., Rasmussen, A., Seibert, P. and Tercier, P., (1996). *'On the Determination of mixing Height: A Review'*, Proc. of the 4th Workshop on Harmonisation within Atmospheric Dispersion Modelling for Regulatory Purposes, 6-9 May 1996, Oostende, Belgium, pp. 155-162.

Burk S. D. and Thomson W.T., (1989). *'A vertically nested regional numerical prediction model with second order closure physics'*. Mon. Wea. Rev., **117**, pp. 2305-2324.

Heffter J. L., (1980). *'Air resources laboratories atmospheric transport and dispersion model'*. NOAA Tech. Memo. ERL ARL **-81**, pp.24.

Hong S.-Y. and Pan H.-L., (1996). '*Nonlocal boundary layer vertical diffusion in a medium-range forecast model'*. Mon. Wea. Rev., **124**, pp. 2322-2339.

Janjinc Zavisa I., (1994). *'The step-mountain eta coordinate model: Further development of the convection, viscous sublayer and turbulent closure schemes'*. Mon. Wea. Rev., **122**, pp.927-945.

Marsik F.J., Kenneth W.F., Tracey D.M., Perry J.S., (1995). *'Comparison of Methods for Estimating Mixing height Used during the 1992 Atlanta Field Intensive'*, J. Appl. Meteor., **34**, pp. 1802-1814.

Pleim J.E. and Chang J.S., (1992). *'A non local model for vertical mixing in the convective boundary layer'*, Atmos. Environ., **26A**, pp. 965-981.

Piringer, M., Baumann K. and Langer, M., (1998). *'Summertime mixing heights at Vienna, Austria, estimated from vertical soundings and by a numerical model',* Boundary-Layer Meteorol., **89**, pp. 25-45.

Tombrou M., E. Founda and D. Boucouvala, (1998).'Nocturnal boundary layer height prediction from surface routine meteorological data'*, Meteorology and Atmospheric Physics, **68**, pp.77-186.*

Zhang D. and Anthes R.A., (1982).'Nocturnal boundary layer height prediction from surface routine meteorological data'*, J. Appl. Meteor., **21**, pp.1594-1609.*

Analysis of Air Pollution Episodes in European Cities

Ranjeet S Sokhi[1], Lakhu Luhana[1], Jaakko Kukkonen[2], Erik Berge[3], Leiv Harvard Slördal[4] and Sandro Finardi[5]

1. ASRG, Department of Environmental Sciences, University of Hertfordshire, Hatfield, AL10 9AB, UK
2. Finnish Meteorological Institute FMI, Air Quality Research, Sahaajankatu 20 E, FIN-00880 Helsinki, FINLAND
3. The Norwegian Meteorological Institute DNMI, Postboks 43, Blindern, N-0313 Oslo, NORWAY
4. The Norwegian Institute for Air Research NILU, Instituttvn 18, PO Box 100, N-2027 Kjeller, NORWAY
5. ARIANET, viale Elvezia 42, 20052 Monza (MI), ITALY

Abstract

This paper reports on the preliminary analysis of air pollution episodes in several European cities: London, Oslo, Milan and Helsinki. Examples of episodes of PM_{10}, NO_2 and O_3 are presented and the causes are examined in relation to local emissions and meteorological conditions. Similarities and differences in relation to the importance of meteorological conditions including inversions are discussed for these major urban regions. The frequency of low wind speed (< 2 m/s) conditions is significant in all of these cities; for example, in London and Helsinki these frequences are typically of the order of 25 and 45 %, respectively. For both particulate matter and nitrogen oxides, low lying inversion and low wind speeds are particularly important in that they tend to lead to high concentration of air pollutants. In the case of PM_{10} episodes, sources such as wood burning and resuspended particulate matter from street surfaces are important in Northern European cities, such as Oslo and Helsinki. Within the UK, studies have indicated that PM_{10} episodes have been caused by air masses bringing high loadings of secondary particles. For NO_2, measurements at three sites within London registered daily averaged concentrations above 200 $\mu g/m^3$ during December 1994. Hourly maximum value during this period at London Bloomsbury showed concentrations reaching 400 $\mu g/m^3$ whilst the wind speeds were at or below 1 m/s. In Milan, episodes of NO_2 are common during anticyclonic conditions with persistent weak wind fields.

1. Introduction

This paper forms part of the work of the COST 715 action "Meteorology Applied to Urban Air Pollution Problems" (e.g., Fisher et al., 2001). It is produced within the above-mentioned action by Working Group 3 “Meteorology during peak pollution episodes”. This paper aims to undertake a preliminary analysis of episodes of PM_{10}, NO_2 and O_3 in four selected European cities, London, Oslo, Milan and Helsinki.

Air pollution episodes in and around cities can pose a serious hazard to human health. Under episodic conditions concentrations of air pollutants such as O_3, NO_2 and particulate matter (measured, e.g., as the mass fractions PM_{10} and $PM_{2.5}$) can considerably exceed national and international standards and limit values (e.g., QUARG 1993, 1996 and Kukkonen, 2001a). The causes of air pollution episodes are complex and depend on various factors including emissions, meteorological parameters, topography, atmospheric chemical processes and solar radiation. The relative importance of such factors is dependent on the climatic, geographical region and the season of the year. For example, particle episodes in many cities have been experienced in winter and spring times. Nitrogen dioxide episodes can occur both in winter and in summer, and ozone levels can be particularly high during summer periods.

Inversions, which lead to stagnant air, are particularly important in relation to episodes and in many cases are responsible for very high levels of pollution (e.g., Karppinen et al., 2001). In addition, regional and long-range transport of pollution, for example fine particulate matter, can also lead to standards being exceeded. Consequently, it is vital to understand the underlying processes on local, regional and continental scales that lead to air pollution episodes. However, as many of the causal factors have varying degree of importance in different regions, an international comparison of cities has been initiated.

For example, in the UK the occurrences of low wind speed (< 2m/s) conditions for the years 1996-1999 was found to be around 25 % using hourly wind data measured at the Heathrow site, see Figure 1. In comparison, the percentage of low wind speed values was 46.0 % above the building roof level (building height 23.0 m, mast height 3.4 m) in Runeberg Street in central Helsinki in 1997. A more rigorous analysis of meteorological conditions relevant to air pollution episodes in the UK has been reported by Middleton and Dixon (2002). Overall, the distribution of meteorological conditions vary from year to year and can have a dramatic impact on the air quality. As reported by Middleton and Dixon (2002) the levels of PM_{10} were exceptionally low for 1998 whereas during 1996 exhibited high PM_{10} concentrations. The authors have also discussed the important role of transboundary contributions especially in relation secondary particles.

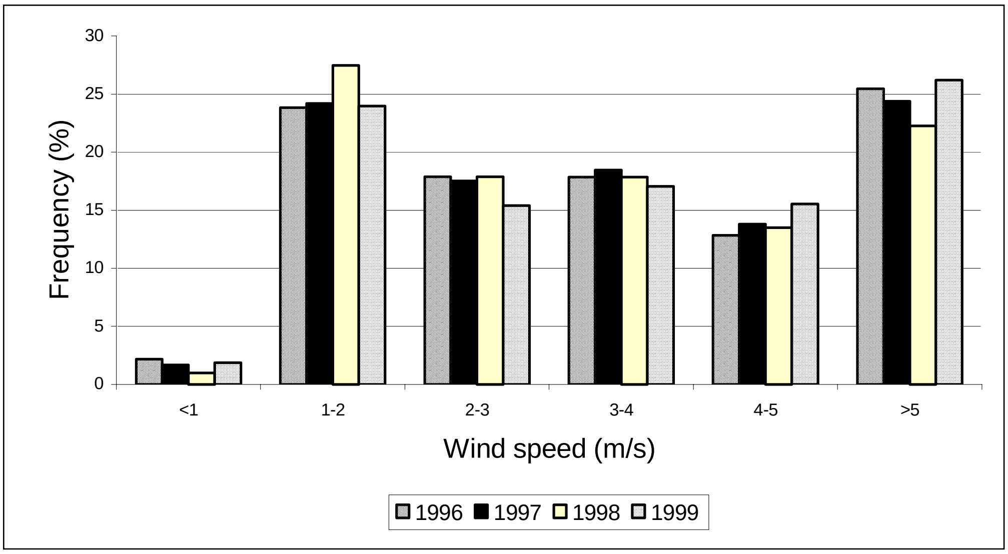

Figure 1. Wind speed frequency for London for 1996-99. Source: British Atmospheric Data Centre, for site at Heathrow, London.

An internationally accepted definition of an air pollution episode does not currently exist. In general an ‘air pollution episode’ is thought to occur when concentrations of a particular pollutant are at an exceptionally high level, with regard to the national or international limit or guideline values. The duration of high concentrations is also important in designating an ‘episode’ and will depend on the main sources as well as on the prevailing weather patterns. It is common for episodes to last for a few hours to a few days depending on the pollutant and meteorological conditions. For examples, for NO_2 the duration can be several hours whereas for PM_{10} the duration can be the order of days. For air quality management purposes levels of pollutants are normally compared with national or international standards or limit values. The current EU limit values for PM_{10}, NO_2 and O_3 are listed in Table 1.

Table 1. EU Limit values for PM10, NO2 (Council Directive 96/622/EC and 1999/30/EC) and O3 (Council Directive 92/72/EC).

Pollutant	**Averaging period**	**Limit Value**
NO_2	Hourly Annual	200 μg/m^3 not to be exceeded more than 18 times a calendar year 40 μg/m^3 (to be achieved by 1 Jan 2010)
PM_{10}	24 hour Annual	50 μg/m^3 not to be exceeded more than 35 times a calendar year 40 μg/m^3 (to be achieved by 1 Jan 2005)
O_3	8 hour (non-overlapping moving average)	110 μg/m^3 (Health protection threshold)

In addition to the concentration values, the averaging period and the measure of tolerance for each pollutant is indicated in Table 1. Therefore, when designating an air pollution event as an ‘episode’ for air quality management purposes, the duration and frequency has to be taken into account. For example, for PM_{10} concentrations, one of the limit values is measured as a 24 hour mean and exceedances are allowed for 35 days over a calendar year.

2. PM_{10} Episodes

PM_{10} episodes are most common during spring or wintertime. This is the case in cities such as Oslo, Helsinki and London. Middleton and Dixon (2002) have analysed a large dataset of PM_{10} concentrations and meteorological conditions spanning from 1949 to 1997. Variables such as wind speed, wind direction and temperature were used to investigate the occurrences of episodes. In particular to a London site (Bloomsbury), the authors found that the easterly direction was especially important in relation to secondary particulate matter.

In Helsinki, PM_{10} episodes occur most commonly in spring, and these are usually related to the resuspended particulate matter from the street surfaces (Kukkonen et al., 1999 and 2001b, Pohjola et al., 2002). During spring and autumn seasons there is significant resuspension of road dust caused by sanding of the streets and wear by tyre studs.

Figure 2 shows PM_{10} and $PM_{2.5}$ episodes during March 1998 at two sites in central Helsinki. Episodes such as these usually last from one to a few days. The elevated PM concentrations during the 1998 March episode were clearly related to conditions of high atmospheric pressure, relatively low ambient temperatures and low wind speeds in predominantly stable atmospheric conditions (Pohjola et al., 2002). The analysis of this episode has shown that the high PM_{10} concentrations originated mainly from local vehicular traffic (direct emissions) coupled with contributions from resuspended dust, while a substantial fraction of the $PM_{2.5}$ concentrations were of regional and long-range origin.

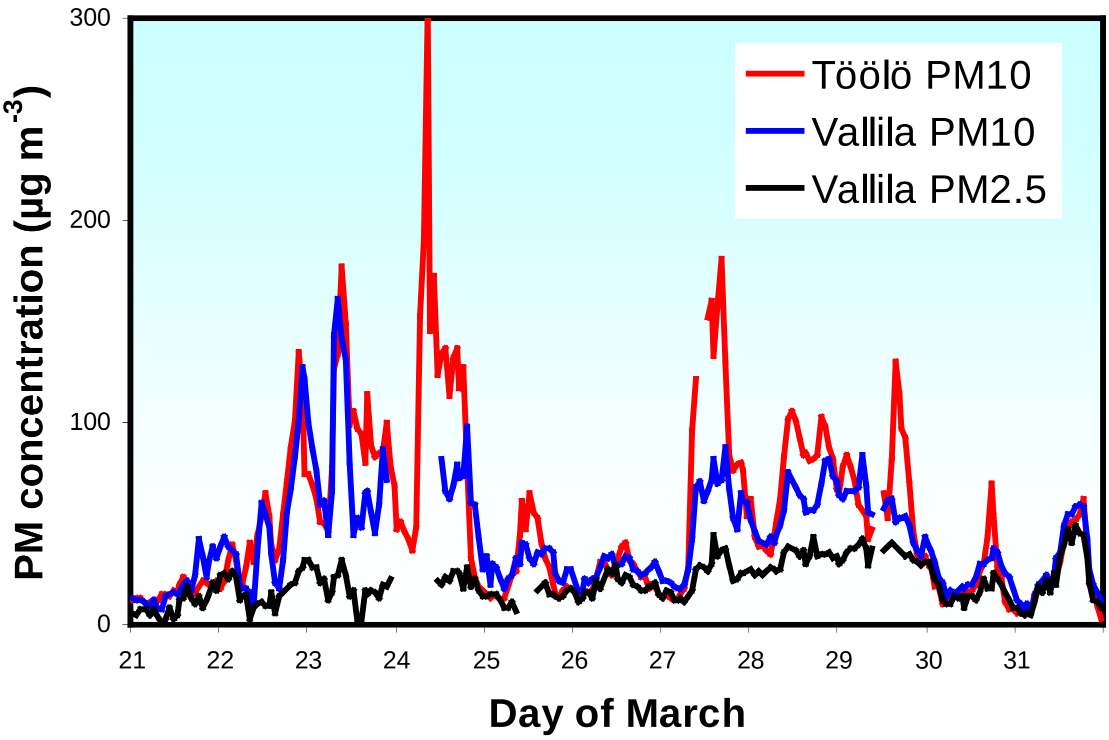

Figure 2. Particulate matter episodes in Helsinki for spring 1998 (from Pohjola et al., 2002). The stations of Töölö and Vallila are located in an urban area in the vicinity of streets with high traffic density.

Similar situations occur in Oslo, where non-vehicular sources and resuspension play a significant role. Table 2 lists the number of days over which the concentration of PM_{10} in several Norwegian urban areas exceeded the 24 hour EU limit value for PM_{10} of 50 µg/m^3. As expected, the highest values are experienced near road locations. As a comparison, the measured values of PM_{10} at a UK road site (Marylebone Road, London) exceeded the 24 hour limit value for 39 days in 2000.

Resuspension of dust from street surfaces can be a significant local source especially under dry condition, and can lead to exceedances. In addition to resuspension, in Oslo, heating with wood also contributes to winter time high peak values. The modelling and measurement work reported by Hagen (2001) and Slørdal and Larssen (2001) has shown that that emissions from wood burning can be responsible for more than 50 % of the outdoor concentration levels of PM_{10} during wintertime episodes. For $PM_{2.5}$, the corresponding contributions are estimated as high as 75 %.

Table 2. The number of exceedances of daily EU PM_{10} limit value (50 µg/m^3) in Norwegian urban Areas during 1992 - 1998.

City	Station	Type	Year	Days
Oslo	Kirkeveien	Roadside	1992/93	63
Oslo	Kirkeveien	Roadside	1994/95	37
Oslo	Kirkeveien	Roadside	1995/96	37
Oslo	Kirkeveien	Roadside	1996/97	40
Oslo	Kirkeveien	Roadside	1997/98	46
Oslo	Tasen	Roadside	1992/93	48
Oslo	Tasen	Roadside	1994/95	36
Oslo	Tasen	Roadside	1995/96	53
Oslo	Tasen	Roadside	1996/97	49
Oslo	Tasen	Roadside	1997/98	76
Oslo	Gamlebyen	Roadside	1992/93	51
Oslo	Gamlebyen	Roadside	1995/96	54
Bergen	Nygardsgt	Roadside	1995/96	55

In Milan, high PM_{10} concentrations are observed during wintertime. During winter months a large number of exceedances of the daily limit value of 50 µg/m^3 are recorded. Monthly averages also often exceed concentrations of 50 µg/m^3. Similar PM_{10} levels are observed in other urban areas located inside the Po Valley, such as Turin. The unfavourable dispersion conditions and the limited frequency of precipitations that characterise the Po valley in wintertime are amongst the factors that lead to such seasonal behaviour. The importance and role of the different source types and of the long range particle transport has not yet been clearly characterised. PM_{10} concentrations during an elevated inversion episode occurred during December 1998 and has been reported by Finardi et al. (2002) in this proceeding.

3. NO_2 and O_3 Episodes

The number of exceedances for NO_2 for two UK sites are given in Table 3 for selected years. Although high concentrations are expected at roadside locations, exceedances are also observed at the urban background site of Bloomsbury, London.

Table 3. NO_2 exceedances of the hourly EU limit value (stated in Table 1) at two measurement stations in London during 1998 - 2000.

Selected Year	Exceedances at Marylebone Road (hours)	Exceedances at Bloomsbury (hours)
1998	62	6
1999	56	4
2000	100	4

Figure 3 shows a typical NO_2 episode in London during the winter of 1994/1995. Data is shown for three sites: roadside site (Cromwell Road), urban centre (Bloomsbury) and urban background (West London). Although West London is classified as an urban background, it is located in an area that has high traffic density and hence can give higher concentrations than the other sites (see Figure 3). Episodes for NO_2 can last from a few hours to a few days depending on the prevailing meteorological conditions. During this episode there were low wind speeds (< 2 m/s), and a low lying inversion associated with low ground level temperatures (the measured temperature near the ground level was ~ -1 ^oC). Solar radiation levels were also strong for much of the day light hours (~ 70 %). As shown by Figure 1 the frequency of low wind speeds can be significant and such conditions can play a critical role in leading to episodic conditions.

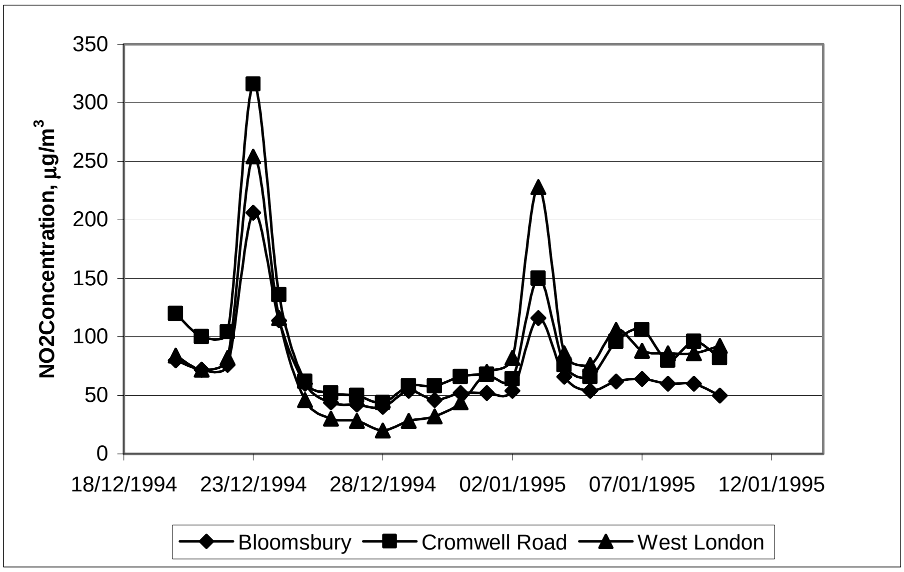

Figure 3. Daily NO_2 concentrations showing the occurrence of an episode at three London sites during the winter of 1994/95.

Hourly concentrations during the period 21-25 December 1994 for London Bloomsbury are shown in Figure 4. The NO_2 concentrations are compared with the prevailing wind speed during the same period. The figure shows that hourly concentrations reached 400 μg/m^3 during the period when the wind speeds were approximately 1 m/s or less. At such low wind speeds ventilation is minimal and this leads to a build up of pollution.

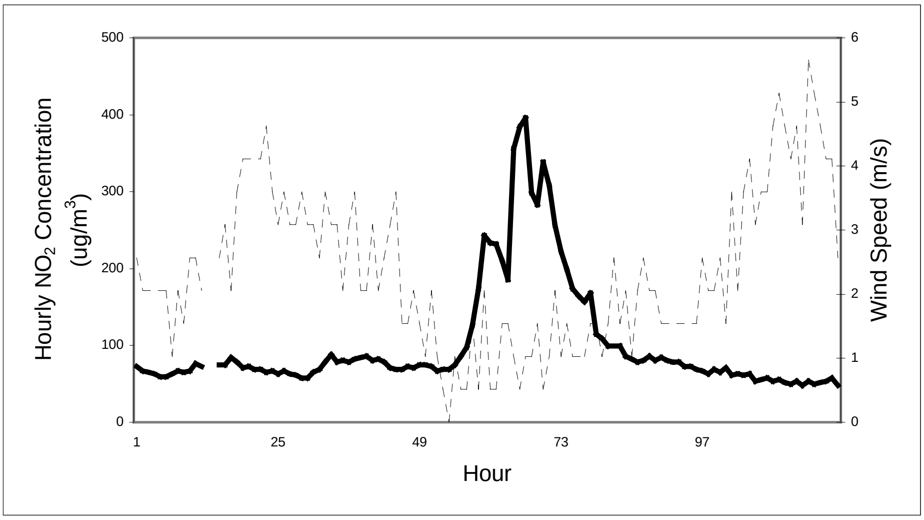

Figure 4. Hourly wind speed and concentrations of NO_2 at London Bloomsbury during 21-25 December 1994 (— NO_2 concentrations in μg/m^3 --- Wind speed in m/s measured at the London Weather Centre).

In Milan, NO_2 episodes also occur during summer time as the strong solar radiation can lead to extra oxidation potential from pollutants such as ozone. Figure 5 shows observations of NO_2 in Milan where hourly values in excess of 200 μg/m^3 were measured by one urban station during June 1998, while other stations recorded values between 100 and 150 μg/m^3. During the same summer period O_3 showed peak hourly values over 150 μg/m^3 at several stations, shown in Figure 6. As expected, high O_3 peak concentrations (exceeding 200 μg/m^3) are observed outside the urban area at the suburban background station of Motta, where NO_2 concentrations are much lower than inside the city (see Figure 5).

The described episode was characterised by anticyclonic conditions and persistent weak winds. Under such stagnant situations high levels of ozone precursors (such as NO_x and VOC's) together with high temperatures and strong solar radiation and, hence efficient photochemistry, can lead to high ozone concentrations.

Winter time NO_2 episodes are also observed, and they are commonly due to persisting fair weather conditions that can cause weak winds and the development of subsidence induced temperature inversions (Finardi et al., 2002, this proceeding). These situations can affect pollutant dispersion by limiting the daily growth of the mixing length to few hundred metres.

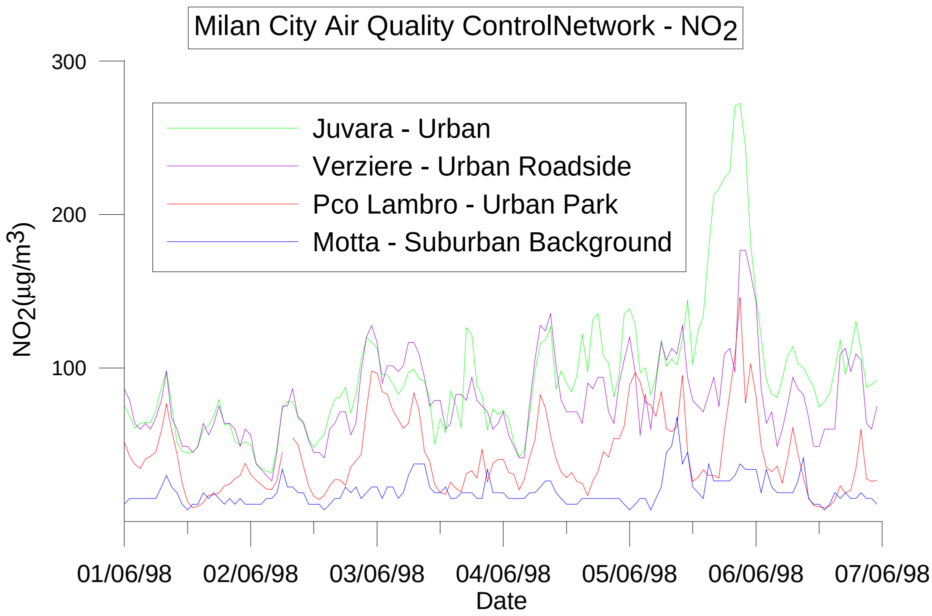

Figure 5. The NO_2 concentrations measured at four stations during an episode in Milan area for June 1998.

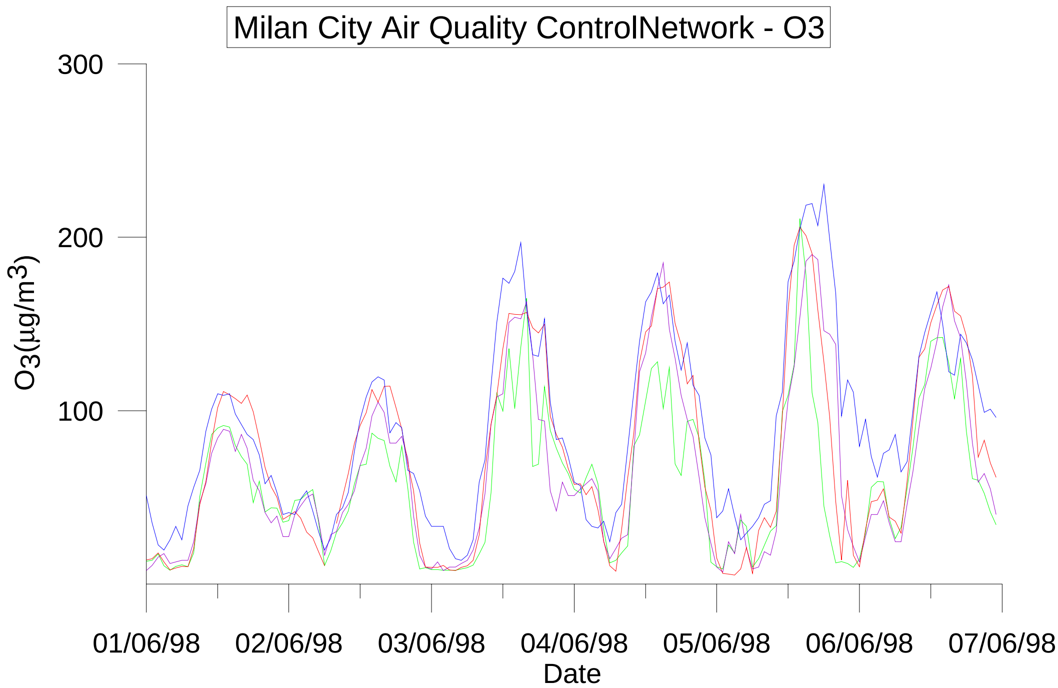

Figure 6. Ozone concentrations measured at the same four stations (as in Figure 5) in Milan during June 1998.

Conclusions

The causes of air pollution episodes depend on several factors including local and regional emissions, topography and meteorological parameters including wind speed, wind direction, temperature and solar radiation. The relative importance of such factors obviously depend on the climatic region and the season of the year. Examples have been cited from London, Oslo, Helsinki and Milan. For instance, for London the frequency of low wind speeds (< 2m/s) can be typically 25 %. Such conditions can lead to local episodes of air pollution.

Particulate matter episodes are observed in spring and winter times, occasionally also in autumn. Local sources such as vehicular exhausts and other non-vehicular sources such as wood burning and excessive resuspension are important in case of PM_{10}. In the case of secondary particulate matter (that has a substantial influence on the $PM_{2.5}$ concentrations) concentrations are mostly determined by regional and long-range transport.

NO_2 episodes can occur during both winter and summer months. During winter time, low level temperature inversions may play a crucial role. During summer months, stagnant conditions can lead to high concentrations. During the summer seasons, under anticyclonic conditions and prevailing weak winds, the levels of ozone precursors, such as VOC's, can be high. This coupled with strong solar radiation and efficient photochemistry can lead to ozone episodes.

References

DEFRA (2000). The Air Quality Strategy for England, Scotland, Wales and Northern Ireland – Working together for Clean Air, HMSO, UK.

Fisher, B E A, J. Kukkonen and M. Schatzmann, 2001. Meteorology applied to urban air pollution problems COST 715. International Journal of Environment and Pollution, Vol. 16, Nos. 1-6.

Hagen, L. O., 2001. Wood burning and particulate matter. Measurement in the Sofienberg Park in Oslo during the winter season 1998/1999. Kjeller (NILU OR 36/2001).

Karppinen, Ari, Sylvain M. Joffre, Jaakko Kukkonen and Pia Bremer, 2001. Evaluation of inversion strengths and mixing heights during extremely stable atmospheric stratification, International Journal of Environment and Pollution, Vol. 16, Nos. 1-6.

Kukkonen J., Salmi T., Saari H., Konttinen M. and Kartastenpää R., 1999. Review of urban air quality in Finland. Boreal Environment Research, Vol. 4, No. 1, pp. 55-65.

Kukkonen, Jaakko (ed.), 2001a. COST action 715, Meteorology applied to Urban Air Pollution Problems, Working Group 3, Status Report. Directorate-General for Research, Information and Communication Unit, European Commission. Brussels, 73 pages.

Kukkonen, Jaakko, Jari Härkönen, Ari Karppinen, Mia Pohjola, Harri Pietarila and Tarja Koskentalo, 2001b. A semi-empirical model for urban PM_{10} concentrations, and its evaluation against data from an urban measurement network. Atmos. Environ. 35, pp. 4433-4442.

Middleton D R and Dixon J 2002. On the Recurrence of Air Pollution Episodes. Turbulence and Diffusion Note No 269, Met Office, UK.

QUARG, 1993. Urban Air Quality in the United Kingdom, First Report of the Quality of Urban Air Review Group, Department of Environment, UK.

QUARG, 1996. Airborne Particulate Matter in the United Kingdom, Third Report of the Quality of Urban Air Review Group, Department of Environment, UK.

Pohjola, M A, Kousa, A, Kukkonen, J, Härkönen, J, Karppinen, A, Aarnio, P, Koskentalo, T, 2002. The Spatial and Temporal Variation of Measured Urban PM_{10} and $PM_{2.5}$ concentrations in the Helsinki Metropolitan Area. Water, Air and Soil Pollution: Focus (in print).

Slørdal, L. H. and S. Larssen, 2001. Indoor wood burning and airborne particles. Model calculations for Oslo for the winter of 1998-1999. Kjeller (NILU OR 37/2001).

Simulations of wintertime inversions in northern European cities by use of NWP-models.

by

Erik Berge[1], Ari Karppinen[2], Jaakko Kukkonen[2], Morten Ø. Køltzow[1] and Leiv Håvard Slørdal[3].

[1]The Norwegian Meteorological Institute
[2]Finnish Meteorological Institute
[3]The Norwegian Institute for Air Research

1 Introduction

The aim of this paper is to present results from Numerical Weather Prediction (NWP) modeling in northern Europe during strong wintertime inversions, and to discuss how realistic these simulations are. Air quality problems in northern Europe are often linked to episodes of strong inversions, and high levels of air pollutants such as NO_2 and particulate matter ($PM_{2.5}$ or PM_{10}) often occur during the episodes. Predictions of the near surface air concentrations are crucially dependent on the prediction of meteorological quantities such as wind speed and direction and the vertical temperature distribution.

Today's meteorological models have become rather elaborate with respect to physical parameterization and treatment of surface processes. Together with present high speed computers, it is now possible to run operational NWP-models with sufficient horizontal and vertical resolution to resolve small scale wind and temperature distributions linked to the wintertime episodes of high levels of pollutants. The simulations discussed in this paper are based on the utilization of an operational fine-scale NWP-system developed for the larger cities in Norway (see Berge et al. 2002). In the present paper, we have applied this NWP-system to study strong winter time inversions in Oslo, Norway and Helsinki, Finland.

2 Model description

For the Oslo study we employ the HIRLAM hydrostatic model. (HIRLAM=HIgh Resolution Limited Area model, (see Kállén 1996)) in order to obtain large scale meteorological fields. The model is operated on a 50 km and a 10 km grid. The 10 km version (henceforth denoted HIRLAM10) has 31 layers in the vertical and covers NW Europe and adjacent seas (see Fig 1). The non-hydrostatic MM5 model version 3 (Fifth Generation NCAR/Penn State University Meso-scale Modeling System, see Dudhia (1993) and Grell et al., 1994) has been nested within the HIRLAM10 model. Details about the nesting of MM5 with HIRLAM10 data and an evaluation of the MM5 model can be found in Berge et al. (2000A and B). For the Oslo region MM5 has been set up for two nests with 3 km and 1 km horizontal resolution respectively as shown in Fig. 1. The inner (1km resolution) domain covers the city plus the nearby hills and the inner part of the Oslo fjord. The meteorological data from this nest is further utilized for air quality simulations in Oslo.

Since Helsinki is located near the lateral boundary of HIRLAM10 (see Fig. 1 left panel) we decided not to apply the HIRLAM10 data, but rather utilize the meteorological data from ECMWF (European Center for Medium Range Weather Forecasting) for the Helsinki case. The horizontal resolution of the ECMWF data is approximately 60 km at 60ºN. Therefore we have added one more nest of 9 km horizontal resolution to the MM5 runs for Helsinki. The MM5 run for Helsinki was therefore set up of three nests with 9 km, 3 km and 1 km horizontal resolution respectively.

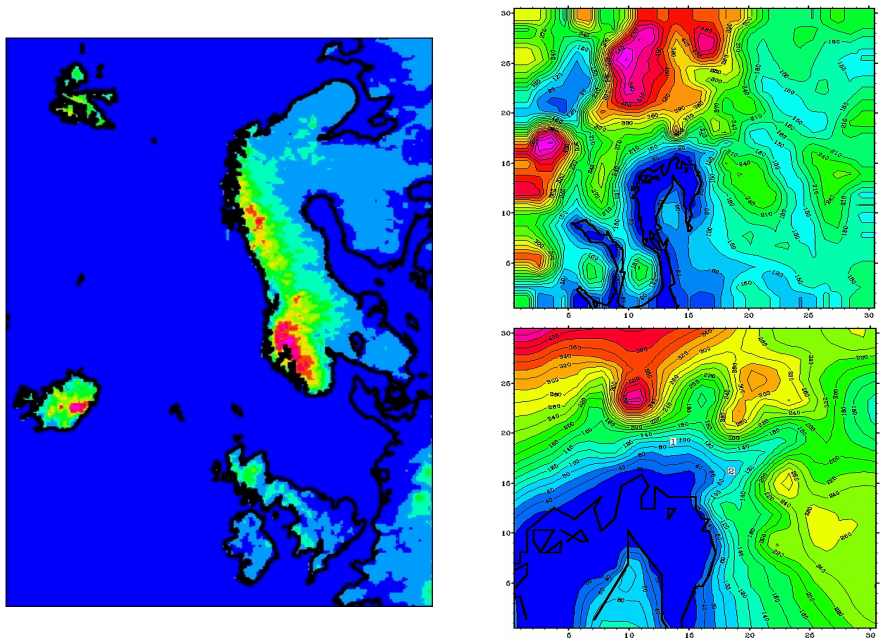

Fig. 1. Model domains for the Oslo case simulation. Left panel: HIRLAM10 domain, upper right panel: MM5 3 km outer nest, lower right panel: MM5 1 km inner nest.

3 Case studies.

3.1 Oslo, Norway.

We have selected to study one case, 11 January 2001, with particular high NO_2 values observed in Oslo. Fig. 2 shows the observed NO_2 and PM_{10} concentrations at the station Alna during this day. The station Alna is located just east of the meteorological station Valle Hovin shown in Fig. 4a. The maximum NO_2 value was about 310 $\mu g/m^3$ just after noon. PM_{10} peaked at about 150 $\mu g/m^3$ at the same time. At a meteorological mast located approximately 2 km WSW of the air quality station, temperatures at 25 m, 8 m and 2 m and winds at 25 m were measured. Fig. 2 also shows temperature differences between the 25 m and 8 m level (T25-T8) and between 25 m and 8 m (T25-2). T25-8 is a direct measurement by a single temperature difference sensor, while T25-2 is the calculated difference of two separate temperature measurements. Fig. 2 shows a very strong surface inversion during the morning hours while the high NO_2 concentrations build up. Just before noon the near surface inversion disappears, but the NO_2 concentrations, although dropping, remain rather high during the afternoon. This is probably due to the low wind speeds persisting throughout the afternoon (see Fig. 3) and the fact that a larger scale inversion up to a few hundred meters remains above the near neutrally mixed layer close to the ground.

Fig. 3 present the model simulations of MM5 and HIRLAM10 compared with the measurements. Firstly, we find a strong inversion at Valle Hovin in the MM5 T25-8 data (Fig. 2) (see Fig. 4a for the location of Valle Hovin). But, the near surface inversion is not broken up around noon as we find from the observations. The temperature panel of Fig. 3 shows rapid increase of the observed temperature after 10:00 from about -5°C to about 0°C, which is probably linked to the break up of the near surface inversion. A corresponding temperature increase is not encountered in the model simulations. MM5 has a realistic temperature curve until 10:00, after this time it remains too cold. HIRLAM10 is somewhat colder than MM5 during the whole day. The underestimated temperature probably causes the discrepancy in the predictions of relative humidity from noon and the following hours.

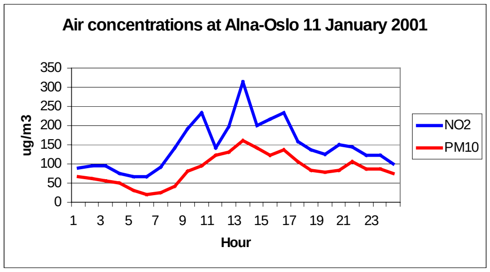

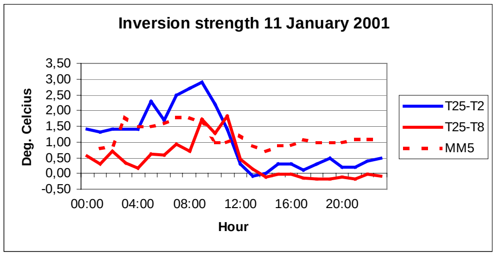

Fig. 2. NO_2 and PM_{10} concentrations (upper panel) at Alna station, Oslo, and inversion strength measured and calculated by MM5 at Valle Hovin during 11.01.2001.

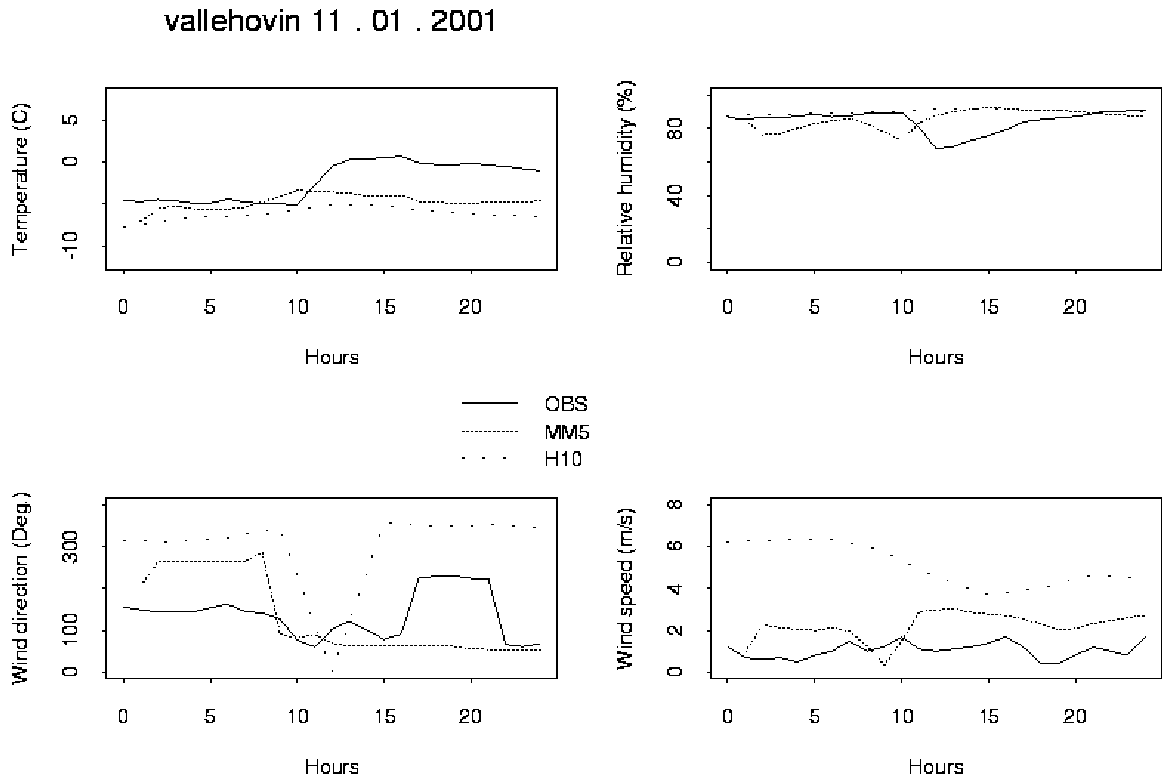

Fig. 3. Observed (OBS) and modeled by MM5 and HIRLAM10 (H10) temperature, relative humidity, wind direction and wind speed during 11.01.2001.

The MM5 wind speed is realistic, but somewhat too high during periods. The wind direction coincides well with the observed easterly directions from about 09:00 until 16:00. During the rest of the day the fit is variable. HIRLAM10 yields NW winds of 4-6 m/s throughout the whole day, which is rather unrealistic. It is likely that the topography around Oslo has a large impact on the local circulation, and that this effect is to a large degree captured by employing MM5 with 1 km resolution. The 10 km grid of HIRLAM10 is too coarse in order to resolve the local features of the wind field. Differences in physical parameterization of the two models may also matter, but this has in the present study not been investigated.

Fig. 4a shows the wind and temperature distribution at 10m at 06 UTC. In Fig. 4b we present a cross-section of temperature that passes the meteorological station Valle Hovin. The winds are very weak in the city area (0-2 m/s) where emissions are high. However, at the hilltops and over the fjord the wind speeds are about 3-5 m/s. Temperatures range from -5°C in the area of Valle Hovin to near 0°C close to the fjord. The cross-section clearly shows the models ability to model a strong inversion close to the surface. Unfortunately, no meteorological data above the mast height of 25 m at Valle Hovin is available in order to verify the height of the inversion. The model data indicate that the inversion height above the bottom of the valley varies from about 50 m in the morning to about 100 m in the afternoon.

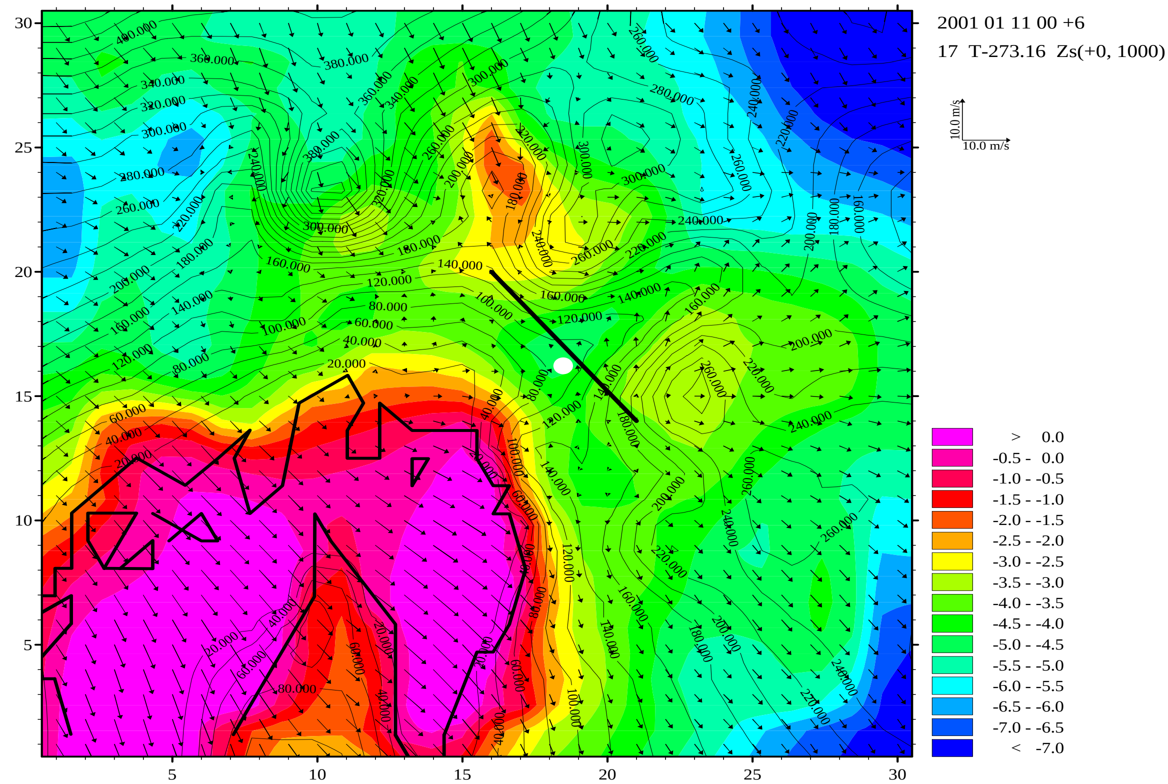

Fig. 4a. MM5 calculated temperature (color scale) and winds (black arrows) at 06 UTC 11.01.2001. The white dot indicate the position of the station Valle Hovin.

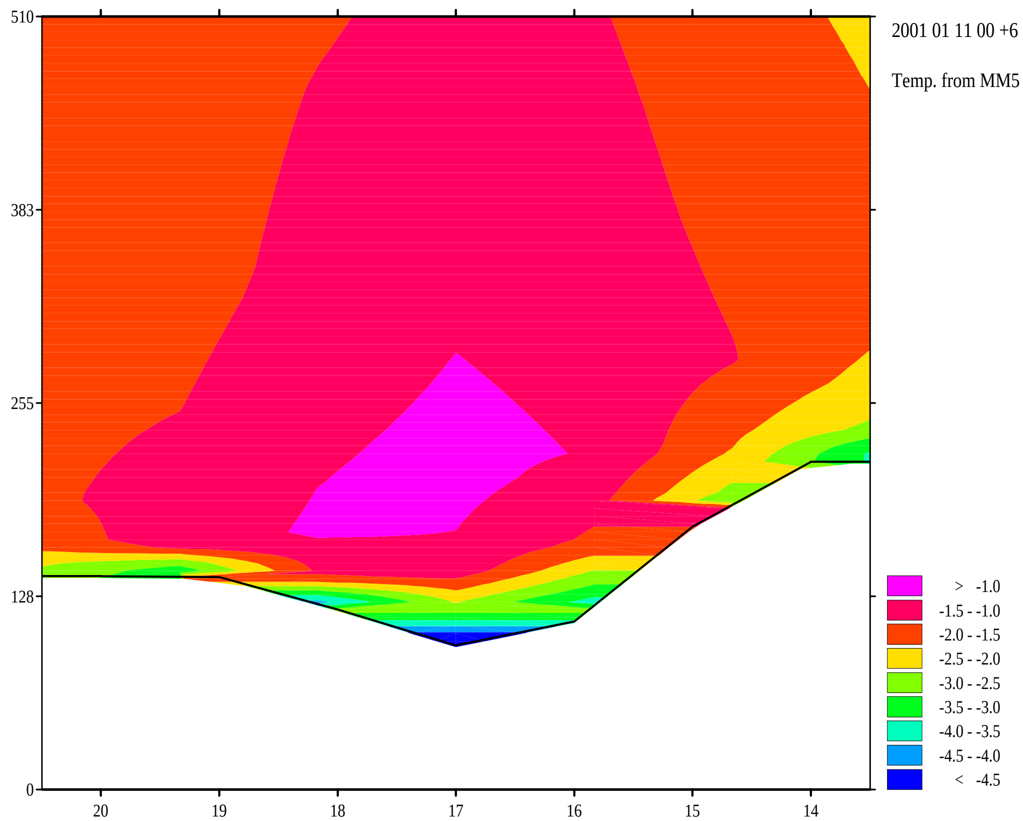

Fig. 4b. Cross-section of temperature at 06 UTC 11.01.2001. The black line in Fig. 4a show the position of the cross-section.

3.2 Helsinki, Finland.

In the next study we focus on a simulation of the local meteorological conditions in the Helsinki area during a severe inversion and air pollution episode by the end of 1995.

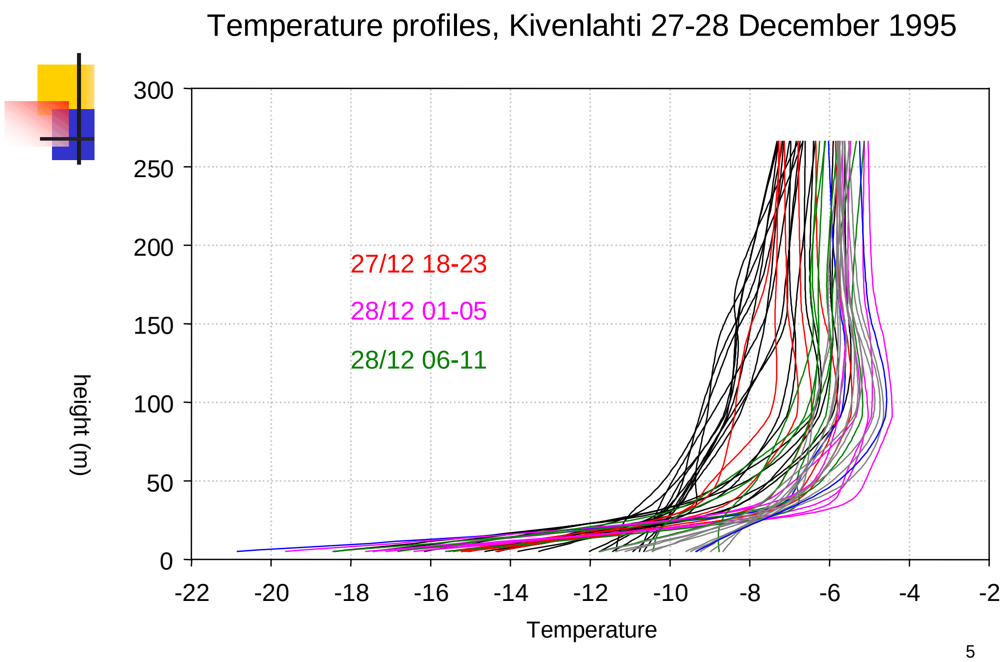

Fig. 5. Vertical temperature profiles at the measuring tower during 27 and 28 December 1995

In Fig. 5 the vertical temperature profiles from the meteorological tower at Kivenlahti a few km west of Helsinki are given for the days 27 and 28 of December 1995 (the position of the tower is indicated by the white dot in Fig. 7b). During periods very strong inversions up to 10°C were found in the lowest 50 m. Much weaker inversions were encountered above approximately 50 m.

MM5 was in this case run with ECMWF initial and boundary data for a 48 hours period starting at midnight 00 UTC 26.12.1995 and ending at 00 UTC 28.12.1995. Fig. 6a shows ECMWF data interpolated to the outer MM5 nest (9 km horizontal resolution) valid at 00 UTC 26.12.1995. A high pressure system was located over the Baltic area while a low was situated over northern Finland and Sweden (not shown). A southwesterly flow dominated over southern Finland and the Helsinki area. Temperatures were decreasing from SW to NE. Fig. 6b shows the winds and temperatures after 30 h simulation in the 9 km grid. Weaker winds and lower temperatures were then predicted over land, while winds over the Baltic Sea and the Finnish Bay still were up to 7-9 m/s.

Figs. 7a and b present results from the 3 km and 1 km MM5 nests after 30 hours of simulation. This coincides with the morning inversion at 06 UTC 27.12.1995. Winds were weak (2-3 m/s) in the Helsinki area, and in the area of the tower. But the winds again speeded up rapidly over the sea. Cross-sections of the modeled temperatures passing through the area of the tower are shown in Figs. 8 a and b (the black line in Fig. 7b indicate the position of the cross-section). It is clearly seen that the initial data from ECMWF hardly depicts any

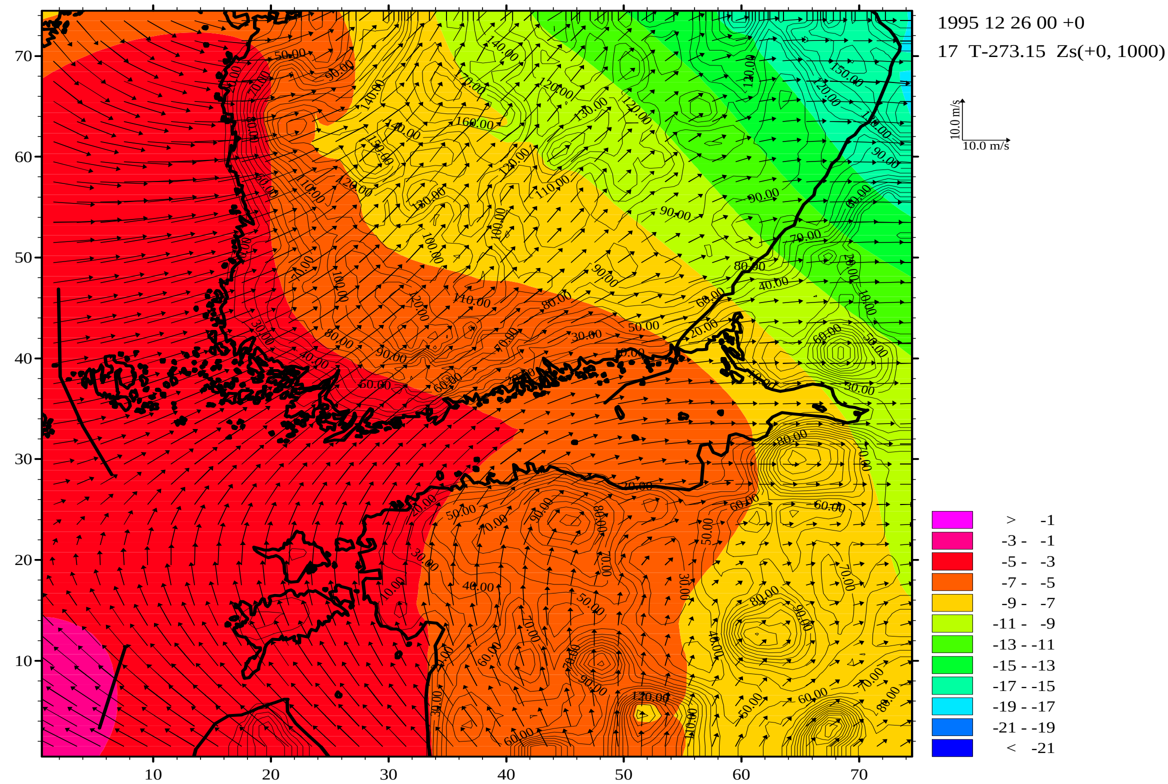

Fig. 6a. Initial wind and temperature fields from ECMWF interpolated to 9 km MM5 grid. Data are valid at 00 UTC 26.12.1995.

inversion. However, after 30 h simulations the 1 km MM5 run creates a surface inversion of about 5°C in the lowest 100 m. Furthermore, from Fig. 9 we see that during nighttime (00 UTC 27.12.02 and 00 UTC 28.12.02) a strong surface inversion of 4-5 °C is encountered in the lowest 50 m. This agrees actually quite well with the observations from the tower during

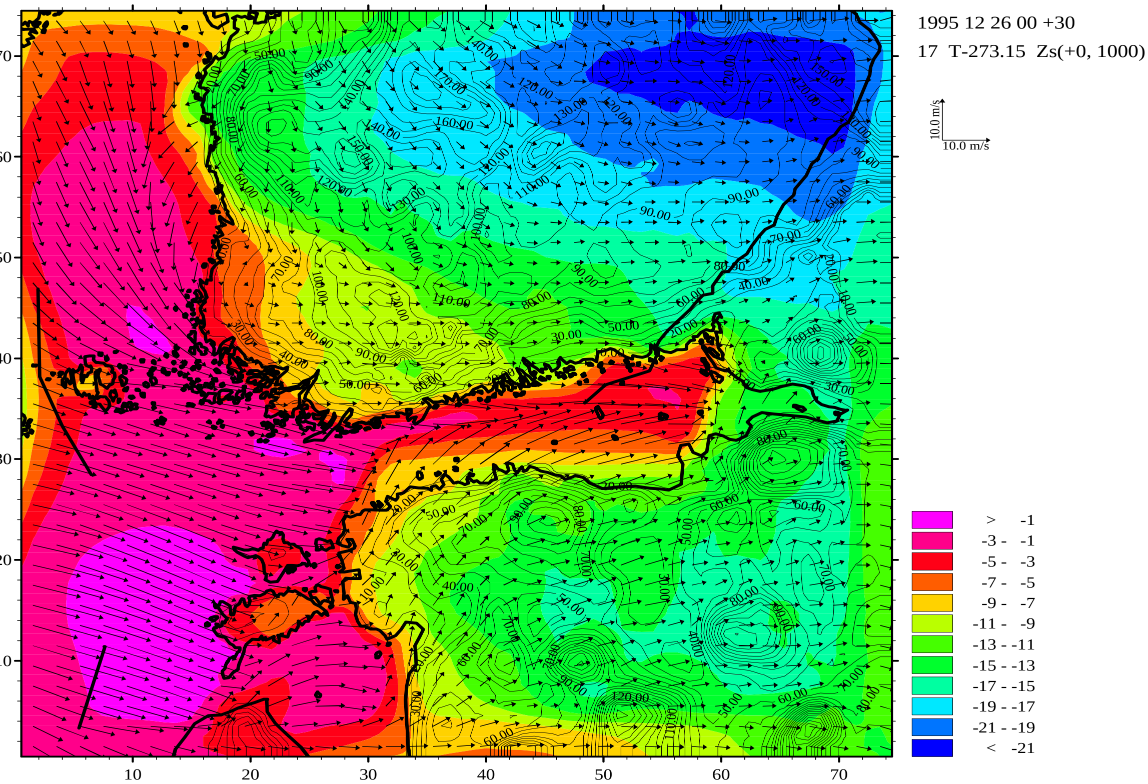

Fig. 6b. Wind and temperature fields from the 9 km MM5 grid after 30 hours of model simulations. Data are valid at 006UTC 27.12.1995.

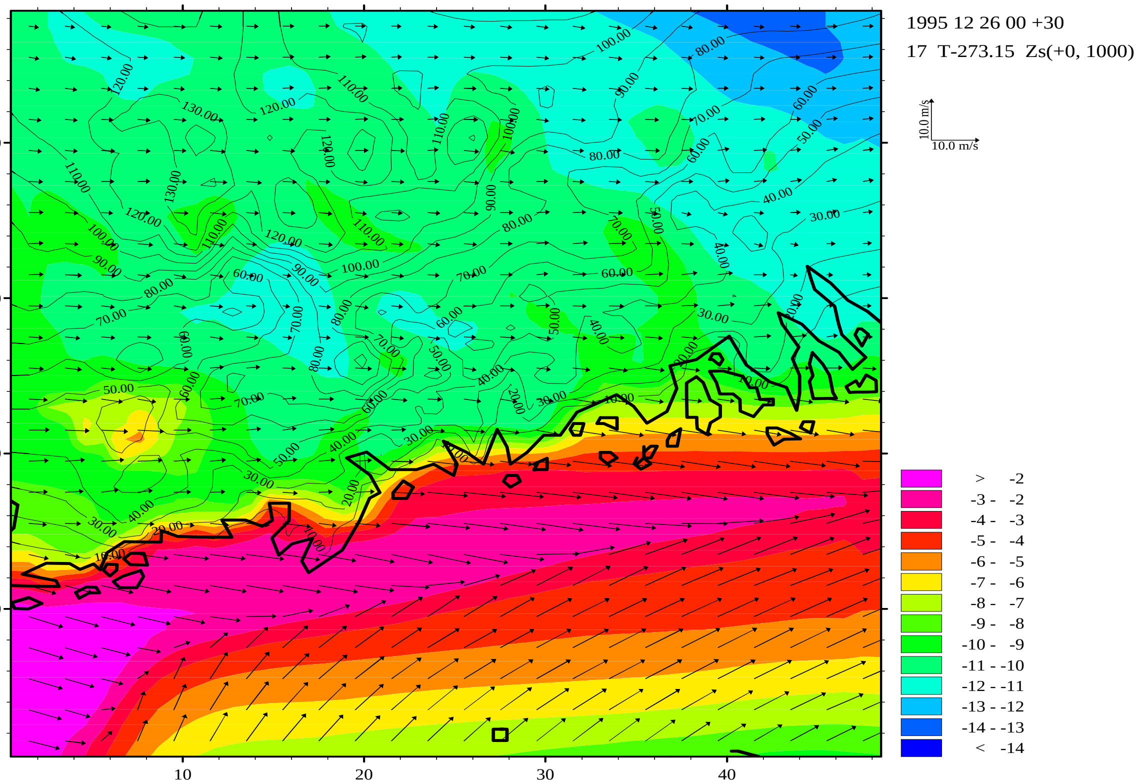

Fig. 7a. Wind and temperature fields from the 3 km MM5 grid after 30 hours of model simulations. Data are valid at 06 UTC 27.12.1995.

the evening 27.12.02 although the observations show an even stronger inversion and 2-4 °C lower temperatures near the surface. (Fig. 5). As already mentioned, the observations indicate an inversion top at about 50 m. We therefore find that the structure of the inversion is realistically simulated although the magnitude is somewhat underestimated.

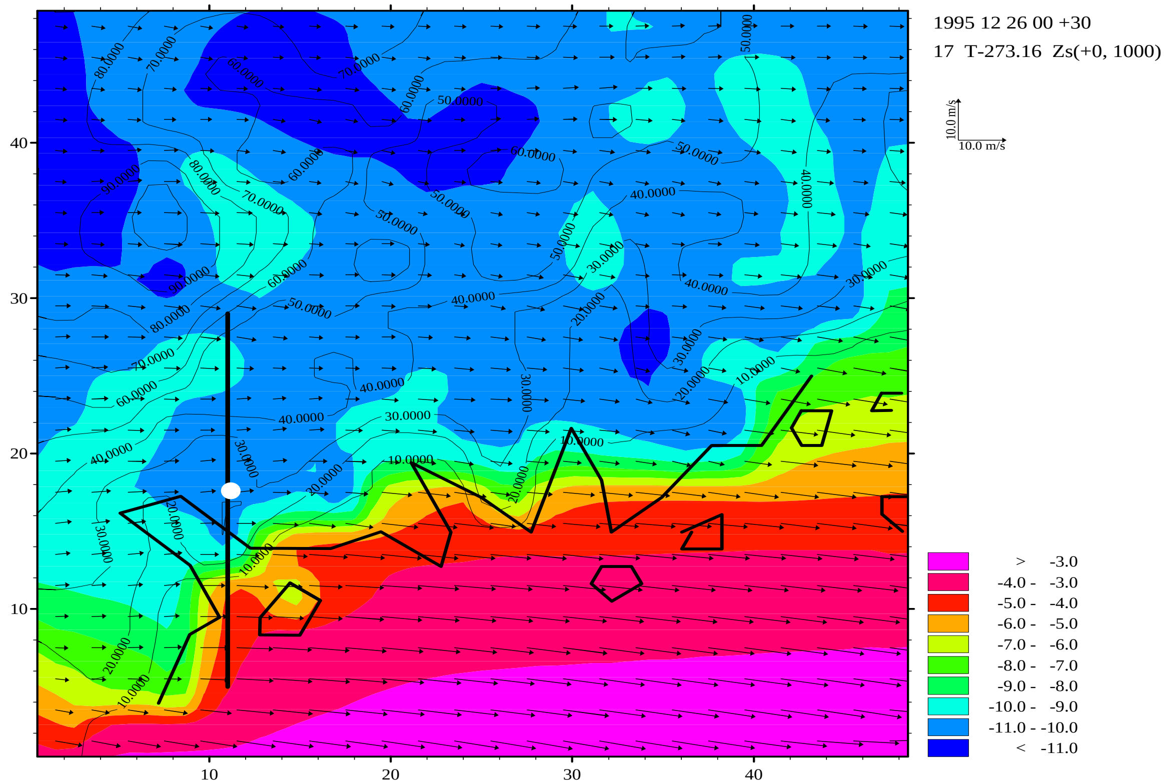

Fig. 7b. Wind and temperature fields from the 1 km MM5 grid after 30 hours of model simulations. Data are valid at 06 UTC 27.12.1995.

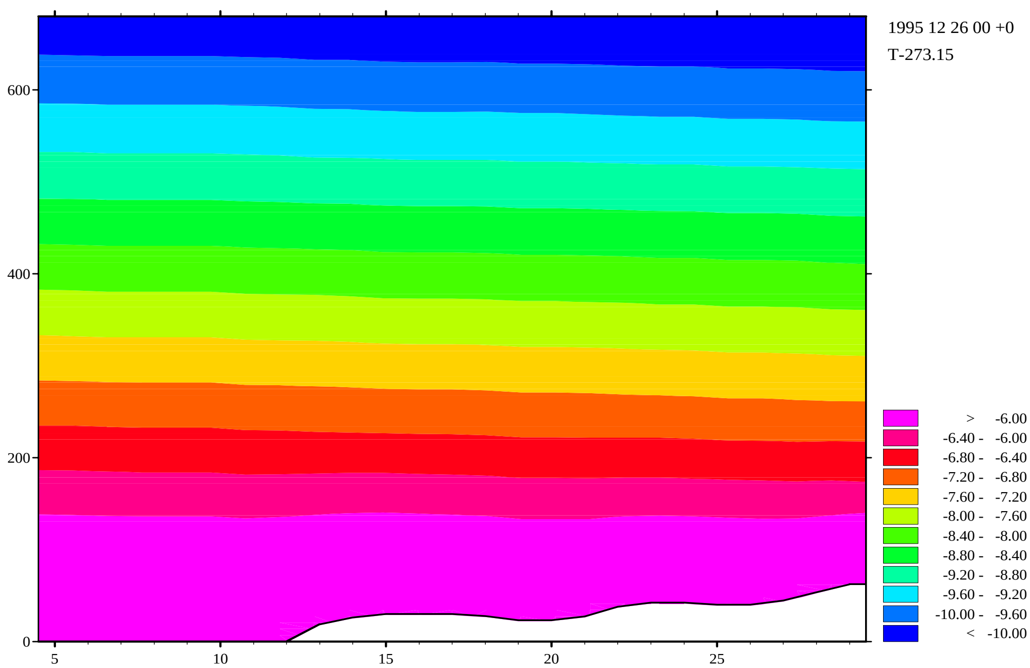

Fig. 8a. Cross-section of temperature at 00 UTC 26.12.1995. The black line in Fig. 7b shows the position of the cross-section.

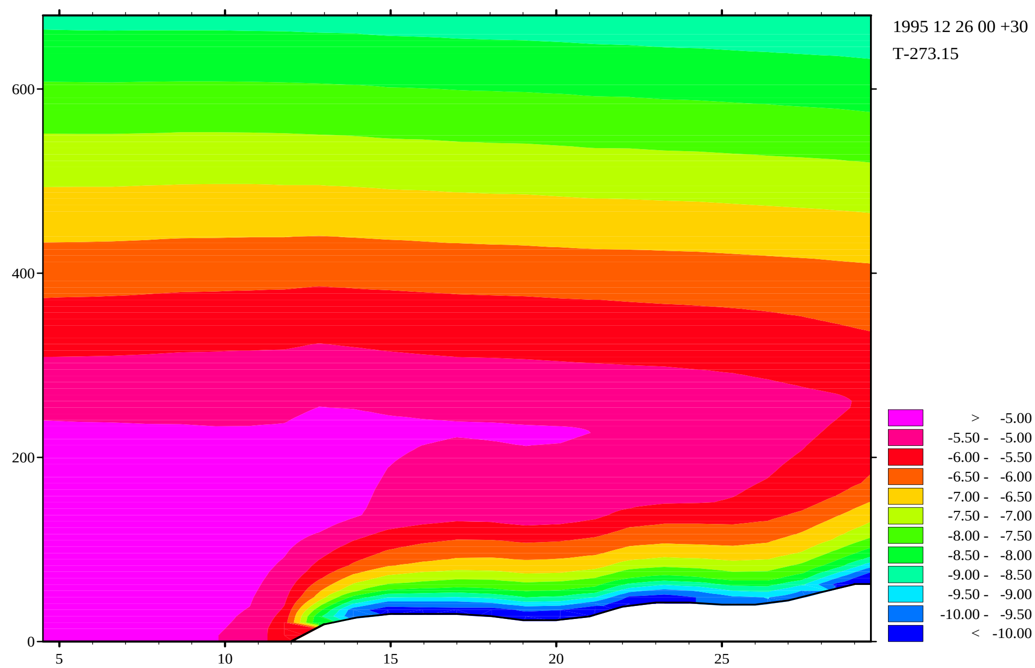

Fig. 8b. Cross-section of temperature at 06 UTC 27.12.1995. The black line in Fig. 7b shows the position of the cross-section.

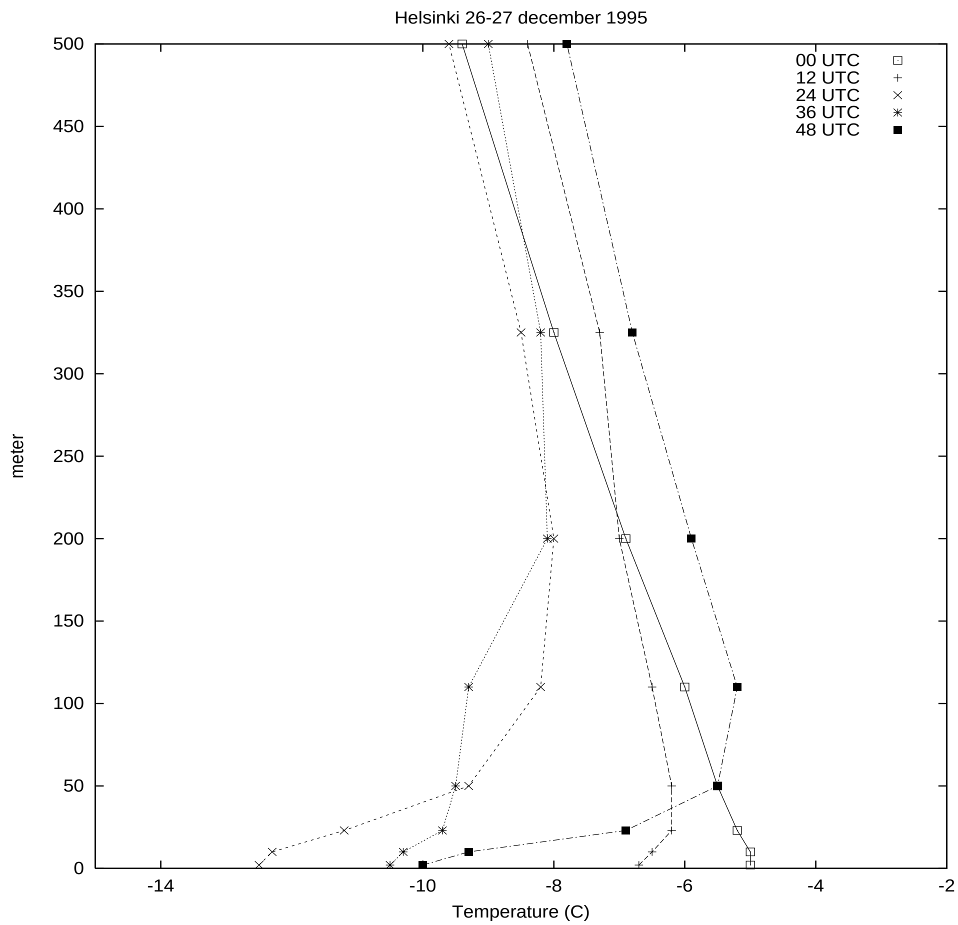

Fig. 9. Vertical profiles from MM5 at the meteorological tower after 00, 12, 24, 36 and 48 hours of simulations.

4 Summary and conclusions.

We have presented two case-studies of fine-scale meteorological simulations of strong surface based inversions carried out with the MM5 model. One of the case-studies is for Oslo, Norway, the other for Helsinki, Finland. Both cities suffer occasionally from high levels of air pollution during strong winter time inversions, and the aim of this paper has been to elucidate the potential of fine-scale NWP modeling in predicting strong inversions and local circulation systems.

The Oslo case reveals that realistic inversion strengths and local circulation patters are set up by MM5 employing 1 km horizontal resolution. However, the peak inversion strength is somewhat underestimated. In the valley east of Oslo where air pollution emissions are high MM5 indicate a 50-100m thick inversion layer during this particular case. NO_2 values up to above 300 $\mu g/m^3$ where recorded in this valley during the episode.

Similarly, for the Helsinki case a realistic vertical profile of the inversion is encountered in the MM5 simulation. Temperature data from a 330 m high meteorological tower show a very strong surface inversion up to approximately 50 m, with temperature differences up to ca. 10°C. MM5 estimates an inversion top at approximately the measured level, however the inversion strength is typically 2-4 °C smaller than the measured values. No wind data comparison has been conducted for the Helsinki case.

It is recommended for the future to employ sensitivity studies in order to understand the reasons for the underestimations of the inversion strength. One may speculate why the model is not able to build up low enough surface temperatures. One explanation could be insufficient surface data on snow and ice coverage and ground temperatures. For the Helsinki case it is also recommended as a next step to compare modeled and measured wind profiles. The measuring tower is situated well away from the urban areas of Helsinki thus the measurements should not be influenced by urban effects. In Oslo however, urban effects may play an important role and develop an urban boundary layer (UBL), and hence it is also recommended to test UBL parameterizations in MM5.

5 References

Berge, E., Walker, S-E., Sorteberg, A., Lenkopane, M., Eastwood, S., Jablonska, H.J. og Ødegaard. M. 2002. A real-time forecast model for meteorology and air quality during peak air pollution episodes in Oslo, Norway. Water Air and Soil Pollution. Special Issue: Urban Air Quality – Recent Advances. In press.

Berge, E, Walker, S-E., Sorteberg, A, Eastwood, S., Kristiansen, J og Tønnesen, D. 2000A. Utvikling og testing av pilotmodell for luftkvaliteten i Oslo. Research Report no. 99, The Norwegian Meteororlogical Institute, Oslo, Norway.

Berge, E., Walker, S-E., Sorteberg, A., Lenkopane, M., Eastwood, S., Jablonska, H.J. og Ødegaard. M. 2000B. Evaluering av prognosemodell for meteorologi og luftkvalitet for 22 vinterdager i Oslo. Research Report no. 100. The Norwegian Meteorological Institute. Oslo. Norway.

Dudhia, J. 1993. A nonhydrostatic version of the Penn State/NCAR mesoscale model: Validation tests and simulation of an Atlantic cyclone and cold front. Mon. Wea. Rev., 121, 1493-1513.

Grell, G.A., Dudhia, J. and Stauffer, D.R. 1994. A description of the fifth-generation Penn State/NCAR mesoscale model (MM5). NCAR Technical Note, NCAR/TN-397+IA, 114p.

Källén, E. 1996. Hirlam documentation manual system 2.5. Available at the Norwegian Meteorological Institute, Oslo, Norway.

Evaluation of meteorological data measured at a radio tower in the Helsinki Metropolitan Area

Ari Karppinen, Sylvain M. Joffre and Jaakko Kukkonen

Finnish Meteorological Institute,
Sahaajankatu 20 E, 00880 HELSINKI, FINLAND

Abstract

We have evaluated the meteorological data measured at a radio tower of 327 m height, called the Kivenlahti mast, situated in the Helsinki Metropolitan Area. Measurement instruments have been located at nine levels from 5 m to 327 m. The archived data contains wind speed and direction, ambient temperature and relative humidity values, averaged within 10 minutes, as well as one-minute minimum and maximum values for wind speed and direction, since 1989. We have analyzed the wind speed and direction data from the mast during a period of ten years, from 1989 to 1998. The roughness length (z_0) in the vicinity of the mast varies from approximately 1.5 m to 3.0 m. The z_0 values are lowest in the South-Western wind direction sector, caused by the surrounding sea areas; as expected, the maximum z_0 value is observed approximately in the direction of the nearest city centre (Espoo). The analysis performed at the height level of 27 m also showed that the wind speed values are disturbed by the presence of the mast itself. Such a disturbance takes place in a specific wind direction sector, in which the instruments are in the lee side of the structure, approximately from 20° to 80°. The dataset is available for studies addressing the structure of urban atmospheres. The data has been utilised especially in evaluating the temporal evolution of temperature inversions in the course of peak pollution episodes.

1. Introduction

Urban areas influence atmospheric flow both mechanically and thermally. Urban roughness elements are commonly heterogeneously distributed; it is therefore difficult to define a specific reference surface regarding wind speed and direction. The classical similarity theories of the surface layer are not generally valid. The vertical surfaces of buildings contribute to an atmospheric energy exchange that is substantially different, compared with that in the surrounding rural environment (e.g., Fisher et al., 2001).

Routine meteorological observations are commonly mostly conducted in rural areas. It is therefore especially important to analyse the meteorological data that has been measured in urban areas. It is also useful to compare such observations with the corresponding values measured in rural areas. Measured data is especially scarce concerning the vertical structure of the boundary layer in urban environments.

In a previous study, we compared the results of the Kivenlahti mast measurements with those extracted from the radiosonde profiles at a rural site located in middle Finland (Karppinen et al., 2001a). Radio towers can be useful platforms for mounting various meteorological instruments (e.g., Middleton, 2002).

The aim of this study was to evaluate and analyse in more detail the data measured at the Kivenlahti tower. However, the data extracted from such measurements needs to be carefully evaluated in order to find out possible disturbances caused by the presence of the tower itself. This concerns especially the wind speed and direction measurements. The aim of this study is to describe the location and environment of the mast, the experimental set-up, the availability of data, and to contribute in analysing the quality of the data obtained. This study is part of the quality control and assurance of the data. We have evaluated especially the influence of the mast itself on the measured wind speeds.

2. Materials and methods

The Kivenlahti mast is situated in the Helsinki Metropolitan Area (World Meteorological Organisation, station number 05601, location: 60°11', 24°39'). The location of the mast is presented in Figure 1.

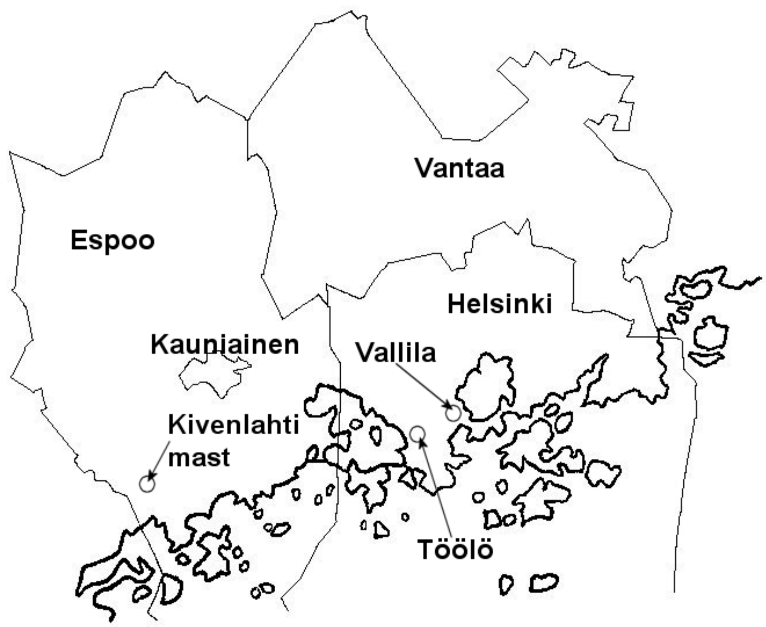

Figure 1. Location of the Kivenlahti meteorological mast within the Helsinki Metropolitan Area, comprising of four cities (Helsinki, Espoo, Vantaa and Kauniainen). The size of the depicted area is approximately 35 km x 25 km. Two air quality stations in central Helsinki have also been shown (Vallila and Töölö).

The mast is located approximately at a distance of 15 km to the west from the centre of Helsinki, and at a distance of 3 km to the south from the centre of the city of Espoo, and at a distance from the seashore of approximately from 5 to 8 km. The mast is located on a small cliff that is approximately 20 to 25 m higher than the surrounding areas. The terrain surrounding the mast is fairly flat; the roughness length in the vicinity of the mast varies from 1.5 m to 3.0 m (Karppinen et al., 2001b). A picture of the mast and the surrounding area to the northern direction is shown in Figure 2.

Figure 2. Aerial photograph of the Kivenlahti radio tower and the surrounding area towards the northern direction. The terrain in the immediate vicinity to the north of the mast is mainly forested area and cultivated fields. The character of terrain to the east of the mast is more urbanised. The figure also shows another shorter (100 m) mast to the right of the higher main mast.

The measurements conducted at the Kivenlahti mast are presented in Table 1. The time resolution of wind measurements is one minute, for the other parameters 10 minutes. The archived wind speed and direction data include minimum, maximum and average values within 10 minutes, and average values of temperature and relative humidity within 10 minutes. The measured data has been archived since 1989.

Table 1. The meteorological measurements conducted at the Kivenlahti mast.

Meteorological parameter	Measurement height (m)								
	5	26	48	91	142	182	266	296	327
Wind speed		x		x		x			x
Wind direction		x		x		x		x	
Temperature	x	x	x	x	x	x	X	x	
Relative humidity		x		x		x		x	

A more detailed picture of the wind sensors at one specific height is presented in Figure 3. Wind sensors (Hydrotech WS-3) are located on the South-Western side of the mast. At each measurement level, sensors are situated on a boom that extends from the mast structure to reduce its disturbing effects.

Figure 3. The wind sensors at the height of 26 m in the Kivenlahti mast (on the left-hand-side of the mast). The photograph has been taken from the southern direction.

3. Results and discussion

We have analysed the wind speed and direction data from the Kivenlahti mast during a period of ten years from 1989 to 1998. Measured vertical wind profiles in neutral atmospheric stratification were utilized to compute the roughness length and displacement height in the vicinity of the mast. Atmospheric stability was determined based on the measured vertical potential temperature profiles between levels at the heights of 26 m and 91 m.

Assuming a logarithmic wind profile in neutral conditions, it can be shown that the friction velocity u_* is connected to the difference of the wind speeds $\Delta u_{ij} = u_j - u_i$ between two height levels (z_i and z_j) by a simple relation:

$$u_*/k = \Delta u_{ij} / \ln[(z_j-d)/(z_i-d)] \equiv k_{ji} \qquad (1)$$

where k is von Karman constant (k = 0.4) and d is the displacement height. This equation is independent of the roughness length (z_o). We seek for the value of d that yields the best agreement between the friction velocities at various height intervals.

Figure 4 illustrates the application of this method. The intersection point of the two lines (k_{21} and k_{32}) yields an estimate of the displacement height.

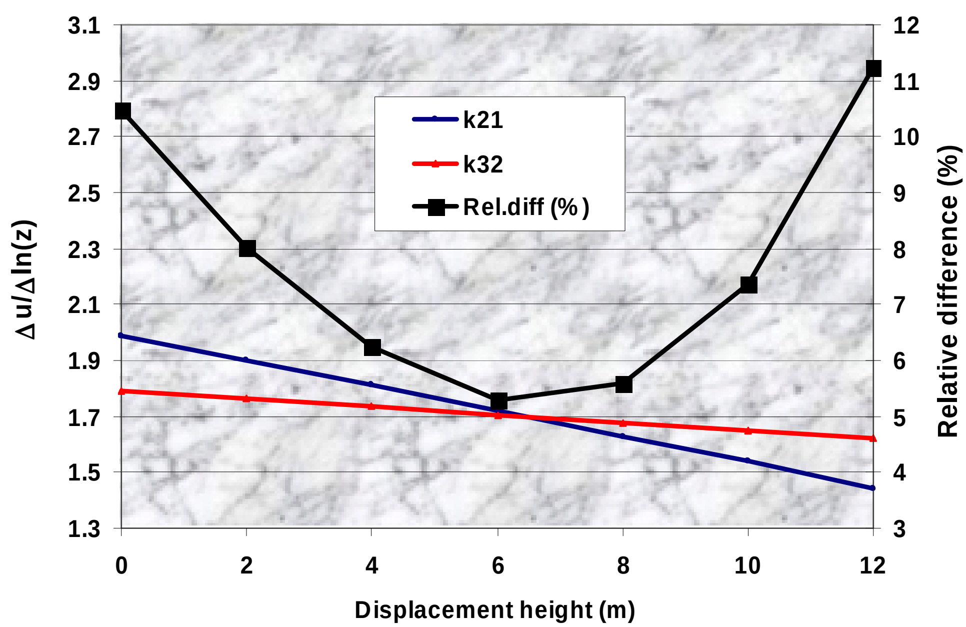

Figure 4. The evaluation of the displacement height, utilising the wind profiles at the levels of 26 m, 91 m and 182 m; these are denoted as the levels number 1, 2 and 3 (k_{21} and k_{32}; left-hand-side vertical axis), respectively. The figure also shows their average relative difference $\Delta k = 2* |k_{21}-k_{32}|/(k_{21}+k_{32})$ as a function of the displacement height (right-hand-side vertical axis).

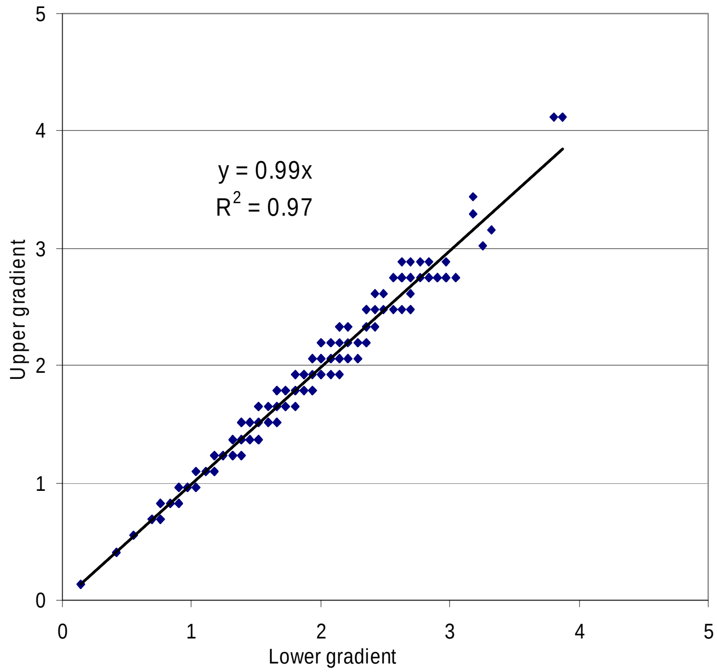

Figure 5. Comparison of the calculated friction velocities (u/k) based on wind speed gradients between the height levels 26 m and 91 m (lower gradient) and between 91 m and 182 m (upper gradient), at the Kivenlahti mast. Only strictly neutral ($\Delta\theta_{(29\text{-}91m)} < 0.1$ ^oK) conditions have been included; displacement height = 6 m.*

The average values of the roughness length and displacement height in terms of the wind direction are presented in Figures 6 a-b. The roughness length (z_o) in the vicinity of the mast is the lowest for the South-Western wind direction sector, it varies from approximately 1.5 m to 2.0 m. Its values are highest in the North-Western and North-Eastern sectors, varying from approximately 2.5 to 3.0 m. Clearly, this variation depends on terrain features in the vicinity of the mast. The fairly low values in the southern direction are influenced by the surrounding sea areas. The maximum value of the roughness length, approximately 3.0 m, is observed approximately in the direction of the city centre of Espoo.

However, the wind direction dependence of displacement length (d) is moderate; it is approximately 6.0 m, and its variation is lower than ± 1 m. This value is qualitatively in agreement with the commonly applied assumption that d = 0.7 H_r, where H_r is the mean height of the physical roughness elements.

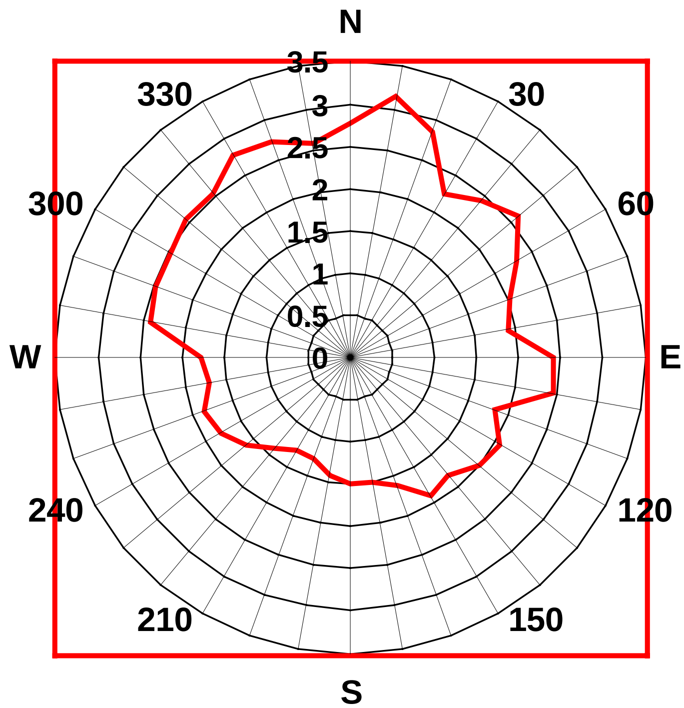

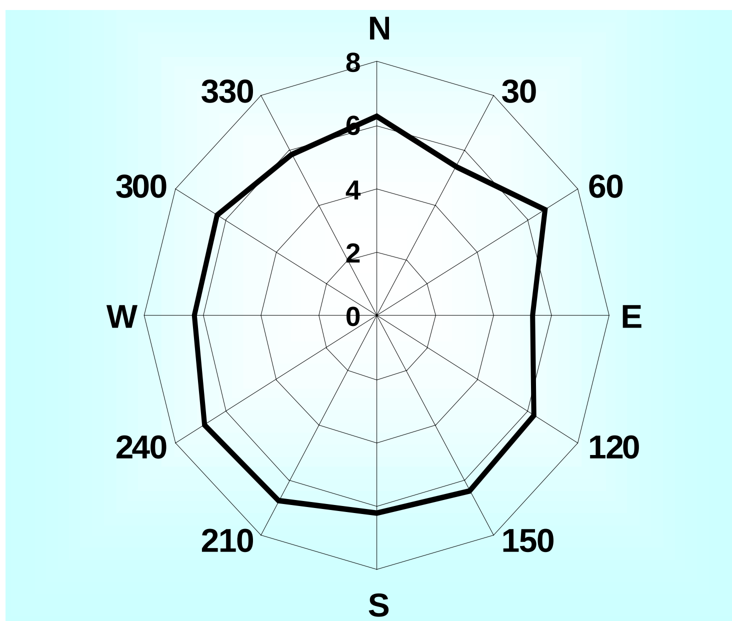

Figures 6 a-b. Wind direction distribution of the average values of the roughness length and displacement height based on the measurements at the Kivenlahti mast during the period 1989 - 1998. Only cases with a neutral atmospheric stratification have been included (the number of cases is 17503).

The averaged wind speed values in terms of the wind direction are presented in Figures 7 a-b at two specific measurement levels. Clearly, the wind speed values are dependent on the synoptic weather conditions and the origin of the air masses. For instance, synoptic weather systems that have been transported from the Northernmost parts of the Atlantic or from the Northernmost parts of Russia can more commonly cause a prevailing stable atmospheric stratification, with associated weak wind speeds. We have therefore included only one stability regime (unstable cases) in the present analysis.

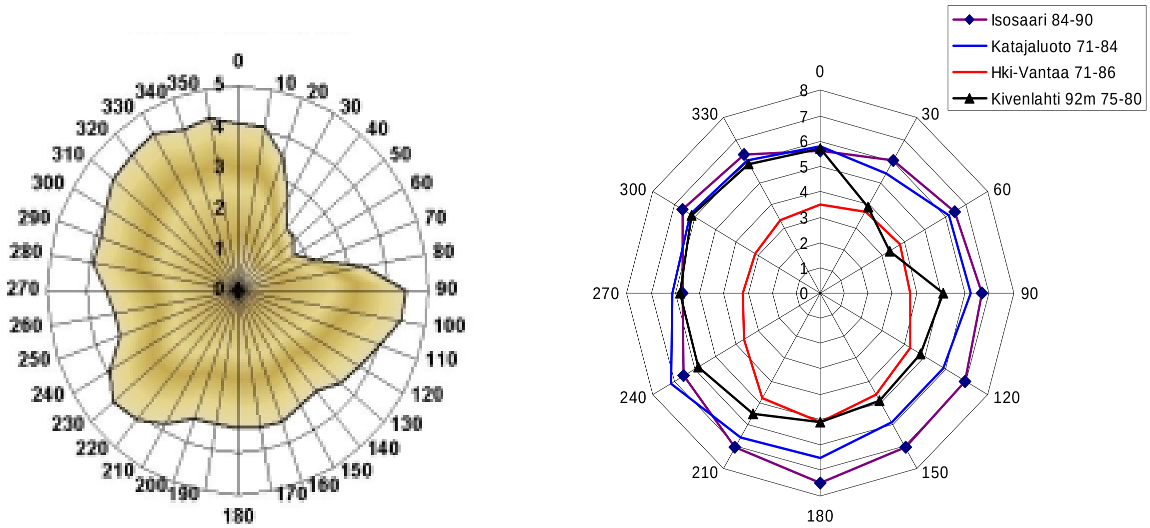

Figures 7 a-b. (a) The average values of the wind speed in terms of the wind direction, based on the measurements at the Kivenlahti mast (unstable stratification) during the period from 1989 to 1998 at the height of 26 meters. (b) The average values of the wind speed in terms of the wind direction, based on the measurements at 3 synoptic stations in the vicinity of the Helsinki area during 1971 - 1990, and the Kivenlahti mast during the period from 1975 to 1980 at the height of 92 meters (Tammelin, 1991).

Figure 7b shows examples of the synoptic-scale influence on the wind speeds in terms of wind direction. Comparison of the data determined at various stations shows that the wind direction dependence of the wind speeds at the station of Kivenlahti is clearly influenced by the presence of the mast itself, and by other equipment and structures attached to the mast.

The results in Figures 7 a-b show a decreased wind speed in the wind direction sector approximately from 20 to 80°. This decrease is caused by the disturbances caused by the mast and other structures attached to it, in the lee side of the structure. We therefore recommend that the data corresponding to this wind direction interval should be removed from any analysis that addresses wind velocities, or other parameters related to the wind velocity.

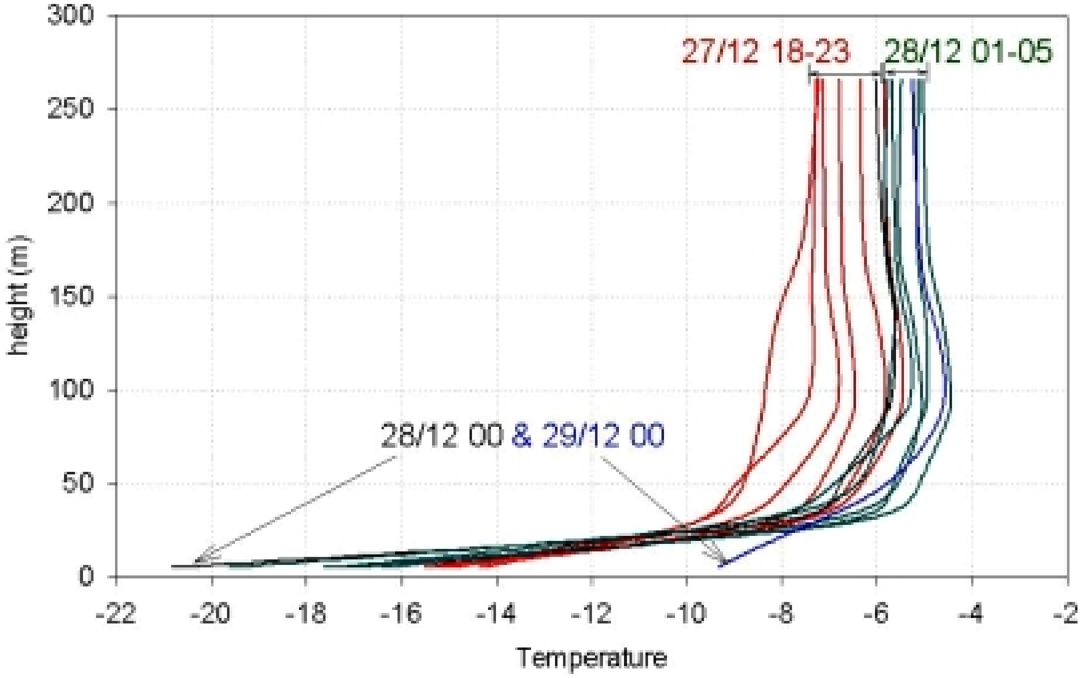

Figure 8. Evolution of a temperature inversion during an air quality episode in December 1995. The curves are numerical fits of the data measured at the Kivenlahti mast.

The temperature profiles measured at a high tower can be very useful in analysing inversions in case of air pollution episodes. As an example, the evolution of temperature profiles measured at the Kivenlahti mast during 27-28 December 1995 is presented in Figure 8. It displays both a warm advection of 2 ˚C above 50 m and a cooling of the layer close to the surface during this period, with a final warming and mixing of the whole layer at the end of the episode. These features, in addition to a vertical inversion of approximately 15˚C over the lowest 30 m of the atmosphere represent a real challenge for boundary layer modelling.

4. Conclusions

Radio towers can be useful platforms for mounting various meteorological instruments (e.g., Middleton, 2002). However, the data extracted from such measurements needs to be carefully evaluated in order to find out possible disturbances caused by the presence of the tower itself. This especially concerns the wind speed and direction measurements.

We have analyzed the wind speed and direction data from the Kivenlahti radio tower during a period of ten years**,** from 1989 to 1998. The roughness length (z_0) in the vicinity of the mast varies from approximately 1.5 m to 3.0 m. As expected, this variation is qualitatively in a good agreement with the structure of the surrounding areas. The tower is located within the Helsinki Metropolitan Area; however, it is in the westernmost part of the area that is not in the immediate vicinity of the major buildings in central Helsinki.

The analysis for unstable cases at the measurement level of 26 and 92 m has shown that the wind speed measurements can be disturbed by the presence of the mast itself, and the attached instruments and equipment. This disturbance is evident in one specific wind direction sector, approximately from 20° to 80°; for this specific sector, the anemometers are in the lee side of the structure. We recommend that the data corresponding to this wind direction sector should be removed from any analysis that addresses wind velocities or other parameters related to the wind velocity. In future work, the corresponding analysis could be performed systematically for all stability regimes and measurement levels.

The temperature profiles measured at such a tower can be very useful in analysing inversions in case of air pollution episodes. The dataset is available for studies addressing the structure of urban atmospheres.

5. References

Fisher, B E A, J. Kukkonen and M. Schatzmann, 2001. Meteorology applied to urban air pollution problems COST 715. *International J. Environ. and Poll.*, **16**, 1-6.

Karppinen, A, J. Kukkonen, T. Elolähde, M. Konttinen, T. Koskentalo and E. Rantakrans, 2000a. A modelling system for predicting urban air pollution, Model description and applications in the Helsinki metropolitan area. *Atmos. Environ*. **34** (22), 3723-3733.

Karppinen, A, Kukkonen, J., Elolähde, T.,Konttinen, M. and Koskentalo, T., 2000b: A modelling system for predicting urban air pollution, Comparison of model predictions with the data of an urban measurement network. *Atmos. Environ*. **34**, 3735-3743.

Karppinen, Ari, Sylvain M. Joffre, Jaakko Kukkonen and Pia Bremer, 2001a. Evaluation of inversion strengths and mixing heights during extremely stable atmospheric stratification. *International J. Environ. and Poll*., **16** (1-6).

Karppinen, A., S. M. Joffre and J. Kukkonen, 2001b. The refinement of a meteorological preprocessor for the urban environment. *International J. of Environ. and Poll.*, **14** (1-6), 565-572.

Middleton, D.R., 2002. Meteorological challenges in urban air pollution. *Clean Air* **32**, 14-19.

Tammelin, B., 1991. Finnish Wind Atlas,. Finnish Meteorological Institute, Valtion painatuskeskus, Helsinki, Finland. (ISBN 951-697-334-5).

Analysis of three air pollution episodes driven by a temperature inversion in a sub-alpine Italian region

Sandro Finardi[1], Gabriele Carboni[2], and Gianni Tinarelli[1]

1. ARIANET s.r.l., viale Elvezia 42, 20052 Monza (MI), ITALY
2. ENEL S.p.A./Produzione, via N.Bixio 39, 29100 Piacenza, ITALY

Abstract

Three different episodes which occurred in northern Italy are analysed: (i) a winter inversion of synoptic origin extending to more than 1000 metres a.g.l., with shallow unstable boundary layer developing during daytime, that caused a severe pollution episode in Milan in December 1998, (ii) an elevated inversion episode observed in the Northern Mediterranean coastal area of Savona on February 1998, and (iii) a persisting ground based inversion in the Alpine valley of Aosta on February 1997. The phenomenology of these episodes is analysed on the basis of local vertical profiles from soundings, meteorological and chemical measurements performed at an air quality network, and synoptic meteorological information. We describe the characteristics of the atmospheric circulation during inversion periods and the behaviour of pollutant concentrations. We also discuss briefly the relevance of modelling of inversion episodes in connection with the application of current EU directives on air quality.

Introduction

Temperature inversions are one of the most crucial atmospheric conditions that are responsible for very high pollution levels during wintertime. The strength and persistence of inversions, and the characteristics of the atmospheric circulation during these conditions are affected by different factors like geographic location, regional and local topography and features of the urban area.

The general situation of air pollution in the Italian urban areas, as resumed by the elaboration of the National Environmental Protection Agency (ANPA) for 1998, shows that the long term air quality standards are generally respected for SO_2 , NO_2 and TSP, while a large number of exceedances are recorded for O_3 nearly everywhere it is measured (countrywide statistics for PM10 are not yet available). However, the situation is different for short term episodes. The major Italian urban areas experience severe pollution episodes, during which the threshold levels for NO_2 (200 $\mu g/m^3$ for the 98th percentile of the hourly averages and "warning level" for hourly averages in urban areas) and O_3 (180 $\mu g/m^3$ for hourly averages) are often exceeded, e.g. during 1997 the worst station in Milan city recorded 100 hours exceeding 200 $\mu g/m^3$ for NO_2, and many other stations in the Province recorded more than 50 exceedances.

This is the situation characterised by the air quality standards presently defined by the Italian legislation. This state of affairs would change quite sharply, if we would consider the air pollutant limit values introduced by the recent EU directives (EC 99/30; EC 2000/69). If the new limit values, to be achieved in 2005 and 2010, are considered, some of the major Italian urban areas would be in a state of non-compliance. The cited EU legislation states limits on the hourly and daily averages of pollutants (e.g. NO_2 and PM10) to be exceeded only a few times each year. The introduction of these limit values will emphasize the prevention of relevant air pollution episodes in urban areas.

Severe pollution conditions are mainly observed during persistent high pressure periods, that cause low wind-speeds and favour pollutant accumulation in the lower atmospheric layers (Finardi et al., 2000). During winter conditions, air pollution peaks are observed mainly for NO_X, PM10 and CO concentrations, while ozone pollution episodes often occur during summer (Silibello et al., 2000).

Temperature inversions are one of the atmospheric phenomena that can cause the worst pollution episodes in urban areas during wintertime. The structure, strength and persistence of inversions and the characteristics of the atmospheric circulation in different geographic locations (Figure 1) is investigated in the following sections through the analysis of experimental data sets. A severe inversion pollution episode which occurred in Milan, December 1998, is analysed on the basis of the air quality network meteorological/chemical measurements, of vertical soundings from Linate airport WMO station and of mesoscale circulation features. Some peculiar characteristics of the atmospheric circulation during temperature inversion inside a deep alpine valley (Aosta, February 1997) and on the Northern Mediterranean coast (Savona, February 1998) are analysed on the basis of local meteorological field campaign data.

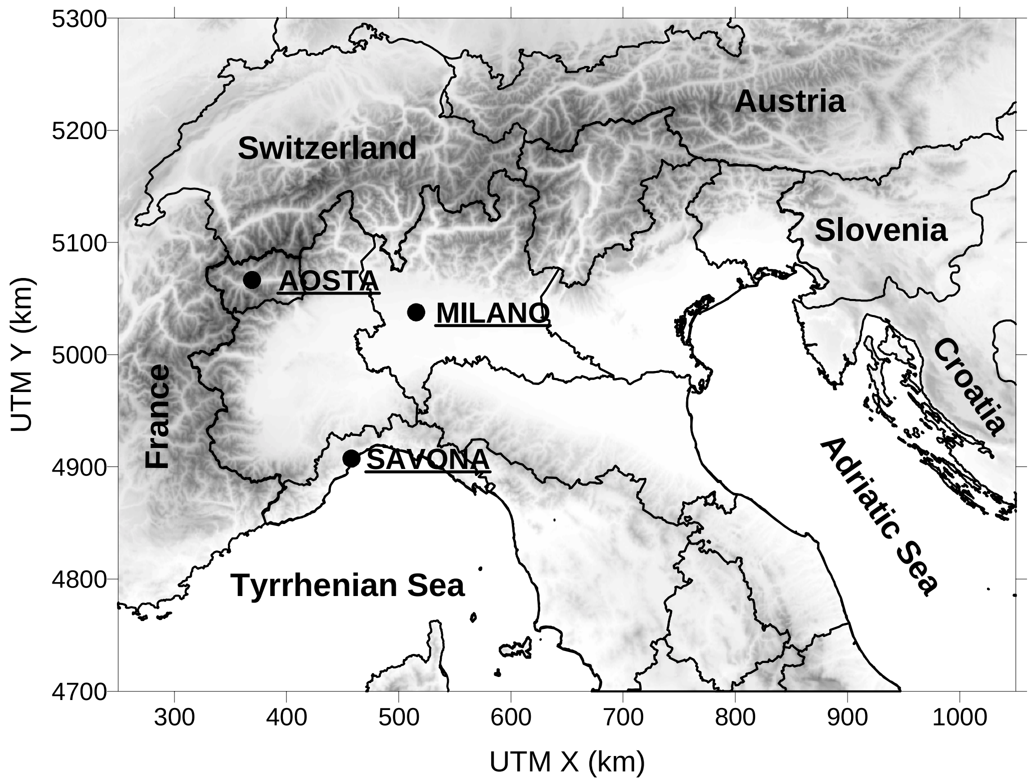

Figure 1 Geographic location of the studied sites. States and Italian Regions boundaries are indicated.

An inversion episode in Milan

Milan city and its surrounding urban area, together with several industrial settlements, is located in the central part of the Po river basin, northern Italy, in a flat area. The whole area is exposed to substantial emission loads. The atmospheric circulation of the Po valley is characterised by the strong modification of synoptic flow due to the high mountains (Alps and Apennines) that surround the valley on three sides. The local atmospheric circulation features, dominated by calms and weak winds, often favour the development of critical pollution episodes. High pollutant concentrations are generally observed during anticyclonic conditions, characterised by weak winds, high humidity and unfavourable stability conditions and limited turbulence intensity, during winter. These conditions can be worsened by temperature inversions which limit the vertical dilution of pollutants.

An air quality episode occurred during December 1998 that was caused by a temperature inversion. Figure 2 shows the time evolution of NO_2 and PM10 concentrations measured by the Milan City air quality control network during December 1998.

A severe pollution episode lasting from December 14th (Monday) to December 19th (Saturday) that can be clearly identified. The NO_2 hourly average concentrations exceed both the warning and alarm thresholds (200 and 400 $\mu g/m^3$, respectively) defined for short term episodes by the Italian law. PM10 daily averages showed values larger than 100 $\mu g/m^3$ for most parts of the period. During the episode the “average” concentrations of different pollutants show values roughly twice their monthly averages.

The observed accumulation of air pollutants is driven by an intense ground based temperature inversion (Figure 3) that develops on December 13th and reaches its maximum depth and intensity (with a temperature growth of about 15 degrees in the first 1000 metres height) on December 15th and lasts until December 19th. The development of the observed inversion is due to the advection of warm air carried by the incoming high pressure ridge, that, during the episode, is located over the western Mediterranean basin (Fig. 4). The maximum warming is observed between 1000 and 1500 metres a.g.l., where the temperature reaches values around 15°C. Surface temperature lowers during the first days, reaching minimum vales on December 15th, and later starts to rise slowly. A very shallow unstable boundary layer is observed during daytime. Its depth ranges only a few hundred meters during the whole episode. The local and mesoscale circulation is characterised by very low wind speeds. Surface wind observations (Figure 5) show a tendency to follow the directions of local breeze circulations.

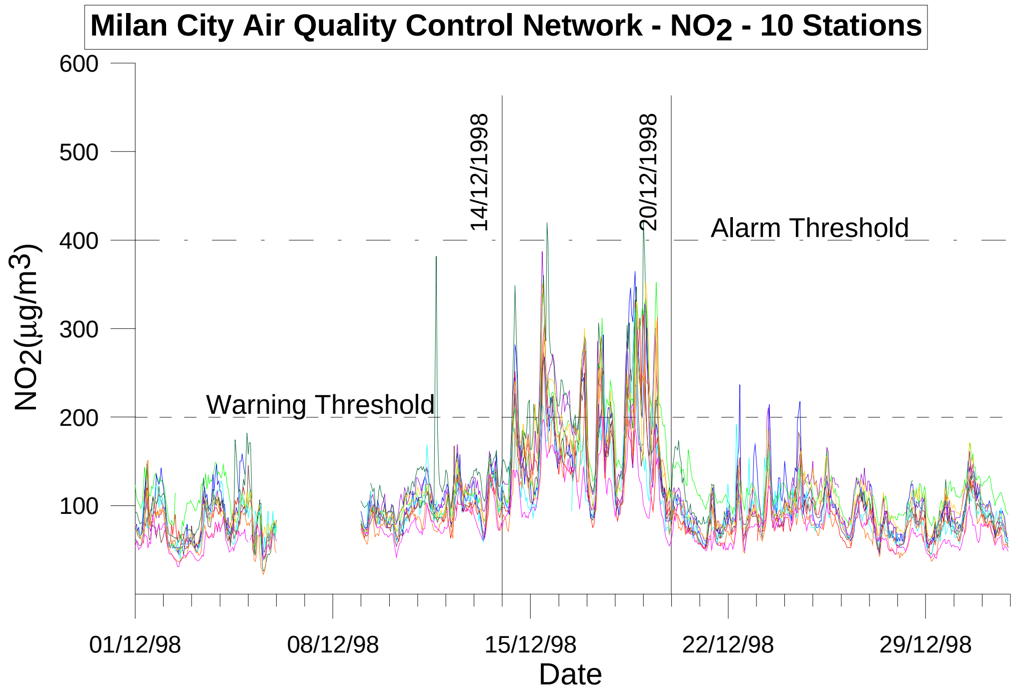

(a)

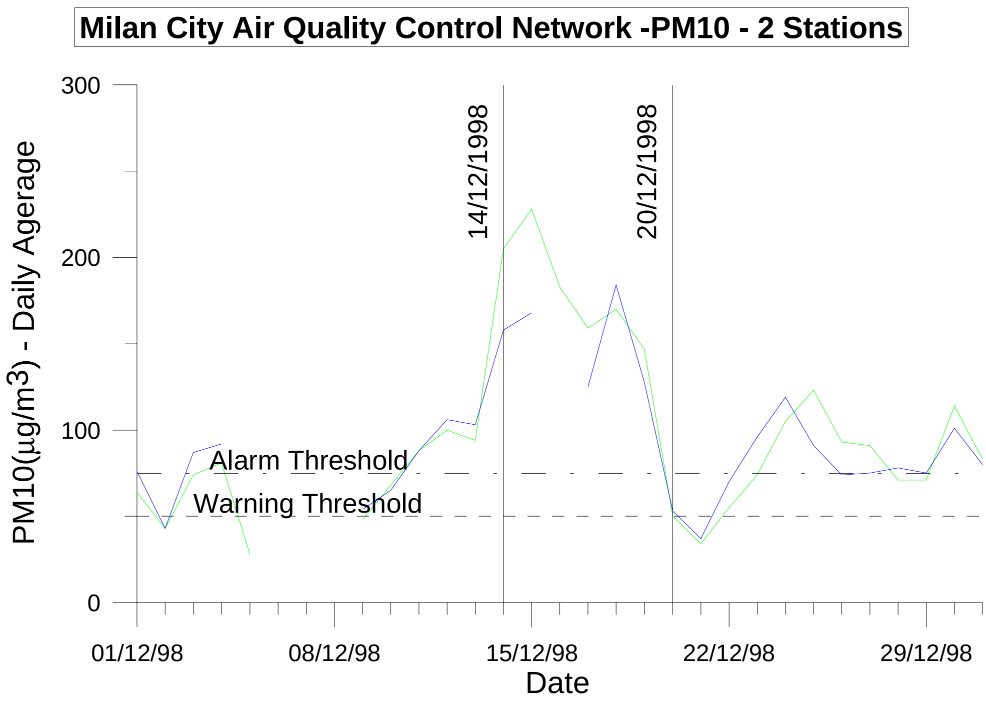

(b)

Figures 2 (a) Hourly average concentrations of NO_2 (10 stations) and (b) daily average concentrations of PM10 (2 stations), measured by the Milan city air quality control network during December 1998.

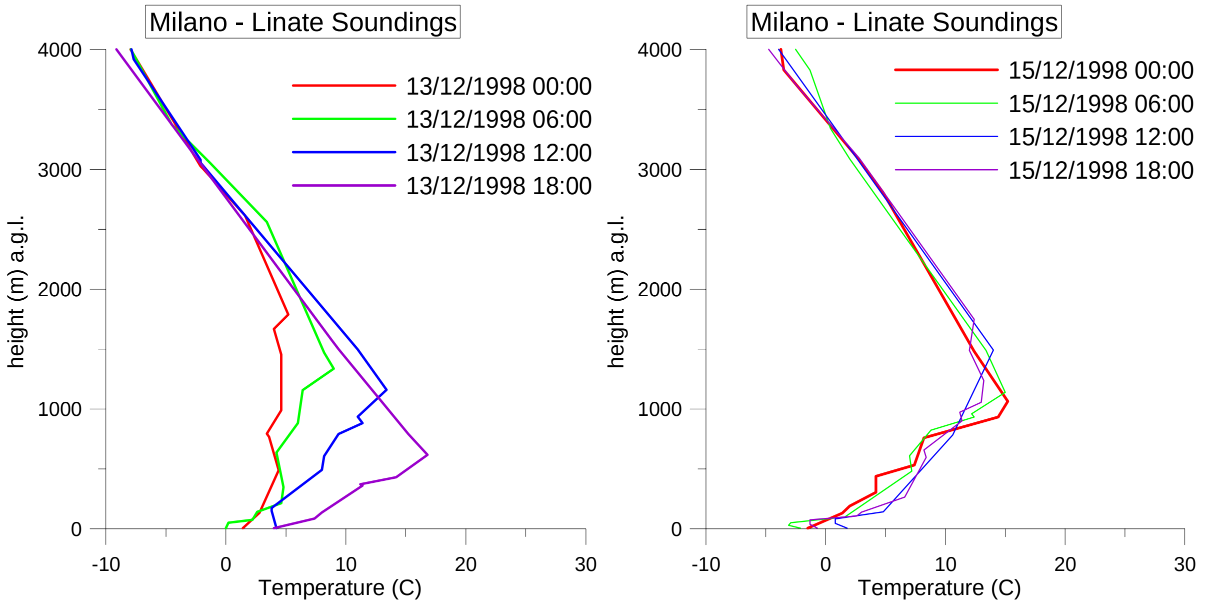

Figure 3. Temperature vertical profile measurements obtained from Milan airport radiosoundings on December 13th (left) and December 15th (right) 1998.

Some interesting differences can be noticed in the behaviour of pollutants during the episode: CO concentrations (not shown) demonstrate a quick response to the inversion development with peaks observed already on day 13 and a growing trend during the whole episode; PM10 seems to be more influenced by the temperature gradient and vertical extension of the inversion, with maximum concentrations observed during the first days of the episode and a decreasing trend; NO_2 behaviour is more complex, it shows a delay of concentration peaks from the inversion development and maximum values are observed both during the first (15/12) and in the last (18-19/12) part of the episode.

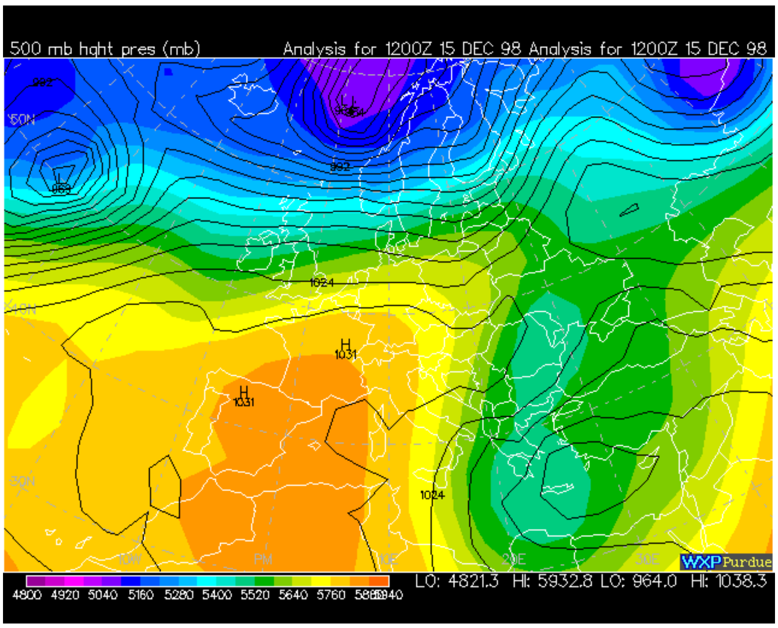

Figure 4. ECMWF 500 HPa geopotential and sea level pressure analyses on December 15th 1998 at 12:00 GMT

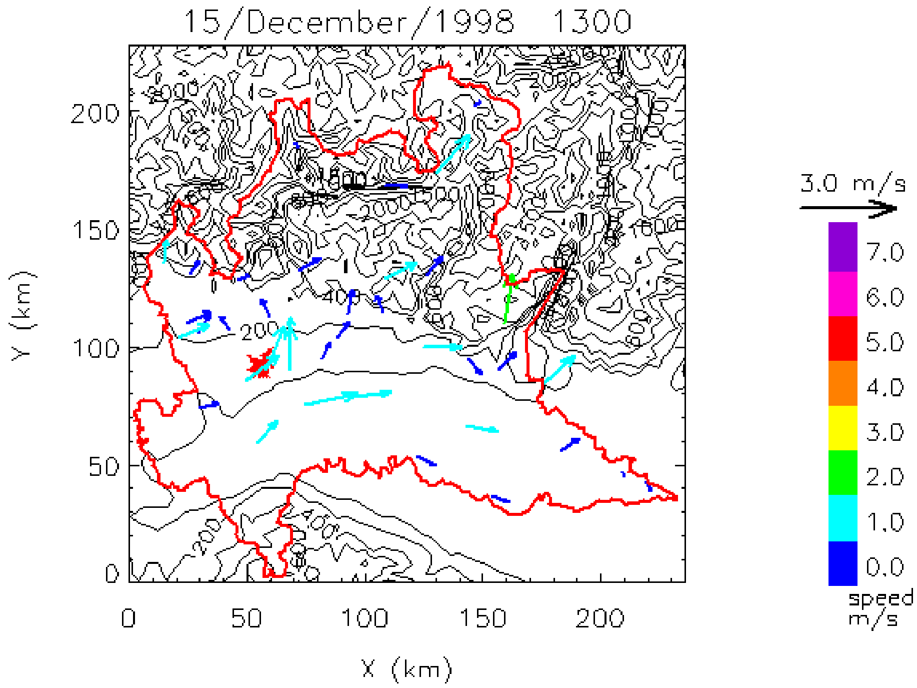

Figure 5. Surface wind measurements on December 15th, 1998 at 13:00 local solar time. Lombardia Region boundaries and Milan city location are printed in red colour.

The influence of an elevated inversion on coastal circulation in Savona

The town of Savona is located on the north-western Mediterranean coast of Italy (Figure 1). The site is characterised by complex terrain with mountains higher than 1000 metres few kilometres inland. Intensive meteorological and air quality field campaigns have been performed on site during summer and winter 1997/1998 operating surface stations, two SODAR's, and conducting regular meteorological soundings. The topography of the area and the locations of measuring stations are illustrated in Figure 6.

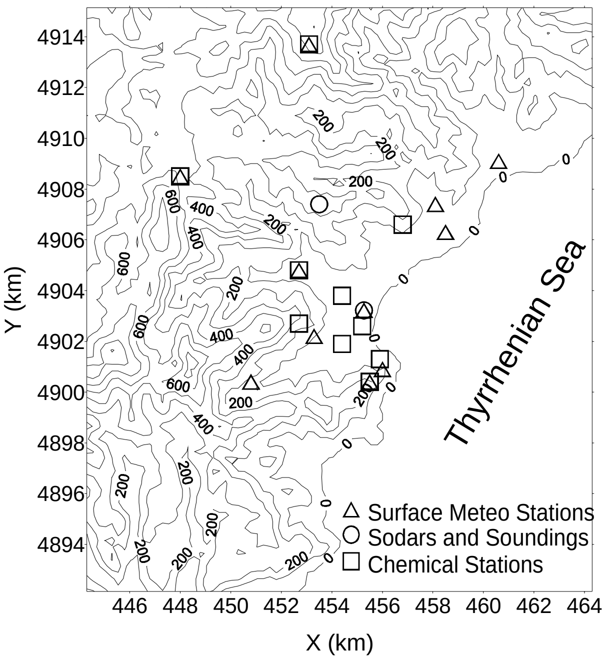

Figure 6. Savona/Vado Ligure: topography and locations of measuring stations. Isolines are plotted with an interval of 100 metres.

During a winter high pressure period (February 10^{th}-13^{th} 1998) a subsidence induced elevated temperature inversion was observed. Figure 7 and 8 shows the vertical wind and temperature profiles measured on February 11^{th} by radiosoundings and pilot balloons. An inversion of 5-7° C located between 800 and 1200 metres is detected. The wind profiles show a strong shear at the height of the inversion. Under the elevated inversion layer, the flow was dominated by local features. At the height of the upper-level inversion, the characteristics of the flow were coherent with the mesoscale circulation. During night-time, a separation of the flow developing in the coastal flat strip and the circulation affecting the hillside stations has been detected.

Figure 9 depicts the distribution of the surface flow measurements on February 12^{th} at 00:00. A north-westerly wind, with slope flow and land breeze features, is observed in the lower layer over the coastal area, while a south-easterly flow is observed over the hills. These characteristics of the flow field are confirmed by the observations from the SODAR's located near the coastline and over a hill. The observed circulation conditions favour pollutant stagnation in the coastal area and determine different dispersion patterns for buoyant plumes and pollutants emitted by ground level sources.

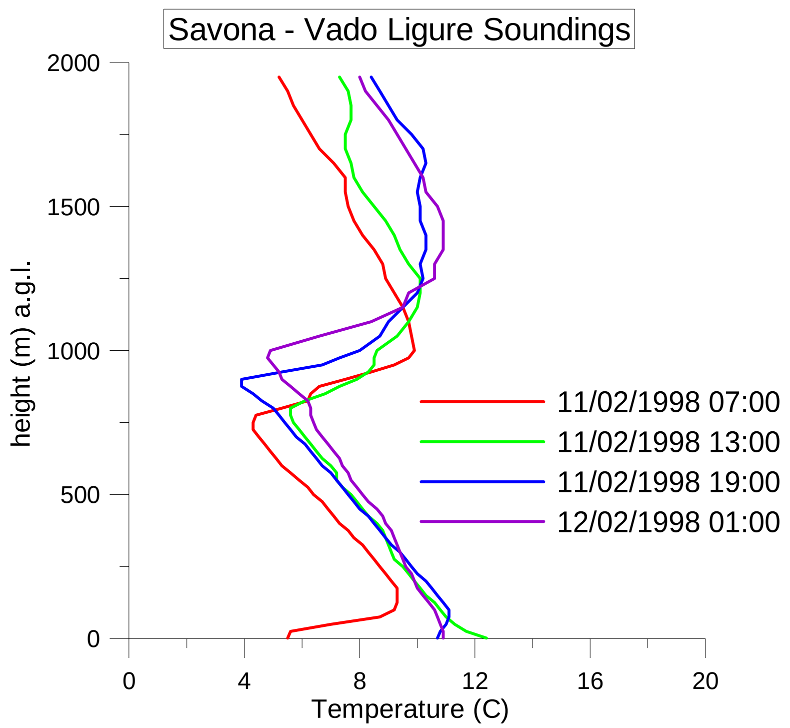

Figure 7. Temperature vertical profile measured by radiosoundings in Savona on February 11th 1998.

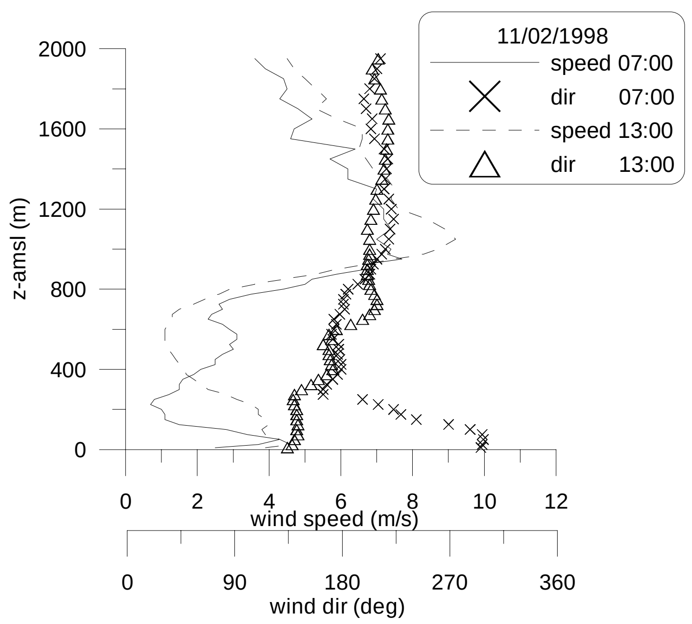

Figure 8. Wind vertical profile measured by radiosoundings launched near the coastline in Vado Ligure, nearby Savona town, on February 11th 1998 at 7:00 and 13:00 local solar time.

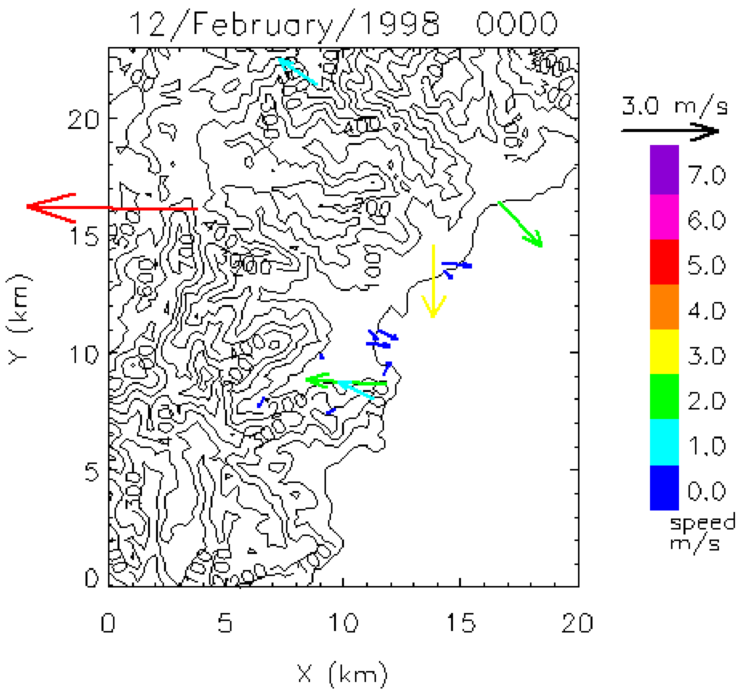

Figure 9 Surface wind observations on February 12th at 00:00 local solar time.

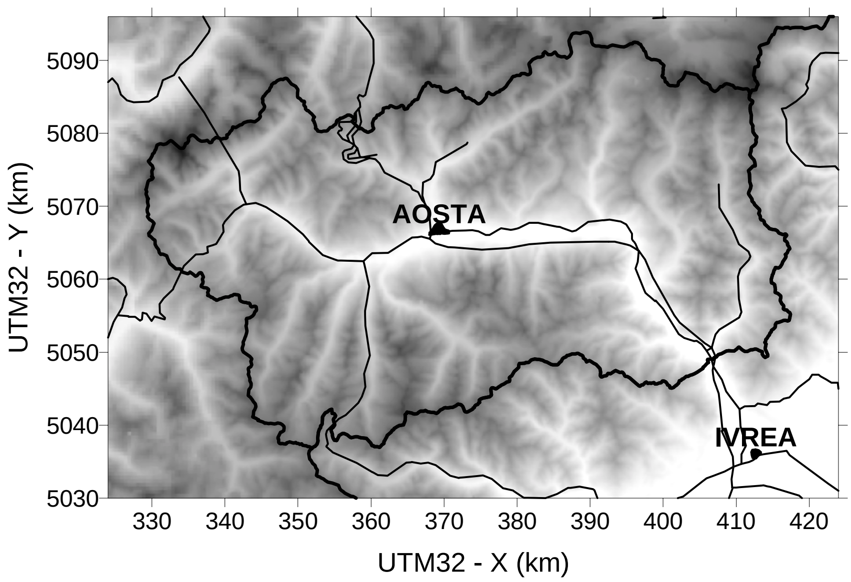

Figure 10. Aosta Valley topographic features. The location of the town of Aosta, the regional boundaries and the major roads are indicated on the map. The Mont Blanc is in the North-western side of the map.

A persisting ground based inversion in a deep alpine valley in Aosta

Deep alpine valleys can experience persisting temperature inversions during wintertime, when the ground surface is generally snow-covered and the solar radiation flux is limited by the shadowing caused by topography. In these conditions air pollution episodes can affect also small towns and weakly urbanised regions. Unluckily, meteorological profile measurements are quite uncommon inside valleys, and few data are available concerning inversion conditions in southern alpine valleys.

A persisting inversion condition was observed in the Aosta Valley (Figure 1) during the period 30/01-07/02/1997 when a meteorological and air quality field campaign took place nearby the town of Aosta. The Aosta Valley is one of the deepest and closest valleys of the Alps (Figure 10). It faces the Mont Blanc from the Italian side, and it is surrounded on three sides by mountains reaching more than 3000 metres high, while the bottom of the valley has a height of about 600 metres (Fig. 10). Moreover the valley axis is oriented west-east, maximising the solar shelter effects of mountains on the bottom of the valley.

The observed temperature inversion developed during a persisting high pressure condition slowly moving over Europe. The temperature profiles measured on January 31 are plotted in Figure 11. The ground based inversion persists all day long. No unstable boundary layer development is detected by measurements. The daily air warming inside the valley simply shifts the temperature profile without modifying its shape. The temperature inversion is limited to the first 500 metres and its strength is of the order of 5° C. The temperature profile features and its daily evolution have some similarities with winter inversion conditions observed in Helsinki (Karppinen et al., 2002), even if the near ground temperature gradient has lower values in the alpine valley. The observed wind profiles showed that inside the inversion layer the flow is very weak and characterised by a daily cycle with the characteristics of a mountain/valley breeze. The observed daily rotation is limited to the first hour of the afternoon. The flow inside the valley appears to be separated from the circulation aloft.

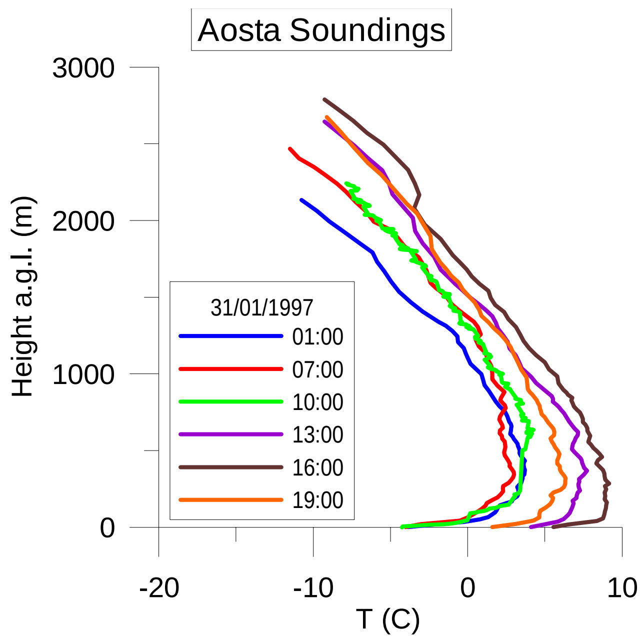

Figure 11. Temperature profiles measured by radiosoundings nearby Aosta on January 31th 1997.

Conclusions

A severe pollution episode caused by temperature inversions during wintertime in the city of Milan has been analysed. Some peculiar characteristics of the atmospheric circulation during temperature inversions have been shown on the basis of measurements recorded during field campaigns performed inside a deep alpine valley and on the northern Mediterranean coast. These data allow to give a detailed local picture of temperature inversion conditions in the areas investigated. The observed inversion episodes are all caused by persisting winter high pressure conditions. In all cases the circulation in the lower layers is decoupled from the synoptic flow and appears to be mainly determined by local and mesoscale terrain features.

The modelling of atmospheric flow and dispersion during temperature inversion conditions is of great interest to forecast and manage potentially harmful urban air pollution episodes. It has to be taken into account that due to the complexity of the circulation within and above an inversion, to the special effects of urban areas like the heat island or flow deceleration, and to the superposition of phenomena of different scales, the high resolution modelling of inversion conditions can still be considered challenging. On the other hand the importance of modelling severe pollution episodes will acquire even more relevance due to the implementation of recent EU directives on air quality. The cited directives allow a very limited number of exceedances of the concentration thresholds stated for the major pollutants, and the occurrence of one or two episodes like the ones described in this paper can cause non-attainment of the air quality standard. Therefore the air quality managers would probably have to move their attention from management to forecasting and prevention of urban air pollution episodes.

References

EC/99/30: Directive 99/30/EC of 22 April 1999 relating to limit values for sulphur dioxide, nitrogen dioxide and oxides of nitrogen, particulate matter and lead in ambient air. *J. Europ. Commun*. L163/41.

EC/2000/69: Directive 2000/69/EC of 16 November 2000 relating to limit values for benzene carbon monoxide in ambient air. *J. Europ. Commun*. L313/12.

Finardi S., Tinarelli G. and Pirovano G., 2000: Local Scale Circulation Reconstruction and Forecast: Problems Connected To Italian Topographic Features, presented to the 6° Convegno Nazionale di Ingegneria del Vento, IN-VENTO-2000, Genova, 18-21 giugno 2000.

Karppinen A., Joffre S. M., and Kukkonen J., 2002, Evaluation of meteorological data measured at a radio tower in the Helsinki Metropolitan Area, Proceedings of the COST715 Workshop on Mixing height and inversions in urban areas, Toulouse, France, 3 - 4 October 2001.

Silibello C., Catenacci G., and Pirovano G., 2000, Modelling Photo-oxidants over Lombardia Region and Milan Area by using a Grid Nesting approach - A contribution to SATURN subproject, presented at Eurotrac-2 2000 Symposium Garmish-Partenkirchen 27-31 March, 2000.

Conclusions and recommendations

Martin Piringer and Jaakko Kukkonen

1. General conclusions

The COST-715 - action aims at providing recommendations for harmonising the measurements, assessments and forecasting of characteristic meteorological parameters in the urban atmosphere. In particular, the action aims at specifying the minimum requirements that meteorological measurements have to satisfy in urban areas.

The action also aims at a more consistent use of available urban meteorological data, especially regarding the application of such data as input values of meteorological pre-processors and atmospheric dispersion models. The action also supports and contributes to new meteorological measurement campaigns in urban areas. Urban meteorological mast data are especially valuable in order to analyse the vertical structure of the urban canopy. In particular, atmospheric turbulence and vertical flux measurements over cities are urgently needed. The action has already initialised some co-operative work for utilising such data more extensively.

The action will undertake comparisons of measured urban and rural meteorological parameters, in order to improve our understanding on urban meteorological processes. Such a comparison is already in progress for wind speed and direction (Working Group-WG 1); some work has also been accomplished concerning temperature inversions (WG 3).

The action needs to collaborate more closely with the World Meteorological Organisation in the future, especially within the "Global Atmospheric Watch, Urban Research Meteorology and Environmental Project – GURME". For instance, the recommendations regarding urban meteorological measurements are of common interest for both of these actions.

2. Conclusions on evaluation of mixing heights

WG2 aims at a more specific definition of the mixing height (MH) for urban areas. Useful background information has been provided by the COST-710 action; however, we also intend to take into consideration the horizontal inhomogeneity and the vertical structure of the boundary layer over the urban area. WG2 recommends that the MH is a useful concept in the context of simpler regulatory dispersion models, although not a very accurate one. Concerning numerical weather prediction (NWP) models, it is not so clear whether the MH is sufficiently accurate to be useful.

WG2 also aims at recommending optimum methods for measuring the urban MH. Experience has been gained based on recent field experiments, such as BUBBLE (The Basle Urban Boundary Layer Experiment) and UBL/ESCOMPTE (The Urban Boundary Layer Experiment in the greater Marseilles area). The effect of climatic differences on the urban MH has to be investigated more thoroughly. There are significant differences between, e.g., Northern and Southern European cities in this respect.

When modelling the mixing height, the mechanisms involved in the formation of the daytime MH are better understood than the corresponding ones at nighttime. WG2 therefore strongly recommends that more emphasis should be given to improving the methods for the nighttime MH determination.

No direct evaluation of the MH is necessary regarding the dispersion of traffic-originated pollution within the roughness sublayer (e.g., within a street canyon). On the other hand, in the urban and meso-scales, the MH is an important parameter for practically all air pollution applications.

WG2 will also try to formulate a list of different methods for the determination of the MH, including their relative advantages and disadvantages, and their limits of application.

3. Conclusions on temperature inversions and peak pollution episodes

WG3 aims at a harmonised definition of an air pollution episode. WG3 also classifies various types of air pollution episodes in Europe, in terms of the pollutants, the main source categories and the seasons of the year. It is particularly relevant for this COST action to investigate the evolution of various meteorological parameters in the course of episodes. The COST 715 action will collaborate with “Formation of Ozone in South European Cities – FOSEC” that has similar objectives specifically for Southern European conditions. The FOSEC action is part of the SATURN project within the EUROTRAC-2 programme.

There is work in progress especially on the dependency of episodes on temperature inversions in both Northern and Southern European countries. The action evaluates the performance of both numerical weather prediction (NWP) models and air quality forecasting models regarding their ability to predict relevant meteorological parameters and air quality. A key question is the ability of such models to forecast urban temperature inversions during episodes.

WG3 will also evaluate the dependency of episodes on the temporal variation in emissions, and the inversions within a city compared with those in surrounding rural areas. A set of meteorological criteria can be specified for predicting the potential formation and occurrence of air quality episodes. Such criteria can include, e.g., limit values in terms of wind velocity, inversion strength or gradient, atmospheric stability and Richardson number. However, any single meteorological parameter or just one criterion will probably not be sufficient.

This action should also keep in mind various policy-relevant issues, such as the conceivable practical measures for air quality protection during episodes. It is therefore important to inform continuously the local authorities and collaborate with them.